Antonio Carlos Brandao de Araujo

Studies on Plantwide Control

Trondheim, January 2007

Doctoral thesis for the degree of PhD

Norwegian University of Science and Technology
Faculty of Natural Sciences and Technology
Department of Chemical Engineering

NTNU
Norwegian University of
Science and Technology

Abstract

Plantwide control is of current interest because of aiming at improved throughput and higher economical value generation, but also for other reasons like increased safety and reduced impact on the environment. Some of these objectives used to be contradictory, but today they more or less all point in the same direction: all improvements usually also imply improved economy of the operations, at least in the long term. Plantwide control obviously implies that one deals with a large-scale system with literally hundreds of measurements and with many mass and energy streams being manipulated. A hierarchical approach is natural so as to build the overall control system from the bottom up, first controlling locally and coordinating actions more and more as one moves up in the hierarchy and at the same time extending the control horizon. Selecting measurements or derived measurements and streams to manipulate and the control structure linking these up is obviously the generic task to be solved here. The self-optimizing method is a sound technology used to select measurements such that the burden of on-line optimizations (as one could expect to keep the process as close as possible to optimality) is drastically reduced or even eliminated in some particular cases. Nonetheless, the application of this technology would not be possible without a proper lower layer regulatory control and a coordinating supervisory control layer.

The first section of this work gives a very general description of the plantwide control framework used throughout the thesis, giving reasons for and describing the plantwide procedure by Skogestad (2004*a*). It directs the chapters that follow in a way that it makes clear the great potential behind the ideas of this procedure when applied to large-scale processes, a subject that has not received much attention to date. This may be considered as a first step into future real-world applications of the technique.

We then use the self-optimizing control procedure to select primary variables to a large-scale process, the HDA plant. The idea is to select controlled variables which when kept constant lead to minimum economic loss. First, the optimal active constraints need to be controlled. Next, controlled variables need to be found for the remaining unconstrained degrees of freedom. In order to avoid the combinatorial problem related to the selection of outputs/measurements for such large plants, a local (linear) analysis based on singular value decomposition (SVD) is used for pre-screening. This is followed by a more detailed analysis using the nonlinear model. Note that a steady-state model, in this case one built in Aspen Plus^{TM}, is sufficient for selecting controlled variables.

After deciding for the primary (economic) controlled variables, the design of a control structure for the HDA plant is considered. Steady-state "top-down" analysis and

optimization of the process was used to select 16 sets of candidate "self-optimizing" primary (economic) variables and then we focus on the remaining "bottom-up" steps dealing with where in the plant the production rate should be set; design of the regulatory control layer; design of the configuration of the supervisory control layer; and nonlinear dynamic simulations to validate the proposed control structure. Emphases is given to the systematic design of the regulatory control layer for it constitutes the backbone on which the optimal operation of higher layer relies on. In regard to the maximization of the production rate, we have found that this process possesses a bottleneck at the reactor inlet pre-heating and that further increase in feed rate is not physically possible. A control structure is then proposed which yields robust, good dynamic performance. In order to carry out the analysis, a dynamic model in Aspen Dynamics^{TM} is extensively used.

In the ammonia synthesis process three modes of operation are considered: (I) Given feed rate, (IIa) Maximum throughput, and (IIb) "Optimized" throughput. There has been found that no bottleneck in the process, and thus there is no Mode IIa of operation. In Mode IIb, the compressors are at their maximum capacity and it is proposed to adjust the feed rate such that the inert concentration is constant. Two control structures, one for Mode I and another for Mode IIb, are therefore proposed. In Mode I, it is proposed to keep constant purge rate and compressor powers. The final control structures result in good dynamic performance.

The chapter on time scale separation aims at combining two different approaches (Skogestad (2000) and Baldea and Daoutidis (2006)) into a method for control structure design for plants with large recycle. The self-optimizing approach (Skogestad, 2000) identifies the variables that must be controlled to achieve acceptable economic operation of the plant, but it gives no information on how fast these variables need to be controlled and how to design the control system. A detailed controllability and dynamic analysis is generally needed for this. One promising alternative is the singular perturbation framework proposed in Baldea and Daoutidis (2006) where one identifies potential controlled and manipulated variables on different time scales. The combined approaches have successfully been applied to a reactor-separator process with recycle and purge.

There is also some disagreement in the literature on whether or not large plant gains are a problem when it comes to input-output controllability. We then decided to derive controllability requirements for two kinds of input errors, namely, restricted (low) input resolution (e.g., caused by a sticky valve) and input disturbances. In both cases, the controllability is limited if the plant gain is large at high frequencies. Limited input resolution causes limit cycle behavior (oscillations) similar to that found with relay feedback. The magnitude of the output variations depends on the plant gain at high frequency, but is independent of the controller tuning. Provided frequent input (valve) movements are acceptable, one may reduce the output magnitude by forcing the system to oscillate at a higher frequency, for example by introducing a faster local feedback (e.g. a valve positioner) or by pulse modulating the input signal.

Acknowledgements

I would like to gratefully acknowledge the opportunity to me given and the supervision of professor Sigurd Skogestad during the course of this laborious thesis, since without his support and contributions this thesis would never have emerged.

Special thanks to my family that, down there in the tropics, has always supported me, and also to Helle for her endless patience and constant love. To them I dedicate this work.

Antonio Araujo
Trondheim, January, 2007

Table of Contents

Chapter 1

Thesis overview

In this chapter the thesis is restricted, the work motivated and placed in a wider perspective. An overview of the thesis together with a brief discussion of related work are given. A list of the publications emerging from this thesis is found at the end of this chapter.

1.1 Motivation and focus

Increasing demands for efficient operation and utilization of energy and raw materials in chemical processes require better knowledge and understanding of the dynamic and steady state behavior of the processes in order to design efficient control systems. There is a need for more sophisticated control schemes to operate the process as close as possible to optimality in spite of disturbances and environment changes. This is in particular important for the most common case of integrated processes where unreacted raw materials are recycled and heat integration accomplished, which gives rise to more complex dynamic and steady-state behaviors.

The main contribution of this thesis is the application of the plantwide control design procedure of Skogestad (2004*a*) to large-scale (very complex) chemical processes with emphasis to the technique of self-optimizing control (Skogestad, 2000), and study the dynamic implications of such an implementation from a practical (engineering) point of view. It is then addressed to the practitioner as well as to the academic community as a remainder that one without the other cannot make science move forward.

1.2 Related work

Plantwide control considers the control philosophy of the overall plant with emphasis on structural decisions (Skogestad, 2004*a*). Control systems in chemical plants are often structured hierarchical into several layers, each operating on a different time scale. Typically, layers include scheduling (weeks), site-wide (real-time)-optimization (day), local optimization (hours), supervisory/predictive control (minutes) and stabilizing/regulatory control (seconds). The layers are interconnected through the *controlled*

variables (Skogestad, 2004*a*).

The set points of the controlled variables ($\mathbf{c}_s$) are the variables that link the layers in a control hierarchy, whereby the upper layer calculate the set points to the lower layer.

In applying the procedure by Skogestad (2004*a*) to large-scale chemical processes, we here focus basically on two issues: (1) The selection of controlled variables via the self-optimizing control technique, and (2) The input-output controllability characteristics of the final selected control structure.

We distinguish between primary and secondary controlled variables. The primary controlled variables deal with achieving some overall optimal operation of the plant. The secondary controlled variables deal with stabilizing and achieving acceptable dynamic performance for the system. Self-optimizing control deals with the selection of primary controlled variable to achieve good steady-state economic performance.

The basis for self-optimizing control was defined by Morari *et al.* (1980) as *the search for a function* $\mathbf{c}$ *of the process variables which when held constant, leads automatically to the optimal adjustments of manipulated variables, and with it, the optimal operating conditions [...].* Related to this is the work of Shinnar (1981) and later by Arbel *et al.* (1996) on "dominant variables" and partial control. Narraway *et al.* (1991) and Narraway and Perkins (1993) stress the need to base the selection of controlled structures of economics.

Skogestad (2000) discusses self-optimizing control, and presents a detail overview of related work. Skogestad (2000) presents qualitative requirements for good controlled variables, namely

R1. Its optimal value should be insensitive to disturbances.

R2. It should be easy to measure and control.

R3. Its value should be sensitive to changes in the manipulated variables.

R4. For cases with two ore more controlled variables, the selected variables should not be closely correlated.

In order to ensure that disturbances to the primary controlled variables can be handled efficiently by the supervisory control layer (it can be the operators in a chemical plant), the secondary controlled variables and the control configuration in the regulatory control layer must be carefully selected. The main issue here is to guarantee "stable" operation of the plant and practical rules for the design of the regulatory control layer are given by Skogestad and Postlethwaite (2005). This is reflected in good input-output controllability features for the regulatory layer.

1.3 Outline of the thesis

Chapter 2 gives an overview of the plantwide control design procedure of Skogestad (2004*a*), discussing its main aspects and charateristics, and forming the groundwork for the chapters that follow.

Chapter 3 describes the application of self-optimizing control to a large-scale process, the HDA plant. The idea is to select controlled variables which when kept constant lead to minimum economic loss. First, the optimal active constraints need to be controlled. Next, controlled variables need to be found for the remaining unconstrained degrees of freedom. In order to avoid the combinatorial problem related to the selection of outputs/measurements for such large plants, a local (linear) analysis based on singular value decomposition (SVD) is used for prescreening. This is followed by a more detailed analysis using the nonlinear model. Note that a steady-state model, in this case one built in Aspen Plus^{TM}, is sufficient for selecting controlled variables. A dynamic model is required to design and test the complete control system which include regulatory control. This is considered in the next chapter.

Chapter 4 describes the design of a control structure for a large-scale process, the HDA plant. Steady-state "top-down" analysis and optimization of the process (Araujo *et al.*, 2006) was used to select 16 sets of candidate "self-optimizing" primary (economic) variables. In this chapter, we focus on the remaining "bottom-up" steps dealing with deciding where in the plant the production rate should be set; design of the regulatory control layer; design of the configuration of the supervisory control layer; and nonlinear dynamic simulations to validate the proposed control structure. Emphases is given to the systematic design of the regulatory control layer for it constitutes the backbone on which the optimal operation of higher layer relies on. In order to carry out the analysis, steady-state and dynamic models are necessary and Aspen Plus^{TM} and Aspen Dynamics^{TM} are used extensively. The final control structure is robust and yields good dynamic performance.

Chapter 5 discusses the application of the plantwide control design procedure of Skogestad (2004*a*) to the ammonia synthesis process. This is a fairly well studied process but so far little has been said about its control structure design such that (near) optimal operation is achieved. We apply the design procedure in a broader perspective by distinguishing between three modes of operation: (I) with given feed rate, (II) with maximum throughput, and (III) with "optimized" throughput. The conclusion is that the ammonia process operates according to Mode III, and it is not economically attractive to increase production rate above the value corresponding to the "optimized" throughput since the profit sharply decreases with increase feed rate. Based on these analyses, two control structures, one for Mode I and another for Mode III, are proposed. The final control structures result in good dynamic performance.

Chapter 6 aims at combining two different approaches (Skogestad (2000) and Baldea and Daoutidis (2006)) into a method for control structure design for plants with large recycle. The self-optimizing approach (Skogestad, 2000) identifies the variables that must be controlled to achieve acceptable economic operation of the plant, but it gives no information on how fast these variables need to be controlled and how to design the control system. A detailed controllability and dynamic analysis is generally needed for this. One promising alternative is the singular perturbation framework proposed in Baldea and Daoutidis (2006) where one identifies potential controlled and manipulated variables on different time scales. The combined approaches has successfully been applied to a reactor-separator process with recycle and purge.

In Chapter 7, controllability requirements are derived for two kinds of input errors, namely restricted (low) input resolution (e.g. caused by a sticky valve) and input disturbances. In both cases, the controllability is limited if the plant gain is large at high frequencies. Limited input resolution causes limit cycle behavior (oscillations) similar to that found with relay feedback. The magnitude of the output variations depends on the plant gain at high frequency, but is independent of the controller tuning. Provided frequent input (valve) movements are acceptable, one may reduce the output magnitude by forcing the system to oscillate at a higher frequency, for example by introducing a faster local feedback (e.g. a valve positioner) or by pulse modulating the input signal.

Chapter 8 sums up and concludes the thesis, where we also discuss directions for further work.

1.4 Publications

Chapter 3

1. Araujo, A., Govatsmark, M., Skogestad, S.: Application of Plantwide Control to Large-Scale Systems. Part I - Self-Optimizing Control of the HDA Process, Presented at the 13th Nordic Process Control Workshop (NPCW), January 26-28, 2006, Copenhagen, Denmark.

2. Araujo, A., Govatsmark, M., Skogestad, S.: Application of Plantwide Control to Large-Scale Systems. Part I - Self-Optimizing Control of the HDA Process, Preprints of the International Symposium on Advanced Control of Chemical Processes (Adchem-2006), Gramado, Brazil, April 2-5, 2006, pp. 1049-1054.

3. Araujo, A., Govatsmark, M., Skogestad, S.: Application of Plantwide Control to the HDA Process. I - Steady-State Optimization and Self-Optimizing Control. Accepted for publication at Control Engineering Practice.

Chapter 4

1. Araujo, A., Hori, E. S., Skogestad, S.: Application of Plantwide Control to the HDA Process. II - Regulatory Control. Submitted for publication to Industrial Engineering Chemistry Research.

Chapter 5

1. Araujo, A. and Skogestad, S.: Control structure design for the ammonia synthesis process. Submitted for publication to Computers and Chemical Engineering.

Chapter 6

1. Araujo, A., Baldea, M., Skogestad, S., Daoutidis, P.: Time scale separation and the link between open-loop and closed-loop dynamics, 16th European Sympo-

sium on computer Aided Process Engineering and 9th International Symposium on Process Systems Engineering, Garmisch-Partenkirchen, Germany, July 9-13, 2006, Elsevier ISBN 0444529705 (Part B), Paper 1276, pp. 1455-1460.

Chapter 7

1. Araujo, A. and Skogestad, S.: Controllability of processes with large gains and valve stiction, AIChE Annual Meeting, Austin, Texas, Nov. 2004, Poster 414b.

2. Araujo, A. and Skogestad, S.: Controllability of processes with large gains, Presented at the Advanced Process Control Applications for Industry Workshop, May 9-11, 2005, Vancouver, Canada. Available on the conference CD-rom.

3. Araujo, A. and Skogestad, S.: Controllability of process with large gains, Presented at the 13th Nordic Process Control Workshop (NPCW), August 19-22, 2005, Gotenburg, Sweden.

4. Araujo, A. and Skogestad, S.: Controllability of process with large gains, 16th IFAC World Congress, Prague, Czech Republic, July 3-8, 2005, Paper Tu-A11-TO/1.

5. Araujo, A. and Skogestad, S.: Limit cycles with imperfect valves: Implications for controllability of processes with large gains. Accepted for publication at Industrial Engineering Chemistry Research.

Chapter 2

Introduction

Increased demand in the process industries requires optimal operation and better utilization of raw materials and energy and the key issue is how to achieve these objectives without the need of big capital investments. We understand that an efficient plantwide control structure can cope with most of the needs for optimal operation and we use the procedure given in Skogestad (2004*a*) to undertake the mission. Alternatively, one strategy for achieving improved production is to use real-time optimization (RTO), based on measured disturbances and process measurements. The optimal solution is usually implemented by updating setpoints to the control system which task is to keep the controlled variables at the setpoint.

The decision is then which variables to control and how to configure the link between them and the available degrees of freedom. Selecting the right controlled variables can be of paramount importance. Many chemical processes are influenced by disturbances that are often *not* measured and where installing new measurements are not economically viable. Thus, finding controlled variables where the optimal value is insensitive to disturbances could eliminate the need of estimating these disturbances online and would reduce the need of frequent setpoint updates. The use of feedback control introduces implementation errors. It is important to select controlled variables that are insensitive to implementation errors. The "optimal" implementation would be to use a dynamic optimizer which, based on full information of the disturbances and the plant outputs, calculates the optimal inputs. In practice, control systems have a hierarchical structure, where different layers operate on different time scales. The ideal situation is to have *self-optimizing* controlled variables where operation remains near-optimal in the presence of disturbances and implementation errors using a constant set point policy. Primary variables related to the economics of the process are therefore selected based upon the self-optimizing control technique as described in Skogestad (2000).

The next step is the identification on where in the process the bottleneck is located. This determines the configuration of inventory loops around the process as well as the throughput manipulator and is therefore a natural transition from the supervisory to the regulatory control layers design.

Secondary variables must also be selected to guarantee "stable" and "smooth" operation of the entire system and this is the key issue we discuss on the regulatory control

layer design along with its configuration, i.e. the link between input and outputs. Simple input-output controllability analysis is then used to assess the performance of the newly design control structure

Although simple at first sight, the approach just described is a powerful tool in designing control structures for large-scale complex chemical processes and the aim of the present thesis is to show the effectiveness of this sound plantwide procedure (Skogestad, 2004*a*) when applied to large-scale processes via the use of commercial simulation tools. Those processes are known by their intrinsic complexities and the result was that the plantwide procedure turned out to provide control structures that excel in economic as well as dynamic performance.

2.1 Plantwide control procedure

In practice, a control system is usually decomposed vertically in several layers, separated by time scale (see Figure 2.1). The layers are linked by the controlled variables, whereby set points computed by the upper layer are implemented by the layer below.

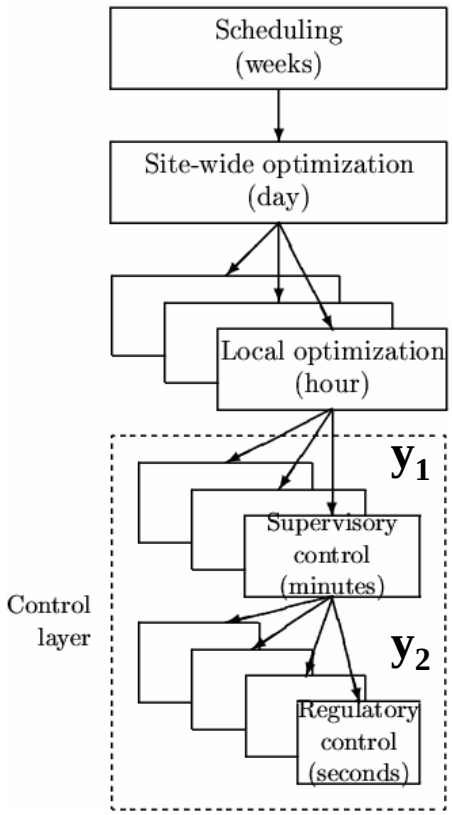

Figure 2.1: *Typical control hierarchy in a chemical plant.*

Control structure design is also known as plantwide control and deals with the structural decisions that must be made to design a control structure for, in our case, a

complete chemical plant. The decisions involve the following main tasks:

1. Selection of manipulated variables ("inputs");
2. Selection of controlled variables ("outputs"; variables with set points);
3. Selection of (extra) measurements (for control purposes including stabilization);
4. Selection of control configuration (the structure of the overall controller that interconnects the controlled, manipulated and measured variables);
5. Selection of controller type (control law specification, e.g. PID, decoupler, LQG, etc.).

The tasks above can be translated into a systematic plantwide procedure for control structure design as summarized in Table 2.1 extracted from Skogestad (2004*a*). The procedure has two main points:

I. *Top-down analysis*, including definition of operational objectives and consideration of degrees of freedom available to meet these (tasks 1 and 2 above; steps 1-4 in Table 2.1).

II. *Bottom-up design* of the control system, starting with the stabilizing control layer (tasks 3, 4 and 5 above; steps 5-8 in Table 2.1).

Each step in Table 2.1 is discussed in more details in sections that follow.

2.1.1 Step 1. Definition of operational objectives

We assume that optimal operation of the system can be quantified in terms of a scalar cost function (performance index) J_0 which is to be minimized with respect to the available degrees of freedom (manipulated variables; inputs) u_0:

$$\min_{u_0} J(x, u_0, d) \tag{2.1}$$

subject to the constraints

$$\begin{aligned} g_1(x, u_0, d) &= 0 \\ g_2(x, u_0, d) &\leq 0 \end{aligned} \tag{2.2}$$

Here d represents the exogenous disturbances that affect the system, including the effect of changes in the model (typically represented by changes in the function g_1), changes in the specifications (constraints), and changes in the parameters (prices) that enter in the cost function (and possibly in the constraints). x represents the internal states. We have available measurements $y = f_0(x, u_0, d)$ that give information about the actual system behavior during operation. Note that y may include measured values

Table 2.1: *Plantwide control structure design procedure.*

Step
(I) Top-down analysis
1. Definition of operational objectives: Identify operational constraints, and preferably identify a scalar cost function J to be minimized. *2. Manipulated variables u and degrees of freedom:* Identify dynamic and steady-state degrees of freedom (DOF). *3. Selection of primary controlled variables:* Which (primary) variables c should we control? - Control active constraints. - Remaining DOFs: control variables for which constant set points give small (economic) loss when disturbances occur (self-optimizing control). *4. Production rate:* Where should the production rate be set? This is a very important choice as it determines the structure of remaining inventory control system.
(II) Bottom-up design (with given primary controlled c and manipulated u variables)
5. Regulatory control layer: *Purpose*: "Stabilize" the plant using low-complexity controllers (single-loop PID controllers) such that a) the plant does not drift too far away from its nominal operating point and b) the supervisory layer (or the operators) can handle the effect of disturbances on the primary outputs ($y_1 = c$). *Main structural issue*: - Selection of secondary controlled variables (measurements) y_2. - Pairing of these y_2 with manipulated variables u_2. *6. Supervisory control layer:* *Purpose*: Keep (primary) controlled outputs $y_1 = c$ at optimal set points c_s, using as degrees of freedom (inputs) the set points $y_{2,sp}$ for the regulatory layer and any unused manipulated variables u_1. *Main structural issue*: - Decentralized (single-loop) control: a) May use simple PI or PID controllers; b) Structural issue: choose input-output pairing. - Multivariable control (usually with explicit handling of constraints (MPC)). Structural issue: Size of each multivariable application. *7. Optimization layer:* *Purpose*: Identify active constraints and compute optimal set points c_s for controlled variables. *Main structural issue*: Do we need real-time optimization (RTO)? *8. Validation:* Nonlinear dynamic simulation of the plant.

of the disturbances d, as well as known or measured values of the independent variables u_0. For simplicity, we assume pseudo-steady-state behavior and do not include time as a variable. The equality constraints ($g_1 = 0$) include the model equations, which give the relationship between the independent variables (u_0 and d) and the states (x). The system must generally satisfy several inequality constraints ($g_2 \leq 0$); for example, product specifications (e.g. minimum purity), manipulated variable constraints (e.g. nonzero flow), other operational limitations (e.g. maximum temperature). The cost function J_0 is in many cases a simple linear function of the independent variables with prices as parameters. In many cases it is more natural to formulate the optimization problem as a maximization of the profit P, which may be formulated as a minimization

problem by selecting $J_0 = -P$.

In most cases some subset g_2' of inequality constraints g_2 are active (i.e. $g_2' = 0$ at the optimal solution). Implementation to achieve this is usually simple: we adjust a corresponding number of degrees of freedom u_0 such that these active constraints are satisfied. In many cases the active constraints consumes all the available degrees of freedom. For example, if the original problem is linear (linear cost function with linear constraints g_1 and g_2), then it is well known from Linear Programming theory that there will be no remaining unconstrained variables. For nonlinear problems (e.g. the model g_1 is nonlinear), the optimal solution may be unconstrained and then we have to choose variables c to be controlled at their desired values (setpoints) c_s by the remaining degrees of freedom in u_0 such that the need for re-optimization when disturbances occur is mitigated - near-optimal operation. Obviously, the idea must be that the optimal value of c, denoted $c_{opt}(d)$, depends only weakly on the disturbances d, such that by keeping c at this value, we indirectly obtain optimal, or at least near-optimal, operation. More precisely, we may define the loss L as the difference between the actual value of the cost function obtained with a specific control strategy, e.g. adjusting u to keep $c = c_s$, and the truly optimal value of the cost function, i.e. $L(u, d) = J(u, d) - J_{opt}(d)$. This is the idea of self-optimizing control.

2.1.2 Step 2. Manipulated variables u and degrees of freedom

It is paramount to determine the number of steady-state degrees of freedom because this determines the number of steady-state controlled variables that we need to choose. To find them for complex plants, it is useful to sum the number of degrees for individual units as given in Table 2.2 (Skogestad, 2002).

Table 2.2: *Typical number of steady-state degrees of freedom for some process units.*

Process unit	DOF
Each external feed stream	1 (feedrate)
Splitter	$n-1$ split fractions (n is the number of exit streams)
Mixer	0
Compressor, turbine, and pump	1 (work)
Adiabatic flash tank	0*
Liquid phase reactor	1 (holdup)
Gas phase reactor	0*
Heat exchanger	1 (duty or net area)
Columns (e.g. distillation) excluding heat exchangers	0* + number of side streams

* Add 1 degree of freedom for each extra pressure that is set (need an extra valve, compressor, or pump), e.g. in flash tank, gas phase reactor, or column.

2.1.3 Step 3. Selection of primary controlled variables

The objective is to achieve self-optimizing control where fixing the primary controlled variables c at constant setpoints c_s indirectly leads to near-optimal operation. More precisely (Skogestad, 2004*a*):

Self-optimizing control is when one can achieve an acceptable loss with constant setpoint values for the controlled variables without the need to re-optimize when disturbances occur.

The main steps to assist in finding the self-optimizing variables are:

1. Identification of important disturbances (typically, feed flow rates, active constraints and input error).

2. Optimization of the problem defined in Section 2.1.1 for the disturbances identified in item 1.

3. Identification of candidate controlled variables c.

4. Evaluation of loss for alternative combinations of controlled variables (loss imposed by keeping constant set points when there are disturbances or implementation errors), including feasibility investigation.

To achieve optimal operation, we first choose to control the active constraints. The difficult issue is to decide which unconstrained variables c to control.

One disadvantage with this "brute force" method is that it is requires a lot of computations, especially because there is no limit on the possible candidate controlled variables that might be evaluated for the loss using the nonlinear model of the process (Steps 3 and 4). It may therefore be important to limit the number of alternatives to evaluate in detail. One effective method is to eliminate choices by recurring to a local (linear) analysis.

Local (linear) analysis

We divide the original independent variables $u_0 = u', u$ in the "constrained" variables u' (used to satisfy the active constraints $g_2' = 0$) and the remaining unconstrained variables u. The value of u' is then a function of the remaining independent variables (u and d). Similarly, the states x are determined by the value of the remaining independent variables. Thus, by solving the model equations ($g_1 = 0$), and for the active constraints ($g_2' = 0$), we may formally write $x = x(u, d)$ and $u' = u'(u, d)$ and we may formally write the cost as a function of u and d: $J = J_0(x, u_0, d) = J_0[x(u, d), u'(u, d), u, d] = J(u, d)$. The remaining unconstrained problem in reduced space then becomes

$$\min_u J(u, d) \tag{2.3}$$

where u represents the set of remaining unconstrained degrees of freedom. This unconstrained problem is the basis for the local method introduced below.

In terms of the unconstrained variables, we can expand locally the loss function around the optimum:

$$L = J(u,d) - J_{opt}(d) = \frac{1}{2}\left\|z\right\|_2^2 \tag{2.4}$$

with $z = J_{uu}^{1/2}(u - u_{opt}) = J_{uu}^{1/2}G^{-1}(c - c_{opt})$, where G is the steady-state gain matrix from the unconstrained degrees of freedom u to the controlled variables c (yet to be selected) and J_{uu} the Hessian of the cost function (2.3) with respect to u. Truly optimal operation corresponds to $L = 0$, but in general $L > 0$. A small value of the loss function L is desired as it implies that the plant is operating close to its optimum. The main issue here is not to find the optimal set points, but rather to find the right variables to keep constant.

Assuming that each controlled variable c_i is scaled such that $||e_c'|| = ||c' - c_{opt}'||_2 \leq 1$, the worst case loss is given by (Halvorsen *et al.*, 2003):

$$L_{max} = \max_{||e_c||_2 \leq 1} L = \frac{1}{2}\frac{1}{\underline{\sigma}(S_1 G J_{uu}^{-1/2})^2} \tag{2.5}$$

where S_1 is the matrix of scalings for c_i:

$$S_1 = diag\{\frac{1}{span(c_i)}\} \tag{2.6}$$

where $span(c_i) = \Delta c_{i,opt}(d) + n_i$ ($\Delta c_{i,opt}(d)$ is the variation of c_i due to variation in disturbances and n_i is the implementation error of c_i).

It may be cumbersome to obtain the matrix J_{uu}, and if we assume that each "base variable" u has been scaled such that a unit change in each input has the same effect on the cost function J (such that the Hessian J_{uu} is a scalar times unitary matrix, i.e. $J_{uu} = \alpha U$), then (2.5) becomes

$$L_{max} = \frac{\alpha}{2}\frac{1}{\underline{\sigma}(S_1 G)^2} \tag{2.7}$$

where $\alpha = \underline{\sigma}(J_{uu})$.

Thus, to minimize the loss L we should maximize $\underline{\sigma}(S_1 G J_{uu}^{-1/2})$ or alternatively maximize $\underline{\sigma}(S_1 G)$; the latter is the original minimum singular value rule of Skogestad (2000).

2.1.4 Step 4. Production rate manipulator

The decision on where to place the production rate manipulator is closely related to where in the process there are bottlenecks that limit the flow of mass and energy. In addition, the decision directly affects the way total inventory (liquid or gas) of individual units are controlled across the process, namely [(Buckley, 1964) and (Price *et al.*, 1994)] (see Figure 2.2):

- Using outflow downstream of the location where the production rate is set, and
- Using inflow upstream of this location.

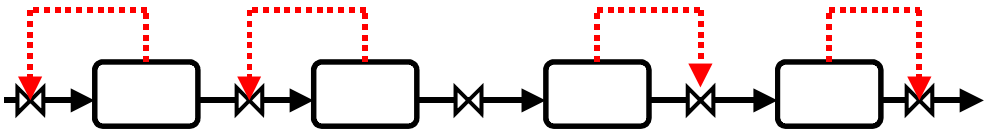

Figure 2.2: *General representation of inventory control (with production rate set inside the plant).*

We distinguish between 3 modes of operation:

- **Mode I: Given throughput**. This mode of operation occurs when (a) the feed rate is given (or limited) or (b) the production rate is given (or limited, e.g. by market conditions). The operational goal is then to minimize utility (energy) consumption, that is, to maximize efficiency.
- **Mode II: Throughput as a degree of freedom**. We here have two cases:
  - **Mode IIa: Maximum throughput**. This mode encompasses feasibility issues and the maximum throughput does not depend on cost data. It occurs when the product prices are sufficiently high and feed is available.
  - **Mode IIb: "Optimized" throughput**. In some cases, it is not optimal economically to maximize throughput, even if feed is available. This happens if the profit reaches a maximum, for example, because purge streams increase sharply at high feed rates.

The production rate is commonly assumed to be set at the inlet to the plant, with outflows used for level control. This is reasonable for Mode I with given feed rate. However, during operation the feed rate is usually a degree of freedom and very often the economic conditions are such that it is optimal to maximize production (Mode II). As feed rate is increased, one eventually reaches a constraint (a bottleneck) where further increase is not feasible (Mode IIa) or economically optimal (Mode IIb). For Mode IIa, in order to maximize production, we must have maximum flow through the bottleneck unit at all times. This gives the following rule for Mode IIa: *Determine the main bottleneck in the plant by identifying the maximum achievable feed rate for various disturbances. To maximize the flow through the bottleneck, the production rate should preferably be set at this location.* To avoid reconfiguration, the same production rate manipulator should be used also in Mode I. As for Mode IIb, there is no bottleneck in the process and one has to operate the process in vicinity of the maximum profit.

2.1.5 Step 5. Regulatory control layer

We here define the regulatory control system as the layer in the control hierarchy which has operation as its main purpose, and which normally contains the control loops that must be in service in order for the supervisory layer (it may be the operators) to be able to operate the plant in an efficient manner. The main objective of this layer is generally to facilitate smooth operation and not to optimize objectives related to profit, which is done at higher layers. Usually, this is a decentralized control system which keeps a subset of measurements y_2 at given set points. The regulatory control layer is usually itself hierarchical, consisting of cascaded loops where the values of the set points of the variables y_2 are determined by the upper layers in the control hierarchy. If there are unstable modes (RHP-poles) then these are usually stabilized first. This layer should also avoid "drift" so the system stays within its linear region which allows the use of linear controllers (Skogestad and Postlethwaite, 2005). In addition, this layer should allow for "fast" control, such that acceptable control is achieved using "slow" control in the layer above. A major structural issue in the design of the regulatory control layer is the selection of controlled variables y_2 and manipulations u_2. Typically, the variables y_2 to be controlled in this layer are levels, flows, pressures, and selected temperatures. A fundamental issue is whether the introduction of a separate regulatory control layer imposes an inherent performance loss in terms of controllability of upper layers.

The subject of regulatory control structure design has called the attention of several researches, for example, Buckley (1964), Hicks *et al.* (1966), Lee and Weekman (1976), Arkun and Stephanopoulos (1980), Shinnar (1981), Hovd and Skogestad (1993), Ponton and Laing (1993), Price and Georgakis (1993), Price *et al.* (1994), Narraway and Perkins (1994), Morari and Perkins (1995), Luyben *et al.* (1998), Stephanopoulos and Ng (2000), Heath *et al.* (2000), and Wang and McAvoy (2001). However, they are either based on heuristics or very complex for practical implementation. Moreover, no systematic rules have been reported to date.

Objectives of the regulatory control layer

The regulatory control layer should usually be of "low complexity". Usually, it consists of single-input/single-output (SISO) PI control loops. The main objective is to "stabilize" the plant. "Stabilize" here means the stabilization of both modes which are mathematically unstable as well as slow modes ("drift") that need to be "stabilized" from an operator point of view. The controlled variables for stabilization are measured output variables y_2, and their set points $y_{2,sp}$ may be used as degrees of freedom by the layers above. More generally, the objective of the regulatory control layer is to locally control secondary measurements (y_2), so that the effect of disturbances on the primary outputs (y_1) can be handled by the layer above (or the operators). In the regulatory control layer, we generally avoid using manipulated variables that may saturate, because otherwise control is lost and reconfiguration of loops is required.

Besides the more general objective, the regulatory control system should also fulfill the following more specific objectives:

O1. It should provide a sufficient quality of control to enable a trained operator to keep the plant running safely without use of the higher levels in the control system. This sharply reduces the need for providing costly backup systems for the higher levels of the control hierarchy in case of failures.

O2. It should be simple to understand and tune. Thus, in most cases simple decentralized control loops are used at this level. There are of course cases for which interactions are so strong that multivariable control may be needed at this level. However, very simple schemes are then preferred to compensate for interactions, such as ratios, sums, and so on.

O3. It should make it possible to use simple (at least in terms of dynamics) models at the higher level. We want to use relatively simple models because of reliability and the prohibitive costs involved in obtaining and maintaining a detailed dynamic model of the plant, and because complex dynamics will add to the computational burden on the higher level control system. This may be achieved by having a regulatory control level at the bottom of the control hierarchy. This may also reduce the effect of model uncertainty and provide for local linearization, for example, by using a cascade on a valve to avoid the nonlinear valve characteristics.

O4. It should make it possible to use longer sampling intervals at the higher levels of the control hierarchy. This will reduce the need for computing power at the higher levels. Preferably, the time scales of the lower-level and higher-level control system should be separated such that response of the lower-level control system, as seen from the higher level, is almost immediate.

O5. It should provide for fast control when this is needed for some variables.

O6. It must be able to follow the set points set by the higher levels in the control hierarchy. The set points of the lower loops are often the manipulated variables for the higher levels in the control hierarchy, and we want to be able to change these variables as directly and with as little interaction as possible. Otherwise, the higher level will need a model of the dynamics and interactions of the lower level control system.

O7. It should provide for local disturbance rejection. This follows from the previous objective, since we want to be able to keep the controlled variables in the regulatory control system at their set points. As disturbances we must also include the unused manipulated variables (additional degrees of freedom) which are adjusted directly by the higher levels of the control system.

O8. It should be designed such that the remaining control problem does not contain unnecessary performance limitations such as RHP-zeros, large RGA-elements, or strong sensitivity to disturbances. The "remaining control problem" is the control problem as seen from the higher level which has as manipulated inputs the "unused" manipulated inputs and the set points to the lower-level control

system. By "unnecessary" is mean limitations that do not exist in the original problem formulation without the lower-level control system in place.

O9. It must stabilize the plant (in the mathematical sense of shifting RHP-poles to the LHP).

O10. It should avoid "drift" so that the system stays within its "linear region" which allows the use of linear controllers.

Objectives O6, O9, and O10 justify the preferred choice of feedback control in the regulatory control layer. Namely, unstable plants can only be stabilized by feedback (Skogestad and Postlethwaite, 2005, pp. 145). In addition, for nonlinear plants, feedback control provides a linearizing effect on the behaviour of the system. Actually, there are two different linearizing effects:

a. A "local" linearizing effect in terms of the validity model: By use of feedback we can control the output y about an operating point and prevent the system from drifting too far away from its desired state. In this way, the system remains in the "linear region" where the linear models $G(s)$ and $G_d(s)$ are valid. This local linearizing effect justifies the use of linear models in feedback controller design and analysis, as used by most practicing control engineers.

b. A "global" linearizing effect in terms of the tracking response from the reference r to the output y: The use of high-gain feedback yields $y \approx r-n$. This holds also for cases where nonlinear effects cause the linear model $G(s)$ to change significantly as we change r. Thus, even though the underlying system is strongly nonlinear (and uncertain) the inputoutput response from r to y is approximately linear (and certain) with a constant gain of 1.

Selection of regulatory control structure

The structural issues that lead to a systematic procedure for the design of the regulatory control structure and that fulfill the objectives listed in the previous Section, are the selection of secondary measurements y_2 and manipulations u_2, and pairing of these.

It is useful to divide the measurements y into two classes as seen from the regulatory control layer:

- y_1: uncontrolled outputs (for which there is an associated control objective). These are the primary variables in upper layers.

- y_2: measured and controlled outputs (with reference value r_2) used in the regulatory control layer.

We also subdivide the available manipulated inputs u in a similar manner:

- u_1: unused inputs (this set may be empty). This set comprises the manipulated variables used in the upper layer in the hierarchy.

- u_2: used inputs for control of y_2 in the regulatory control layer. We usually have a square plant with $n_{u2} = n_{y2}$.

Essentially, you can think of y_1 as the variables we would really like to control and y_2 as the variables we control locally to make control of y_1 easier, meaning the regulatory control layer should assist in achieving the overall operational goals.

There are basically two cases to be considered:

C1. **Cascade and indirect control**. The variables y_2 are controlled solely to assist in achieving good control of y_1. In this case r_2 is available as manipulated variables of the layer above for the control of y_1.

C2. **Decentralized control (using sequential design)**. The variables y_2 are important in themselves. In this case, their reference values r_2 are usually not available for the control of y_1, but rather act as disturbances to the control of y_1.

Case C1 is the most common practice in most chemical plants and we assume from this point on that r_2 is always available for control of y_1.

Simple rules for selecting regulatory controlled variables and pairing decision

Selection of measurements y_2:

R1. y_2 should be easy to measure.

R2. Avoid "unreliable" measurements because the regulatory control layer should not fail.

R3. y_2 should have good controllability, that is favorable dynamics for control: Avoid variables y_2 with large (effective) delay.

R4. y_2 should be located "close" to the manipulated variable u_2 (as a consequence of Rule R3, because for good controllability we want a small effective delay).

R5. The (scaled) gain from u_2 to y_2 should be large.

Note: Rules R2 and R3 normally exclude compositions as secondary controlled variables y_2.

Selection of input u_2 (to be paired with y_2):

R6. Select u_2 so that controllability for y_2 is good, that is u_2 has a "large" and "direct" effect on y_2. Here "large" means that the gain is large, and "direct" means good dynamics with no inverse response and a small effective delay.

R7. Avoid using variables u_2 that may "saturate".

R8. Avoid variables u_2 where (frequent) changes are undesirable, for example, because they disturb other parts of the process or they can wear out the equipment they are related to (compressors or large control valves).

By "saturate" in Rule R7, we mean that the desired value of the input u_2 exceeds a physical constraint; for example, on its magnitude or rate. When an input saturates, we have effectively lost control, and reconfiguration may be required. Preferably, we would like to minimize the need for reconfiguration and its associated logic in the regulatory control layer, and rather leave such tasks for the upper layers in the control hierarchy.

The pairing issue arises because we aim at using decentralized SISO control, if at all possible. In many cases, it is "clear" from physical considerations and experience what the pairings can be. However, we have put the word "clear" in quotes, because it may sometimes be useful to question the conventional control wisdom. We will below discuss on "partial control", which is a useful tool to be used for a more exact analysis of the effects of various choices for y_2 and u_2.

Distillation column control provides a good example of the importance of selecting appropriate inputs. In this case, the level control constitutes the regulatory control system, and it is well known that closing the level loops with the "LV configuration" (corresponding to having reflux L and boilup V as the remaining unused inputs for composition control) may turn the remaining composition control problem difficult because of serious interactions (resulting in large RGA values. See Skogestad *et al.* (1990)). Note that the lower-level control system for the LV-configuration meets essentially all of the regulatory control objectives previously mentioned, with the exception of avoiding performance limitations in the remaining problem.

2.1.6 Step 6. Supervisory control layer

The purpose of the supervisor control layer is to keep the (primary) controlled outputs y_1 at their optimal set points y_{1s}, using as degrees of freedom the set points $y'_{1,sp}/y_{2,sp}$ in the composition control/regulatory layer and any unused manipulated inputs. The variables to control at this layer can be determined by the self-optimizing control technique. The main issue about this layer is to decide on whether to use a decentralized or a multivariable control configuration, e.g. MPC. For the purpose of this thesis, we assume the discussion around the decentralized configuration alternative only. Decentralized single-loop configuration is the simplest and it is preferred for non-interacting process and cases where active constraints remain constant. Advantages with decentralized control are:

+ Tuning may be done on-line;

+ None or minimal model requirements;

+ Easy to fix and change.

On the other hand, the disadvantages are:

- Need to determine pairing;
- Performance loss compared to multivariable control;
- Complicated logic required for reconfiguration when active constraints move.

The decision on how to pair inputs ($y_{2,sp}$ and u_1) and outputs c is often done based on process insight. In more difficult cases a RGA-analysis may be useful, and the rule is pair such that the resulting transfer matrix is close to identity matrix at the crossover expected frequency, provided the element is not negative at steady-state. For a more detailed analysis one should also consider disturbances and compute the closed-loop disturbance gain (CLDG) (Skogestad and Postlethwaite, 2005).

2.1.7 Step 7. Optimization layer

The purpose of the optimization is to identify the active constraints and recompute optimal set points c_s for controlled variables. The main structural issue is to decide if it is necessary to use real-time optimization (RTO). Real-time optimization is costly in the sense that it requires a detailed steady-state model to be maintained and continuously updated. If the active constraints do not change and we are able to find good self-optimizing controlled variables, then RTO gives little benefit and should not be used. In this thesis, we do not use this strategy and the optimization layer is then not designed.

2.1.8 Step 8. Validation

Finally, after having determined the preliminary plantwide control structure, it may be necessary to validate the structure, for example, using nonlinear dynamic simulation of the plant. We use Aspen Dynamics^{TM} extensively for this purpose.

2.2 Further considerations

In this thesis, we essentially apply the procedure just described to two large-scale processes in order to credit its efficiency and hope to open the doors for its application to real-world chemical plants.

Chapter 3

Application of Plantwide Control to the HDA Process. I - Steady-State Optimization and Self-Optimizing Control

Based on the paper accepted for publication in Control Engineering Practice

This chapter describes the application of self-optimizing control to a large-scale process, the HDA plant. The idea is to select controlled variables which when kept constant lead to minimum economic loss relative to the maximum attainable benefit. First, the optimal active constraints need to be controlled. Next, controlled variables need to be found for the remaining unconstrained degrees of freedom. In order to avoid the combinatorial problem related to the selection of outputs/measurements for such large plants, a local (linear) analysis based on singular value decomposition (SVD) is used for prescreening. This is followed by a more detailed analysis using the nonlinear model. Note that a steady-state model, in this case one built in Aspen Plus^{TM}, is sufficient for selecting controlled variables. A dynamic model is required to design and test the complete control system which include regulatory control. This is considered in the next chapter.

3.1 Synopsis

This chapter deals with the selection of controlled variables for the HDA process. One objective is to avoid the combinatorial control structure issue for such large-scale processes by using local methods based on the singular value decomposition of the linearized model of the process.

We base the selection of controlled variables on steady-state economics and use the ideas of self-optimizing control to find the best set(s). Self-optimizing control is when an acceptable (economic) loss can be achieved using constant set points for the controlled

variables, without the need to reoptimize when disturbances occur (Skogestad, 2000). The constant set point policy is simple but will not be optimal (and thus have a positive loss) as a result of the following two factors: (1) disturbances, i.e., changes in (independent) variables and parameters that cause the optimal set points to change, and (2) implementation errors, i.e., differences between the setpoints and the actual values of the controlled variables (e.g., because of measurement errors or poor control). The effect of these factors (or more specifically the loss) depends on the choice of controlled variables, and the objective is to find a set of controlled variables for which the loss is acceptable.

The HDA process (Figure 3.1) was first presented in a contest which the American Institute of Chemical Engineers arranged to find better solutions to typical design problems (McKetta, 1977). It has been exhaustively studied by several authors with different objectives, such as steady-state design, controllability and operability of the dynamic model and control structure selection and controller design.

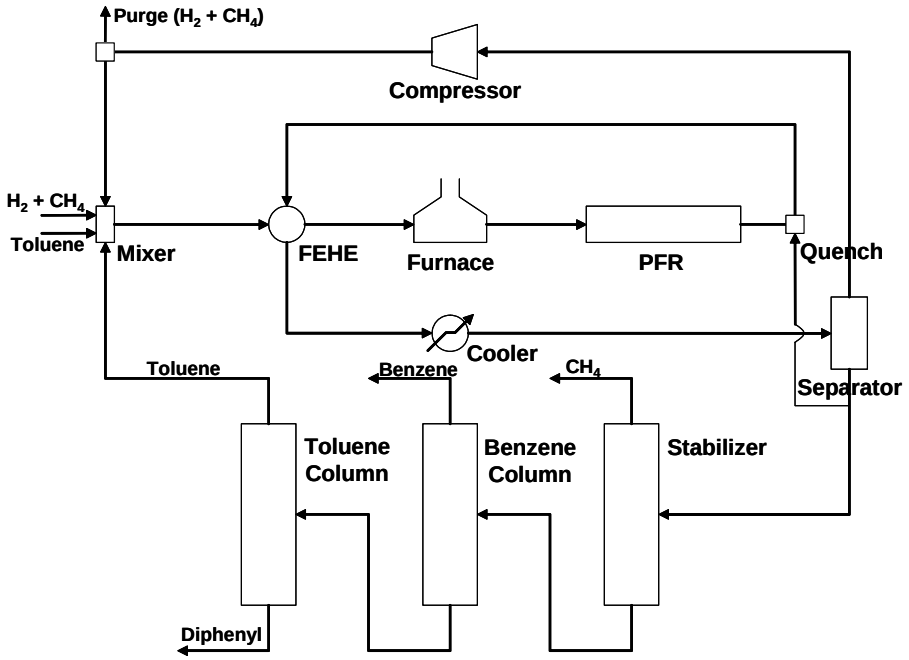

Figure 3.1: *HDA process flowsheet.*

This chapter is organized as follows: Section 3.2 examines previous proposed control structures for the HDA process. Section 3.3 shortly introduces the self-optimizing control technique. Section 3.4 describes the HDA process and the features of the model used in the present chapter. Section 3.5 summarizes the results found by applying the self-optimizing control procedure and the SVD analysis to the selection of controlled variables for the HDA process. A discussion of the results is found in Section 3.6 followed by a conclusion in Section 3.7.

3.2 Previous work on the HDA process

Stephanopoulos (1984) followed the approach proposed by Buckley (1964) based on material balance and product quality control. He used an HDA plant model where steam is generated from the effluent of the feed effluent heat exchanger through a series of steam coolers. From the material balance viewpoint, the selected controlled variables of choice were fresh toluene feed flow rate (production rate control), recycle gas flow rate, hydrogen contents in the recycle gas, purge flow rate, and quencher flow rate. Product quality is controlled through product compositions in the distillation columns and the controlled variables selected are product purity in benzene column and reactor inlet temperature.

Later, Douglas (1988) used another version of the HDA process to demonstrate a steady-state procedure for flowsheet design.

Brognaux (1992) implemented both a steady-state and dynamic model of the HDA plant in Speedup^{TM} based on the model developed by Douglas (1988) and used it as an example to compute operability measurements, define control objectives, and perform controllability analysis. He found that it is optimal to control the active constraints found by optimization.

Wolff (1994) used an HDA model based on Brognaux (1992)) to illustrate a procedure for operability analysis. He concluded that the HDA process is controllable provided the instability of the heat-integrated reactor is resolved. After some additional heuristic consideration, the controlled variables were selected to be the same as used by Brognaux (1992).

Ng and Stephanopoulos (1996) used the HDA process to illustrate how plantwide control systems can be synthesized based on a hierarchical framework. The selection of controlled variables is performed somehow heuristically by prioritizing the implementation of the control objectives. In other words, it is necessary to control the material balances of hydrogen, methane and toluene, the energy balance is controlled by the amount of energy added to the process (as fuel in the furnace, cooling water, and steam), production rate, and product purity.

Cao *et al.* used the HDA process as a case study in several papers, but mainly to study input selection, whereas the focus of our work is on output selection. In Cao and Biss (1996), Cao and Rossiter (1997), Cao *et al.* (1997*a*), and Cao and Rossiter (1998) issues involving input selection are discussed. Cao *et al.* (1997*b*) considered input and output selection for control structure design purposes using the singular value decomposition (SVD). Cao *et al.* (1998*a*) applied a branch and bound algorithm based on local (linear) analysis. All the papers by Cao *et al.* utilize the same controlled variables selected heuristically by Wolff (1994). Cao *et al.* (1998*b*) discuss the importance of modelling in order to achieve the most effective control structure and improves the HDA process model for such purpose.

Ponton and Laing (1993) presented a unified heuristic hierarchical approach to process and control system design based on the ideas of Douglas (1988) and used the HDA process throughout. The controlled variables selected at each stage are: Toluene flow rate, hydrogen concentration in the reactor, and methane contents in

the compressor inlet (feed and product rate control stage); separator liquid stream outlet temperature and toluene contents at the bottom of the toluene column (recycle structure, rates and compositions stage); and separator separator pressure, benzene contents at stabilizer overhead, and toluene contents at benzene column overhead are related to product and intermediate stream composition stage. The stages related to energy integration and inventory regulation do not cover the HDA process directly, so no controlled variables are assigned at these stages.

Luyben *et al.* (1998) applied a heuristic nine-step procedure together with dynamic simulations to the HDA process and concluded that control performance is worse when the steady-state economic optimal design is used. They chose to control the inventory of all components in the process (hydrogen, methane, benzene, toluene, and diphenyl) to ensure that the component material balance are satisfied; the temperatures around the reactor are controlled to ensure exothermic heat removal from the process; total toluene flow or reactor inlet temperature (it is not exactly clear which one was selected) can be used to set production rate and product purity by the benzene contents in the benzene column distillate. Luyben (2002) uses the rigorous commercial flowsheet simulators Hysys^{TM}, Aspen Plus^{TM} and Aspen Dyanmics^{TM} to propose a heuristic-based control structure for the HDA process.

Herrmann *et al.* (2003) consider the HDA process to be an important test-bed problem for design of new control structures due to its high integration and non-minimum phase behavior. They re-implemented Brognaux (1992)'s model in Aspen Custom Modeler^{TM} and design a model-based, multivariable H_∞ controller for the process. They considered the same controlled variables used by Wolff (1994).

Konda *et al.* (2005*b*) used an integrated framework of simulation and heuristics and proposed a control structure for the HDA process. A Hysys^{TM} model of the plant was built to assist the simulations. They selected fresh toluene feed flow rate to set production rate, product purity at benzene column distillate to fulfill the product specification, overall toluene conversion in the reactor to regulate the toluene recycle loop, ratio of hydrogen to aromatics and quencher outlet temperature to fulfill process constraint, and methane contents in the purge stream to avoid its accumulation in the process.

Table 3.1 summarizes the selection of (steady-state) controlled variables by various authors. It seems clear that the systematic selection of controlled variable for this plant has not been fully investigated although the process has been extensively considered by several authors. In this work, a set(s) of controlled variables for the HDA process is to be systematically selected.

3.3 Selection controlled variables by self-optimizing control

We here consider selection of primary controlled variables. The objective is to achieve self-optimizing control where fixing the primary controlled variables c at constant set-points c_s indirectly leads to near-optimal operation (see Figure 3.2).

Table 3.1: *Steady-state controlled variables selected by various authors.*

		Stephanopoulos (1984)	Brognaux (1992), Wolff (1994), Cao et al., and Herrmann *et al.* (2003)	Ng and Stephanopoulos (1996)	Ponton and Laing (1993)	Luyben et al. (1998) and Luyben (2002)	Konda *et al.* (2005)	This work
	Number of steady-state (economic) controlled variables[1]	**8**	**7**	**6**	**8**	**8**	**9**	**13**
Y20[2]	Fresh toluene feed rate **(active constraint)**[3]	x			x		x	x
Y71	Recycle gas flow rate	x						
Y48	Recycle gas hydrogen mole fraction	x						
Y49	Recycle gas methane mole fraction			x	x	x	x	
Y62	Reactor inlet pressure **(active constraint)**							x
Y68	Compressor power	x	x	x	x	x	x	
Y72	Total toluene flow rate to the reaction section					x		
Y28	Mixer outlet methane mole fraction							x
Y5	Reactor inlet temperature	x	x			x		
Y19	Separator temperature **(active constraint)**		x		x		x	x
Y64	Separator pressure		x	x	x		x	
Y70	Hydrogen to aromatics ratio at the reactor inlet **(active constraint)**		x				x	x
Y73	Hydrogen mole fraction in the reactor outlet				x			
Y69	Overall toluene conversion in the reactor						x	
Y27	Quencher flow rate	x						
Y16	Quencher outlet temperature **(active constraint)**					x	x	x
Y26	Purge flow rate	x						
Y46	Separator liquid toluene mole fraction							x
Y74	Hydrogen mole fraction in stabilizer distillate			x				
Y53	Benzene mole fraction in stabilizer distillate				x			x
Y54	Methane mole fraction in stabilizer bottoms							x
Y55	Benzene product purity **(active constraint)**	x	x	x		x	x	x
Y56	Benzene mole fraction in benzene column bottoms							x
Y75	Production rate (benzene column distillate flow rate)		x					
Y76	Temperature in an intermediate stage of the benzene column					x		
Y77	Temperature in an intermediate stage of the toluene column					x		
Y78	Toluene mole fraction in toluene column distillate			x				x
Y58	Toluene mole fraction in toluene column bottoms				x			
Y57	Diphenyl mole fraction in toluene column distillate							x

[1] The total number of steady-state degrees of freedom is 13, so there are additional controlled variables, or fixed inputs, which are not clearly specified by some authors.

[2] Y-variables refer to candidates in Table 3.4.

[3] Active constraints found in this work.

More precisely (Skogestad, 2004*a*):

Self-optimizing control is when one can achieve an acceptable loss with constant setpoint values for the controlled variables without the need to re-optimize when disturbances occur.

For continuous processes with infrequent grade changes, like the HDA process, a steady-state analysis is usually sufficient because the economics can be assumed to be determined by the steady-state operation.

We assume that the optimal operation of the system can be quantified in terms of a scalar cost function (performance index) J_0, which is to be minimized with respect to the available degrees of freedom u_0

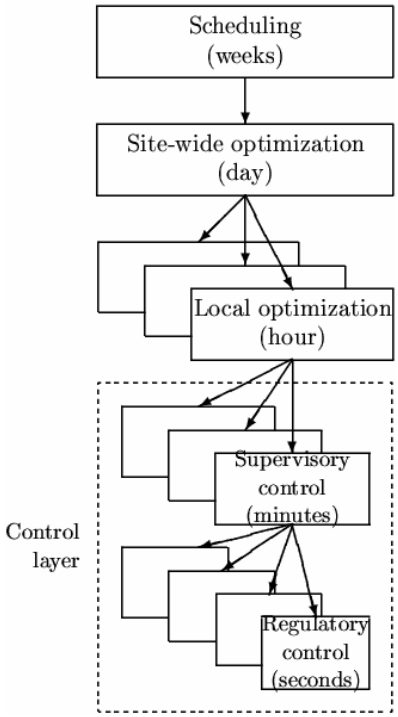

Figure 3.2: *Typical control hierarchy in a chemical plant.*

$$\min_{u_0} J_0(x, u_0, d) \tag{3.1}$$

subject to the constraints

$$g_1(x, u_0, d) = 0;\ g_2(x, u_0, d) \leq 0 \tag{3.2}$$

Here d represents all of the disturbances, including exogenous changes that affect the system (e.g., a change in the feed), changes in the model (typically represented by changes in the function g_1), changes in the specifications (constraints), and changes in the parameters (prices) that enter in the cost function and the constraints. x represents the internal variables (states). One way to approach this problem is to evaluate the cost function for the expected set of disturbances and implementation errors. The main steps of this procedure are as follows (Skogestad, 2000):

1. Degree of freedom analysis.
2. Definition of optimal operation (cost and constraints).
3. Identification of important disturbances (typically, feed flow rates, active constraints and input error).
4. Optimization.

5. Identification of candidate controlled variables c.

6. Evaluation of loss for alternative combinations of controlled variables (loss imposed by keeping constant set points when there are disturbances or implementation errors), including feasibility investigation.

7. Final evaluation and selection (including controllability analysis).

To achieve optimal operation, we first choose to control the active constraints. The difficult issue is to decide which unconstrained variables c to control.

Unconstrained problem: We divide the original independent variables $u_0 = u', u$ in the "constrained" variables u' (used to satisfy the active constraints $g_2' = 0$) and the remaining unconstrained variables u. The value of u' is then a function of the remaining independent variables (u and d). Similarly, the states x are determined by the value of the remaining independent variables. Thus, by solving the model equations ($g_1 = 0$), and for the active constraints ($g_2' = 0$), we may formally write $x = x(u, d)$ and $u' = u'(u, d)$ and we may formally write the cost as a function of u and d: $J = J_0(x, u_0, d) = J_0[x(u, d), u'(u, d), u, d] = J(u, d)$. The remaining unconstrained problem in reduced space then becomes

$$\min_u J(u, d) \tag{3.3}$$

where u represents the set of remaining unconstrained degrees of freedom. This unconstrained problem is the basis for the local method introduced below.

3.3.1 Degrees of freedom analysis

It is paramount to determine the number of steady-state degrees of freedom because this determines the number of steady-state controlled variables that we need to choose. To find them for complex plants, it is useful to sum the number of degrees for individual units as given in Table 3.2 (Skogestad, 2002).

3.3.2 Local (linear) method

In terms of the unconstrained variables, we can expand locally the loss function around the optimum:

$$L = J(u, d) - J_{opt}(d) = \frac{1}{2} \|z\|_2^2 \tag{3.4}$$

with $z = J_{uu}^{1/2}(u - u_{opt}) = J_{uu}^{1/2} G^{-1}(c - c_{opt})$, where G is the steady-state gain matrix from the unconstrained degrees of freedom u to the controlled variables c (yet to be selected) and J_{uu} the Hessian of the cost function with respect to the u. Truly optimal operation corresponds to $L = 0$, but in general $L > 0$. A small value of the loss function L is desired as it implies that the plant is operating close to its optimum. The main issue here is not to find the optimal set points, but rather to find the right variables to keep constant.

Table 3.2: *Typical number of steady-state degrees of freedom for some process units.*

Process unit	DOF
Each external feed stream	1 (feedrate)
Splitter	$n-1$ split fractions (n is the number of exit streams)
Mixer	0
Compressor, turbine, and pump	1 (work)
Adiabatic flash tank	0*
Liquid phase reactor	1 (holdup)
Gas phase reactor	0*
Heat exchanger	1 (duty or net area)
Columns (e.g. distillation) excluding heat exchangers	0* + number of side streams

* Add 1 degree of freedom for each extra pressure that is set (need an extra valve, compressor, or pump), e.g. in flash tank, gas phase reactor, or column.

Assuming that each controlled variable c_i is scaled such that $||e'_c|| = ||c' - c'_{opt}||_2 \leq 1$, the worst case loss is given by (Halvorsen *et al.*, 2003):

$$L_{max} = \max_{||e_c||_2 \leq 1} L = \frac{1}{2} \frac{1}{\underline{\sigma}(S_1 G J_{uu}^{-1/2})^2} \tag{3.5}$$

where S_1 is the matrix of scalings for c_i:

$$S_1 = diag\{\frac{1}{span(c_i)}\} \tag{3.6}$$

where $span(c_i) = \Delta c_{i,opt}(d) + n_i$ ($\Delta c_{i,opt}(d)$ is the variation of c_i due to variation in disturbances and n_i is the implementation error of c_i)

It may be cumbersome to obtain the matrix J_{uu}, and if we assume that each "base variable" u has been scaled such that a unit change in each input has the same effect on the cost function J (such that the Hessian J_{uu} is a scalar times unitary matrix, i.e. $J_{uu} = \alpha U$), then (3.5) becomes

$$L_{max} = \frac{\alpha}{2} \frac{1}{\underline{\sigma}(S_1 G)^2} \tag{3.7}$$

where $\alpha = \underline{\sigma}(J_{uu})$.

Thus, to minimize the loss L we should maximize $\underline{\sigma}(S_1 G J_{uu}^{-1/2})$ or alternatively maximize $\underline{\sigma}(S_1 G)$; the latter is the original minimum singular value rule of Skogestad (2000).

Originally, a MatLab^{TM} model was used to obtain the optimal variation $\Delta c_{opt}(d)$, the steady-state gain matrix G and the Hessian J_{uu}, but in the present version Aspen Plus^{TM} is used instead (see the Appendix for details). The use of a commercial

flowsheet simulator like Aspen Plus^{TM} demonstrates the practical usefulness of the approach.

3.4 HDA process description

In the HDA process, fresh toluene (pure) and hydrogen (97% hydrogen and 3% methane) are mixed with recycled toluene and hydrogen (Figure 3.1). This reactant mixture is first preheated in a feed-effluent heat exchanger (FEHE) using the reactor effluent stream and then to the reaction temperature in a furnace before being fed to an adiabatic plug-flow reactor.

A main reaction and a side reaction take place in the reactor as follows:

$$Toluene + H_2 \rightarrow Benzene + Methane \tag{3.8}$$

$$2\ Benzene \rightleftharpoons Diphenyl + H_2 \tag{3.9}$$

The reactor effluent is quenched by a portion of the recycle separator liquid flow to prevent coking, and further cooled in the FEHE and cooler before being fed to the vapor-liquid separator. Part of the vapor containing unconverted hydrogen and methane is purged to avoid accumulation of methane within the process while the remainder is compressed and recycled to the process. The liquid from the separator is processed in the separation section consisting of three distillation columns. The stabilizer column removes small amounts of hydrogen and methane in the overhead product, and the benzene column takes of the benzene product in the overhead. Finally, in the toluene column, unreacted toluene is separated from diphenyl and recycled to the process.

3.4.1 Details of the HDA process model in Aspen Plus^{TM}

The model of the HDA process used in this chapter is a modified version of the model developed by Luyben (2002). A schematic flowsheet of the Aspen Plus^{TM} model is depicted in Figure 3.3 and the corresponding stream table is shown in Table 5.1.

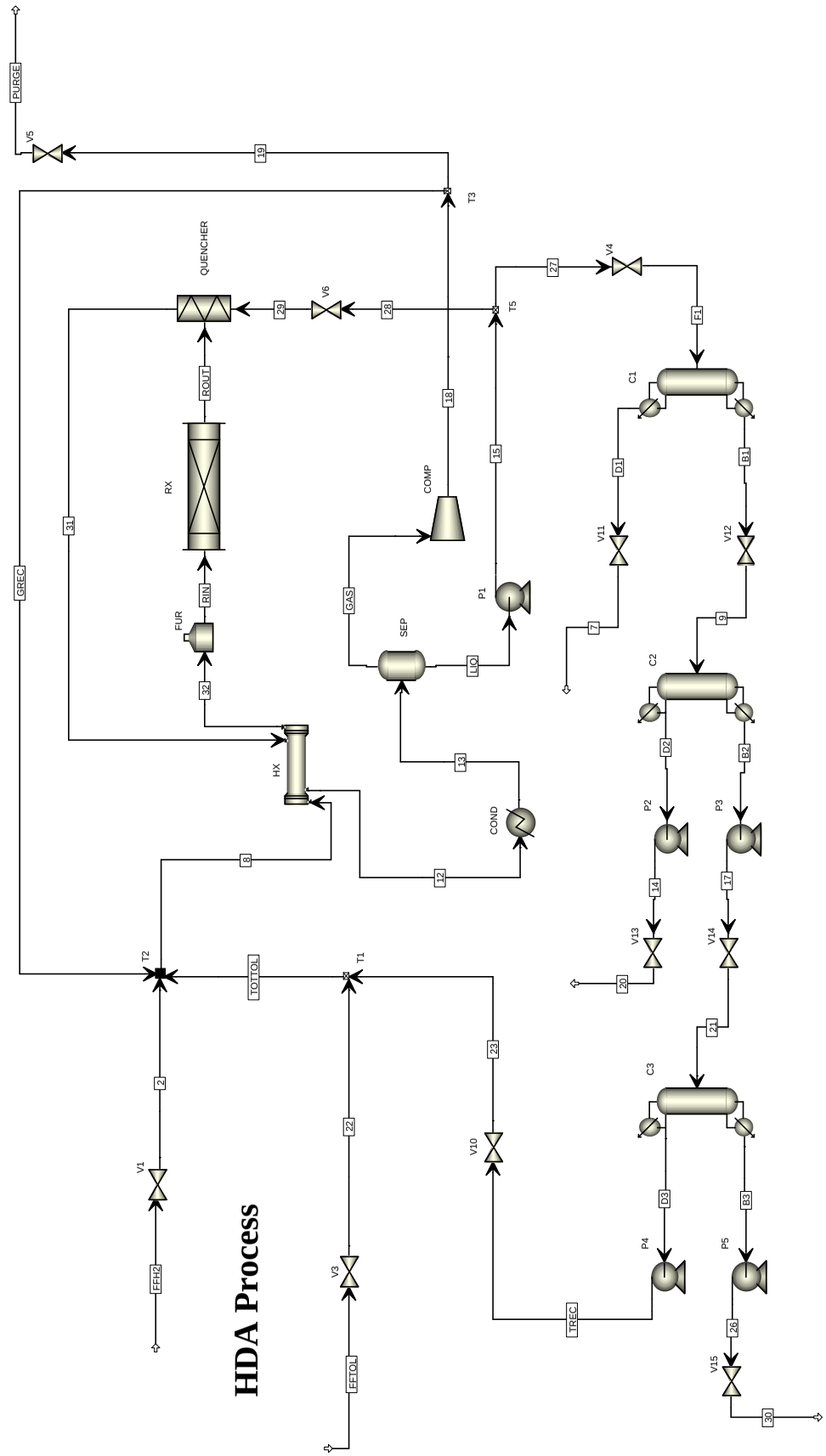

Figure 3.3: *HDA Aspen Plus^{TM} process flowsheet.*

Table 3.3: *Stream table for the nominally optimal operating point for the HDA process. See Figure 3.3 for the stream names.*

Stream	2	7	8	9	12	13	14	15	17	18	19	20	21	22	23	26	27	28	29	30
Mole Flow [lbmol/h]																				
Hydrogen	433.37	1.0841	1809.1	0	1519.4	1519.4	0	1.7618	0	1517.7	141.9	0	0	0	0	0	1.0841	0.6777	0.6777	0
Methane	13.403	14.438	2910.1	0	3219	3219	0	23.464	0	3195.5	298.78	0	0	0	0	0	14.438	9.0258	9.0258	0
Benzene	0	0.0016	45.023	276.36	498.76	498.76	276.33	449.13	0.0329	49.631	4.6405	276.33	0.0329	0	0.0329	0	276.36	172.77	172.77	0
Toluene	0	0	316.8	15.946	26.948	26.948	0.0831	25.914	15.862	1.0342	0.0967	0.0831	15.862	300	15.859	0.0038	15.946	9.9684	9.9684	0.0038
Diphenyl	0	0	0.0101	9.43	15.328	15.328	0	15.325	9.43	0.0031	0.0003	0	9.43	0	0.0073	9.4227	9.43	5.8951	5.8951	9.4227
Mole Fraction																				
Hydrogen	0.97	0.0698	0.3561	0	0.2878	0.2878	0	0.0034	0	0.3186	0.3186	0	0	0	0	0	0.0034	0.0034	0.0034	0
Methane	0.03	0.9301	0.5727	0	0.6097	0.6097	0	0.0455	0	0.6708	0.6708	0	0	0	0	0	0.0455	0.0455	0.0455	0
Benzene	0	1E-04	0.0089	0.9159	0.0945	0.0945	0.9997	0.8711	0.0013	0.0104	0.0104	0.9997	0.0013	0	0.0021	0	0.8711	0.8711	0.8711	0
Toluene	0	0	0.0623	0.0528	0.0051	0.0051	0.0003	0.0503	0.6263	0.0002	0.0002	0.0003	0.6263	1	0.9975	0.0004	0.0503	0.0503	0.0503	0.0004
Diphenyl	0	0	2E-06	0.0313	0.0029	0.0029	0	0.0297	0.3724	6E-07	6E-07	0	0.3724	0	0.0005	0.9996	0.0297	0.0297	0.0297	0.9996
Total Flow [lbmol/h]	446.77	15.524	5081.1	301.74	5279.5	5279.5	276.41	515.6	25.325	4763.9	445.42	276.41	25.325	300	15.899	9.4264	317.26	198.33	198.33	9.4264
Temperature [^{o}F]	100.11	-93.394	120.25	235.26	357.67	95	223.92	95.359	333	124.89	124.89	224.02	325.6	100.27	289.14	566.56	95.359	95.359	95.578	565.56
Pressure [psi]	555	50	530	31.714	477.4	477	80	530	84	555	555	50	30.75	555	555	82	530	530	487.4	32
Vapor Fraction	1	1	0.932	0.4557	1	0.9023	0	0	0	1	1	0	0.0337	0	0	0	0	0	0	0.005
Enthalpy [MBtu/h]	-0.3551	-0.4846	-88.217	9.8177	-68.617	-90.323	7.2579	10.044	0.8809	-99.2	-9.2752	7.2579	0.8809	1.8353	0.2276	0.7991	6.1802	3.8635	3.8635	0.7991

Stream	31	32	B1	B2	B3	D1	D2	D3	F1	FFH2	FFTOL	GAS	GREC	LIQ	PURGE	RIN	ROUT	TOTTOL	TREC
Mole Flow [lbmol/h]																			
Hydrogen	1519.4	1809.1	0	0	0	1.0841	0	0	1.0841	433.37	0	1517.7	1375.8	1.7618	141.9	1809.1	1518.8	0	0
Methane	3219	2910.1	0.0003	0	0	14.438	0	0	14.438	13.403	0	3195.5	2896.7	23.464	298.78	2910.1	3210	0	0
Benzene	498.76	45.023	276.36	0.0329	0	0.0016	276.33	0.0329	276.36	0	0	49.631	44.99	449.13	4.6405	45.023	325.99	0.0329	0.0329
Toluene	26.948	316.8	15.946	15.862	0.0038	0	0.0831	15.859	15.946	0	300	1.0342	0.9375	25.914	0.0967	316.8	16.98	315.86	15.859
Diphenyl	15.328	0.0101	9.43	9.43	9.4227	0	0	0.0073	9.43	0	0	0.0031	0.0028	15.325	0.0003	0.0101	9.4331	0.0073	0.0073
Mole Fraction																			
Hydrogen	0.2878	0.3561	0	0	0	0.0698	0	0	0.0034	0.97	0	0.3186	0.3186	0.0034	0.3186	0.3561	0.2989	0	0
Methane	0.6097	0.5727	1E-06	0	0	0.9301	0	0	0.0455	0.03	0	0.6708	0.6708	0.0455	0.6708	0.5727	0.6317	0	0
Benzene	0.0945	0.0089	0.9159	0.0013	0	1E-04	0.9997	0.0021	0.8711	0	0	0.0104	0.0104	0.8711	0.0104	0.0089	0.0642	0.0001	0.0021
Toluene	0.0051	0.0623	0.0528	0.6263	0.0004	0	0.0003	0.9975	0.0503	0	1	0.0002	0.0002	0.0503	0.0002	0.0623	0.0033	0.9999	0.9975
Diphenyl	0.0029	2E-06	0.0313	0.3724	0.9996	0	0	0.0005	0.0297	0	0	6E-07	6E-07	0.0297	6E-07	2E-06	0.0019	2E-05	0.0005
Total Flow [lbmol/h]	5279.5	5081.1	301.74	25.325	9.4264	15.524	276.41	15.899	317.26	446.77	300	4763.9	4318.5	515.6	445.42	5081.1	5081.1	315.9	15.899
Temperature [^{o}F]	1150	1004.8	371.4	332.65	565.54	-83.814	223.52	283.61	97.982	100	100	94.979	124.89	94.979	123.85	1201.2	1277.2	110.72	288.76
Pressure [psi]	487.4	510	154	34	32	150	30	30	160	605	605	476	555	476	505	500	496	555	675
Vapor Fraction	1	1	0	0	0	1	0	0	0.0293	1	0	1	1	0	1	1	1	0	0
Enthalpy [MBtu/h]	-7.2542	-26.854	9.8177	0.8801	0.7981	-0.4846	7.2521	0.2222	6.1802	-0.3551	1.8353	-100.36	-89.925	10.033	-9.2752	-11.118	-11.118	2.0629	0.2276

Details on this model can be found in Luyben (2002). The main difference between our model and Luyben's lies on the distillation train. As optimization of the entire plant is difficult for this problem, we decided to first optimize the distillation train separately (see Section 3.5.4). The distillation train may then be represented by simple material balances with given specifications. This was implemented in Aspen Plus^{TM} using an Excel^{TM} spreadsheet, and optimization of the remaining plant is then relatively simple.

3.5 Results

This section describes the self-optimizing control procedure applied to the HDA process model in Aspen Plus^{TM} starting with the degree of freedom analysis.

3.5.1 Step 1. Degree of freedom analysis

We consider 20 manipulated variables (Table 3.6), 70 candidate measurements (the first 70 in Table 3.4), and 12 disturbances (Table 6.3). The 20 manipulated variables correspond to 20 dynamic degrees of freedom. However, at steady state there are only 13 degrees of freedom because there are 7 liquid levels that need to be controlled which have no steady-state effect. This is confirmed by the alternative steady-state degree of freedom analysis in Table 3.5.

With 13 degrees of freedom and 70 candidate controlled variables, there are $\binom{70}{13} = \frac{70!}{13!57!} = 4.7466 \cdot 10^{13}$ (!) control structures, without including the alternative ways of controlling liquid levels. Clearly, an analysis of all of them is intractable. To avoid this combinatorial explosion, we first determine the active constraints which should be controlled to achieve optimal operation and next apply a local analysis to eliminate further sets.

3.5.2 Step 2. Definition of optimal operation

The following profit function $(-J)$ [M$/year] given by Douglas (1988)'s economic potential (EP) is to be maximized:

$$\begin{aligned}(-J) \quad = \quad & (p_{ben}D_{ben} + p_{fuel}Q_{fuel}) - (p_{tol}F_{tol} + p_{gas}F_{gas} + p_{fuel}Q_{fur} + \\ & p_{cw}Q_{cw} + p_{pow}W_{pow} + p_{stm}Q_{stm})\end{aligned} \tag{3.10}$$

subject to the constraints

1. Minimum production rate

$$D_{benzene} \geq 265\ lbmol/h \tag{3.11}$$

2. Hydrogen to aromatic ratio in reactor inlet (to prevent coking formation)

$$\frac{F_{H_2}}{(F_{benzene} + F_{toluene} + F_{diphenyl})} \geq 5 \tag{3.12}$$

Table 3.4: *Selected candidate controlled variables for the HDA process (excluding levels).*

Y1	Mixer outlet temperature	Y22	Mixer outlet flow rate
Y2	FEHE hot side outlet temperature	Y23	Quencher outlet flow rate
Y3	Furnace inlet temperature	Y24	Separator vapor outlet flow rate
Y4	Furnace outlet temperature	Y25	Separator liquid outlet flow rate
Y5	Reactor section 1 temperature	Y26	Purge flow rate
Y6	Reactor section 2 temperature	Y27	Flow of cooling stream to quencher
Y7	Reactor section 3 temperature	Y28	Mixer outlet hydrogen mole fraction
Y8	Reactor section 4 temperature	Y29	Mixer outlet methane mole fraction
Y9	Reactor section 5 temperature	Y30	Mixer outlet benzene mole fraction
Y10	Reactor section 6 temperature	Y31	Mixer outlet toluene mole fraction
Y11	Reactor section 7 temperature	Y32	Mixer outlet diphenyl mole fraction
Y12	Reactor section 8 temperature	Y33	Quencher outlet hydrogen mole fraction
Y13	Reactor section 9 temperature	Y34	Quencher outlet methane mole fraction
Y14	Reactor section 10 temperature	Y35	Quencher outlet benzene mole fraction
Y15	Reactor section 11 temperature	Y36	Quencher outlet toluene mole fraction
Y16	Quencher outlet temperature (active constraint)	Y37	Quencher outlet diphenyl mole fraction
Y17	Compressor inlet temperature	Y38	Separator overhead vapor hydrogen mole fraction
Y18	Compressor outlet temperature	Y39	Separator overhead vapor methane mole fraction
Y19	Separator temperature (active constraint)	Y40	Separator overhead vapor benzene mole fraction
Y20	Fresh toluene feed rate (active constraint)	Y41	Separator overhead vapor toluene mole fraction
Y21	Fresh gas feed flow rate	Y42	Separator overhead vapor diphenyl mole fraction

Table 3.4: *Selected candidate controlled variables for the HDA process (excluding levels) (cont').*

Y43	Separator liquid outlet hydrogen mole fraction	Y61	Furnace inlet pressure
Y44	Separator liquid outlet methane mole fraction	Y62	Reactor inlet pressure (active constraint)
Y45	Separator liquid outlet benzene mole fraction	Y63	Reactor outlet pressure
Y46	Separator liquid outlet toluene mole fraction	Y64	Separator pressure
Y47	Separator liquid outlet diphenyl mole fraction	Y65	Compressor outlet pressure
Y48	Gas recycle hydrogen mole fraction	Y66	Furnace heat duty
Y49	Gas recycle methane mole fraction	Y67	Cooler heat duty
Y50	Gas recycle benzene mole fraction	Y68	Compressor power
Y51	Gas recycle toluene mole fraction	Y69	Toluene conversion at reactor outlet
Y52	Gas recycle diphenyl mole fraction	Y70	Hydrogen to aromatic ratio in reactor inlet (active constraint)
Y53	Benzene mole fraction in stabilizer distillate (active constraint)	Y71	Recycle gas flow rate
Y54	Methane mole fraction in stabilizer bottoms (active constraint)	Y72	Total toluene flow rate to the reaction section
Y55	Benzene mole fraction in benzene column distillate (active constraint)	Y73	Hydrogen mole fraction in the reactor outlet
Y56	Benzene mole fraction in benzene column bottoms (active constraint)	Y74	Hydrogen mole fraction in stabilizer distillate
Y57	Diphenyl mole fraction in toluene column distillate (active constraint)	Y75	Production rate (benzene column distillate flow rate)
Y58	Toluene mole fraction in toluene column bottoms (active constraint)	Y76	Temperature in an intermediate stage of the benzene column
Y59	Mixer outlet pressure	Y77	Temperature in an intermediate stage of the toluene column
Y60	FEHE hot side outlet pressure	Y78	Toluene mole fraction in toluene column distillate

Table 3.5: *Steady-state degrees of freedom analysis based on Table 3.2.*

Process unit	DOF
External feed streams	$2 \cdot 1 = 2$
Splitters (purge and quench)	$2 \cdot 1 = 2$
Compressor	$1 \cdot 1 = 1$
Adiabatic flash$^{(*)}$ (quencher and separator)	$2 \cdot 0 = 0$
Gas phase reactor$^{(*)}$	$1 \cdot 0 = 0$
Heat exchangers in recycle section$^{(**)}$ (furnace and cooler)	$2 \cdot 1 = 2$
Heat exchangers in 3 distillation columns	$3 \cdot 2 = 6$
Total	13

$^{(*)}$ Assuming no adjustable valves for pressure control (assume fully open valve before separator).
$^{(**)}$ The FEHE (feed effluent heat exchanger) duty is not a degree of freedom because there is no adjustable bypass.

Table 3.6: *List of manipulable variables.*

	Manipulated variable	Status in this work
U1	Fresh toluene feed rate	Steady state
U2	Fresh gas feed rate	Steady state
U3	Furnace heat duty	Steady state
U4	Cooler heat duty	Steady state
U5	Compressor power	Steady state
U6	Purge flow rate	Steady state
U7	Flow of cooling stream to quencher	Steady state
U8	Liquid flow to stabilizer	Dynamic only (level control)
U9	Stabilizer reflux rate	Steady state
U10	Stabilizer distillate rate	Dynamic only (level control)
U11	Stabilizer reboiler duty	Steady state
U12	Stabilizer bottoms rate	Dynamic only (level control)
U13	Benzene column reflux rate	Steady state
U14	Benzene column distillate rate	Dynamic only (level control)
U15	Benzene column reboiler duty	Steady state
U16	Benzene column bottoms rate	Dynamic only (level control)
U17	Toluene column reflux rate	Steady state
U18	Toluene column distillate rate	Dynamic only (level control)
U19	Toluene column reboiler duty	Steady state
U20	Toluene column bottoms rate	Dynamic only (level control)

3. Maximum toluene feed rate

$$F_{toluene} \leq 300 lbmol/h \tag{3.13}$$

4. Reactor inlet pressure

$$P_{reactor,in} \leq 500\ psia \tag{3.14}$$

5. Reactor outlet temperature

$$T_{reactor,out} \leq 1300^o F \tag{3.15}$$

6. Quencher outlet temperature

$$T_{quencher,out} \leq 1150^o F \tag{3.16}$$

7. Product purity at the benzene column distillate

$$x_{D,benzene} \geq 0.9997 \tag{3.17}$$

8. Separator inlet temperature

$$95^o F \leq T_{separator,in} \leq 105^o F \tag{3.18}$$

9. Reactor inlet temperature (to get a high enough reaction rate)

$$T_{reactor,in} \geq 1150^o F \tag{3.19}$$

10. In addition, all flows and concentrations must be non-negative

It is assumed that all by-products (purge, stabilizer distillate, and toluene column bottom) are sold as fuel.

Here:

1. p_{ben}, p_{tol}, p_{gas}, p_{fuel}, p_{cw}, p_{pow}, and p_{stm} are the prices of benzene, fresh toluene feed, fresh gas feed, fuel to the furnace, cooling water, power to the compressor, and steam, respectively (see Table 3.7 for data);

2. D_{ben}, F_{tol}, F_{gas}, Q_{fur}, Q_{cw}, W_{pow}, and Q_{stm} are the flows of product benzene, fresh toluene feed, fresh gas (hydrogen) feed, energy fuel to the furnace, cooling water, power to the compressor, and steam, respectively;

3. $Q_{cw} = Q_{cw,cooler} + Q_{cw,stab} + Q_{cw,ben-col} + Q_{cw,tol-col}$;

4. $Q_{stm} = Q_{stm,stab} + Q_{stm,ben-col} + Q_{stm,tol-col}$;

5. Q_{fuel} is the fuel value of the by-product streams F_{purge} (flow through the purge), $D_{stab,i}$ (flow through the stabilizer distillate), and $B_{tol-col,i}$ (flow through the toluene column bottom);

6. 8150 hours of operation per year.

Table 3.7: *Economic data for the HDA process based on Douglas (1988).*

p_{ben}	9.04\$/lbmol
p_{tol}	6.04\$/lbmol
p_{gas}	1.32\$/lbmol
p_{fuel}	$4.00 \cdot 10^{-6}$\$/Btu
p_{cw}	$2.34 \cdot 10^{-8}$\$/Btu
p_{pow}	0.042\$/bhp
p_{stm}	$2.50 \cdot 10^{-6}$\$/Btu

3.5.3 Step 3. Identification of important disturbances

We consider the 12 disturbances listed in Table 6.3. They include changes in the feed and in the active constraints.

Table 3.8: *Disturbances to the process.*

		Nominal	Disturbance
D1	Fresh toluene feed rate [lbmol/h]	300	-15
D2	Fresh toluene feed rate [lbmol/h]	300	+15
D3	Fresh gas feed rate methane mole fraction	0.03	+0.05
D4	Hydrogen to aromatic ratio in reactor inlet	5.0	+0.5
D5	Reactor inlet pressure [psi]	500	+20
D6	Quencher outlet temperature [°F]	1150	+20
D7	Product purity in the benzene column distillate	0.9997	-0.0037
D8	Benzene mole fraction in stabilizer distillate	$1 \cdot 10^{-4}$	$+2 \cdot 10^{-4}$
D9	Methane mole fraction in stabilizer bottoms	$1 \cdot 10^{-6}$	$+4 \cdot 10^{-6}$
D10	Benzene mole fraction in benzene column bottoms	$1.3 \cdot 10^{-3}$	$+0.7 \cdot 10^{-3}$
D11	Diphenyl mole fraction in toluene column distillate	$0.5 \cdot 10^{-3}$	$+0.5 \cdot 10^{-3}$
D12	Toluene mole fraction in toluene column bottoms	$0.4 \cdot 10^{-3}$	$+0.6 \cdot 10^{-3}$

3.5.4 Step 4. Optimization

Optimization of the distillation columns

The six steady-state degrees of freedom for the three distillation columns should ideally be used to optimize the profit for the entire plant, but as mentioned in Section 3.4, a simplified recovery model is used for the distillation columns when modeling the entire plant to make the optimization feasible. The error imposed by this is expected to be very small. The distillation columns were therefore optimized separately using detailed models. Assumed internal prices were defined to take care of the interaction with the remaining process. For distillation columns, to avoid product give-away, it is always optimal to have the most valuable product at its constraint. In our case, there is only

one product constraint, namely $x_{D,benzene} \geq 0.9997$, and this should always be active as benzene is the main (and most valuable) product. For the remaining distillation products, the optimal conditions were obtained by a trade-off between maximizing the recovery of valuable component and minimizing energy (favored by a large mole fraction). Figure 3.4 shows the relations between the reboiler duty and the respective mole fraction of valuable component for each distillation column. When the mole fraction is less than about 10^{-3}, its economic effect on the recovery is small. In general, we get a good trade-off if we have a small mole fraction (about 10^{-3} or less) in the "flat" region.

The resulting "optimal" values for the five remaining degrees of freedom (product compositions) are given in Table 3.9.

Table 3.9: *Specifications for distillation columns.*

Column/Specification	Value	Comment
Stabilizer		
Y53 $x_{D,benzene}$	$1 \cdot 10^{-4}$	(A)
Y54 $x_{B,methane}$	$1 \cdot 10^{-6}$	(B)
Benzene column		
Y55 $x_{D,benzene}$	0.9997	Active constraint
Y56 $x_{B,benzene}$	$1.3 \cdot 10^{-3}$	(A)
Toluene column		
Y57 $x_{D,diphenyl}$	$0.5 \cdot 10^{-3}$	(C)
Y58 $x_{B,toluene}$	$0.4 \cdot 10^{-3}$	(A)

(A) Determined by trade-off between energy usage and recovery (Figure 3.4).

(B) $x_{B,methane}$ should be small to avoid methane impurity in distillate of benzene column.

(C) Diphenyl should not be recycled because it may reduce the available production rate if there is bottleneck in the plant.

The reason why the impurities in Table 3.9 are so small is that "our columns" have many stages so that it does not cost much energy to achieve higher purity. This also means that the optimal point is "flat" (which is good) as it is also illustrated by Figure 3.5. For the stabilizer column, the separation is very simple and improving the purity has almost no penalty in terms of reboiler duty.

Note we have chosen to use product compositions as controlled variables (specifications) for the distillation columns. There are two reasons for this: First, with fixed product compositions only mass balances are needed to represent the distillation columns when simulating the overall process in Aspen Plus^{TM}. Second, compositions are good self-optimizing variables in most cases (e.g. Skogestad (2000)). Also note that the product compositions should normally be given in terms of impurity of key components (Luyben *et al.*, 1998) as this avoids problems with non-unique specifications.

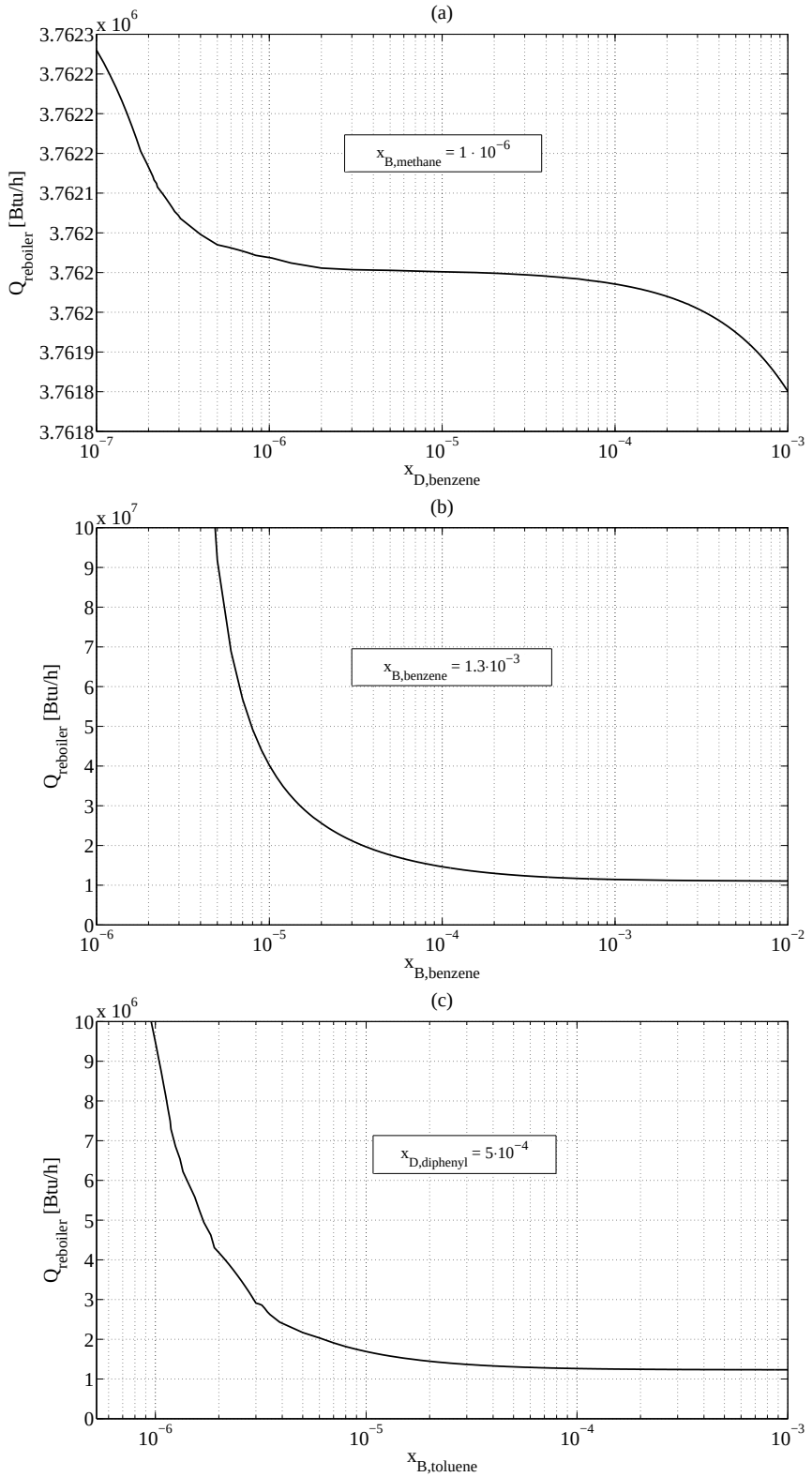

Figure 3.4: *Typical relations between reboiler duty and product purity. (a) Stabilizer distillate; (b) Benzene column bottoms; (c) Toluene column bottoms.*

These six specifications for the distillation columns consume six steady-state degrees of freedom. There are then $13 - 6 = 7$ degrees of freedom left.

Optimization of the entire process (reactor and recycle)

Optimization with respect to the 7 remaining steady-state degrees of freedom was performed using an SQP algorithm in Aspen Plus^{TM}. Figure 3.5 gives the effect of disturbances on the profit ($-J$). Note that disturbances D8 - D12 in the distillation product compositions have almost no effect. This is expected,,since the five distillation composition specifications (Table 3.9) are in the "flat" region and have practically no influence in the profit. A change in the given purity for the benzene product (disturbance D7) has, as expected, a quite large effect. The detailed results for disturbances D1 to D7 are summarized in Table 3.10.

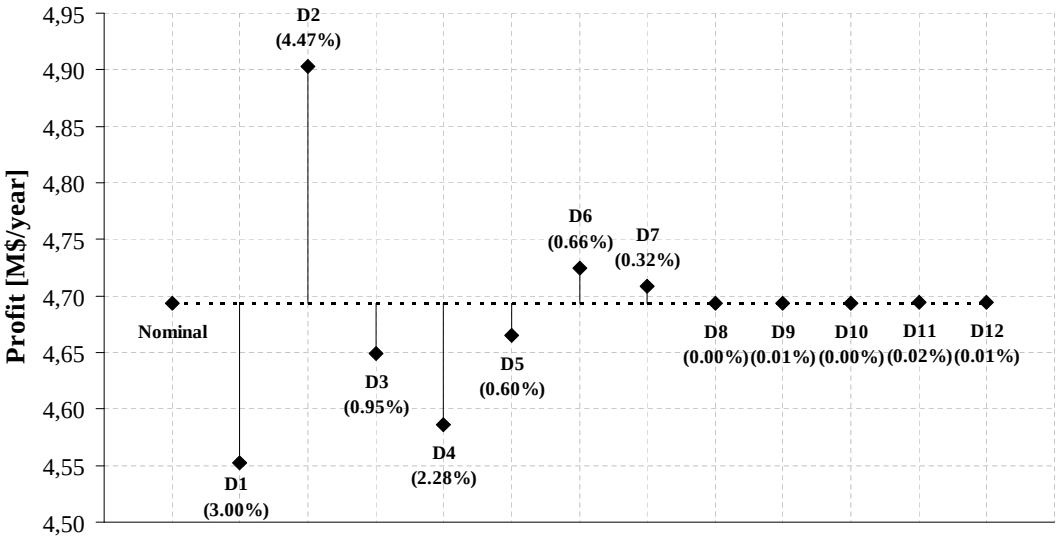

Figure 3.5: *Effect of disturbances (see Table 6.3) on optimal operation. Percentages in parentheses are changes with respect to the nominal optimum.*

From Table 3.10, 5 constraints are optimally active in all operating points:

Y16. Quencher outlet temperature (upper bound)

Y19. Separator temperature (lower bound)

Y20. Fresh toluene feed rate (upper bound)

Y62. Reactor inlet pressure (upper bound)

Y70. Hydrogen to aromatic ratio in reactor inlet (lower bound)

Table 3.10: *Effect of disturbances on optimal values for selected variables.*

Variable	Nominal	D1	D2	D3	D4	D5	D6	D7
Profit	4,693.4	4,552.7	4,903.2	4,649.0	4,585.6	4,664.7	4,722.5	4,705.5
Y4	1201.15	1198.20	1202.89	1204.66	1206.66	1196.44	1201.88	1199.33
Y15	1277.21	1273.64	1279.25	1277.71	1279.65	1272.25	1276.89	1274.99
Y16$^{(*)}$	1150	1150	1150	1150	1150	1150	1170	1150
Y19$^{(*)}$	95	95	95	95	95	95	95	95
Y20$^{(*)}$	300	285	315	300	300	300	300	300
Y21	446.59	431.29	470.33	476.29	460.03	446.75	444.73	445.46
Y26	445.27	429.78	468.91	474.95	458.44	445.27	443.23	443.90
Y28	0.3558	0.3548	0.3577	0.3454	0.3703	0.3558	0.3526	0.3560
Y29	0.5729	0.5742	0.5707	0.5854	0.5622	0.5730	0.5767	0.5727
Y45	0.8721	0.8671	0.8703	0.8667	0.8792	0.8683	0.8692	0.8662
Y46	0.0491	0.0544	0.0511	0.5419	0.4534	0.5322	0.5205	0.5549
Y49	0.6710	0.6717	0.6691	0.6803	0.6534	0.6708	0.6737	0.6705
Y53$^{(**)}$	$1 \cdot 10^{-4}$	$1 \cdot 10^{-4}$	$1 \cdot 10^{-4}$	$1 \cdot 10^{-4}$	$1 \cdot 10^{-4}$	$1 \cdot 10^{-4}$	$1 \cdot 10^{-4}$	$1 \cdot 10^{-4}$
Y54$^{(**)}$	$1 \cdot 10^{-6}$	$1 \cdot 10^{-6}$	$1 \cdot 10^{-6}$	$1 \cdot 10^{-6}$	$1 \cdot 10^{-6}$	$1 \cdot 10^{-6}$	$1 \cdot 10^{-6}$	$1 \cdot 10^{-6}$
Y55$^{(**)}$	0.9997	0.9997	0.9997	0.9997	0.9997	0.9997	0.9997	0.996
Y56$^{(**)}$	$1.3 \cdot 10^{-3}$	$1.3 \cdot 10^{-3}$	$1.3 \cdot 10^{-3}$	$1.3 \cdot 10^{-3}$	$1.3 \cdot 10^{-3}$	$1.3 \cdot 10^{-3}$	$1.3 \cdot 10^{-3}$	$1.3 \cdot 10^{-3}$
Y57$^{(**)}$	$5 \cdot 10^{-4}$	$5 \cdot 10^{-4}$	$5 \cdot 10^{-4}$	$5 \cdot 10^{-4}$	$5 \cdot 10^{-4}$	$5 \cdot 10^{-4}$	$5 \cdot 10^{-4}$	$5 \cdot 10^{-4}$
Y58$^{(**)}$	$4 \cdot 10^{-4}$	$4 \cdot 10^{-4}$	$4 \cdot 10^{-4}$	$4 \cdot 10^{-4}$	$4 \cdot 10^{-4}$	$4 \cdot 10^{-4}$	$4 \cdot 10^{-4}$	$4 \cdot 10^{-4}$
Y62$^{(*)}$	500	500	500	500	500	520	500	500
Y68	454.39	443.20	474.93	473.22	485.53	564.09	460.82	455.41
Y70$^{(*)}$	5.0	5.0	5.0	5.0	5.5	5.0	5.0	5.0

$^{(*)}$ Active constraints.

$^{(**)}$ Distillation specification.

As expected, the benzene purity at the outlet of the process is kept at its bound for economic reasons. Moreover, fresh feed toluene is maintained at its maximum flow rate to maximize the profit. The separator inlet temperature is kept at its lower bound in order to maximize the recycle of hydrogen and to avoid the accumulation of methane in the process. Luyben's rule of keeping all recycle loops under flow control is not economically optimal in this process since it is best to let the recycle flow fluctuate.

All the 5 active constraints should be controlled to achieve optimal operation (Maarleveld and Rijnsdorp, 1970). Consequently, the remaining number of unconstrained degrees of freedom is 2 ($7 - 5 = 2$). This reduces the number of possible sets of controlled variables to $\binom{59}{2} = \frac{59!}{2!57!} = 1,711$, where the number 59 is found by subtracting from the initial 70 candidate measurements in Table 3.4 the 6 distillation specifications and 5 active constraints of the reactor and recycle process. However, this number is still too large to consider all alternatives in detail.

The next step uses local analysis to find promising candidate sets of 2 controlled variables.

3.5.5 Step 5. Identification of candidate controlled variables

A branch-and-bound algorithm (Cao *et al.*, 1998*a*) for maximizing the minimum singular value of $S_1 G J_{uu}^{-1/2}$ and $S_1 G$ was used to obtain the candidate sets of controlled variables (details on the calculation of S_1, G, and J_{uu} are given in the Appendix). Note that the steady-state gain matrix G is obtained with the 5 active constraints fixed at their optimal values. The minimum singular value of the 16 candidate sets are given

in Table 3.12 and the 15 (out of 59) measurements involved in the 16 sets are listed in Table 3.11, with their nominally optimal values, the optimal variations, and assumed implementation errors (i.e, the total span is the sum of the optimal variation and the implementation error). From Table 3.12 we see that the same best 10 sets were identified for both criteria of maximizing $\underline{\sigma}(S_1 G J_{uu}^{-1/2})$ and $\underline{\sigma}(S_1 G)$. Also note the 10 best sets all include the reactor feed inert (methane) mole fraction (Y29) plus another composition (of benzene, toluene, or diphenyl) as controlled variable. The remaining 6 sets (XI - XVI) are some other common choices that are reasonable to consider, including inert (methane) recycle concentration (Y49), the furnace outlet temperature (Y4), the purge rate (Y26), and the compressor power (Y68). Set XII with fixed furnace outlet temperature (Y4) and inert (methane) concentration (Y49) is similar to the structure of Luyben (2002), although Luyben does not control all the active constraints.

Table 3.11: *Candidate controlled variables with small losses in local analysis.*

Variable	Name	Nominal optimal	Optimal variation	Implementation error	Total span
Y4	Furnace outlet temperature	1201.15	5.52	60.06	65.57
Y26	Purge flow rate	445.27	29.73	22.26	52
Y29	Mixer outlet inert (methane) mole fraction	0.5729	0.0125	0.0001	0.0126
Y30	Mixer outlet benzene mole fraction	0.0091	0.000068	0.0001	0.000168
Y35	Quencher outlet benzene mole fraction	0.0996	0.0059	0.0001	0.006
Y36	Quencher outlet toluene mole fraction	0.0031	0.0007	0.0001	0.0008
Y37	Quencher outlet diphenyl mole fraction	0.0033	0.0003	0.0001	0.0004
Y40	Separator overhead vapor benzene mole fraction	0.0107	0.000081	0.0001	0.000181
Y45	Separator liquid benzene mole fraction	0.8721	0.0071	0.0001	0.0072
Y46	Separator liquid toluene mole fraction	0.0491	0.0071	0.0001	0.0072
Y47	Separator liquid diphenyl mole fraction	0.0318	0.0023	0.0001	0.0024
Y49	Gas recycle inert (methane) mole fraction	0.6710	0.0175	0.0001	0.0176
Y50	Gas recycle benzene mole fraction	0.0107	0.000081	0.0001	0.000181
Y68	Compressor power	454.39	109.69	4.54	114.23
Y69	Toluene conversion at reactor outlet	0.9124	0.0076	0.01	0.0176

3.5.6 Step 6. Detailed evaluation of the loss

The next step is to evaluate the loss for the promising sets of controlled variables in Table 3.12 by keeping constant setpoint policy when there are disturbances and/or implementation errors. The computations were performed on the nonlinear model in Aspen Plus^{TM} for disturbances D1 through D7 (the losses for disturbances D8 to D12 are negligible, as discussed above) and the results are shown in Table 3.13.

As seen in Tables 3.12 and 3.13, the results from the linear and nonlinear analysis give the same ranking for the sets of candidate controlled variables, with the best sets having both the largest value of $\underline{\sigma}(S_1 G_{2\times 2} J_{uu}^{-1/2})$ (as one would expect from (3.7)) and the lowest value of the actual loss. Note from Table 3.13 that all the structures were found to be feasible for the given disturbances.

Compared to the controlled structure proposed by Luyben (2002) the sets of controlled variables selected by the self-optimizing control approach give smaller economic losses. This is because the steady-state nominal point of Luyben (2002) is not optimal: It gives a profit of $(-J) = 3.955.2$ k\$/year, which is about 16% smaller than our

Table 3.12: *Local analysis: Minimum singular values for candidate sets of unconstrained controlled variables.*

Set	Variable 1	Variable 2	$1000 \cdot \underline{\sigma}(S_1 G_{2\times 2})$	$1000 \cdot \underline{\sigma}(S_1 G_{2\times 2} J_{uu}^{-1/2})$
Full(*)			6.2523	6.3436
I	Y29	Y36	2.2942	2.3331
II	Y29	Y69	2.2523	2.2761
III	Y29	Y45	2.2133	2.2545
IV	Y29	Y46	2.2102	2.2398
V	Y29	Y40	2.2072	2.2201
VI	Y29	Y50	2.1981	2.2199
VII	Y29	Y35	1.8452	1.8247
VIII	Y29	Y47	1.8344	1.8044
IX	Y29	Y30	1.7855	1.7851
X	Y29	Y37	1.7149	1.6825
XI	Y4	Y26	1.2439	1.2815
XII	Y4	Y49	0.2008	0.1957
XIII	Y26	Y49	1.3352	1.2902
XIV	Y4	Y68	0.1198	0.1201
XV	Y26	Y68	1.2196	1.2785
XVI	Y49	Y68	0.0198	0.0201

(*) With all 59 variables: $G_{full} = G_{59\times 2}$.

Table 3.13: *Loss in k$/year caused by disturbances and implementation errors for the alternative sets of controlled variables from Table 3.12.*

Set	D1	D2	D3	D4	D5	D6	D7	n_{y1}(*)	n_{y2}	Average
I	70.40	5.37	14.41	4.57	12.85	12.57	9.66	5.33	3.37	15.39
II	86.16	10.91	25.78	18.98	27.11	13.31	17.77	5.33	33.58	26.55
III	100.01	13.22	35.40	26.66	55.52	13.60	21.82	5.33	10.92	31.39
IV	118.45	16.04	38.22	39.52	60.30	37.98	43.17	5.33	4.57	40.40
V	136.60	16.92	48.46	53.16	69.07	41.48	78.59	5.33	16.17	51.75
VI	143.54	19.70	48.47	58.17	79.12	51.23	106.07	5.33	12.02	58.18
VII	149.94	22.01	58.42	67.39	79.27	64.68	112.07	5.33	12.05	63.46
VIII	140.83	23.40	59.81	85.09	81.44	76.60	118.25	5.33	12.03	66.97
IX	150.37	25.25	67.70	96.31	83.30	85.55	136.07	5.33	3.40	72.59
X	151.61	31.07	70.11	99.91	88.29	106.15	141.18	5.33	4.19	77.54
XI	163.29	43.10	97.70	133.87	104.15	127.00	150.84	243.97	176.86	137.87
XII(**)	188.09	55.86	125.35	169.45	128.55	151.18	178.46	243.97	25.46	140.71
XIII	162.78	37.49	88.99	144.73	128.55	124.42	148.47	176.86	25.46	115.31
XIV	193.80	61.99	131.70	157.08	137.96	154.38	188.23	243.97	302.04	174.57
XV	179.48	43.24	89.21	183.32	155.35	122.78	159.47	176.86	302.04	156.86
XVI	233.26	188.87	259.70	364.56	186.68	171.82	224.66	25.46	302.04	217.45

(*) n_{y1} and n_{y2} are the implementation errors associated with each variable in the set.
(**) This is similar to the structure of Luyben (2002), but with control of active constraints.

nominal optimally operation (4,693.4k$/year). First, Luyben (2002) considers only 12 degrees of freedom at steady state as compressor power is assumed fixed. Second, Luyben (2002) does not control all the active constraints in the process. Specifically, the hydrogen-to-aromatics ratio, which is an important variable in the process and should be kept at its lower bound of 5 (see (5.6)), is not controlled. Instead, Luyben (2002) controls inert (methane) composition in the recycle gas and reactor inlet temperature which results in large economic losses.

3.6 Discussion

In this chapter, we have considered the standard operation mode with given feed rate (indirectly, through an upper bound on toluene feed). Yet another important mode of operation is maximum throughput, which occurs when prices are such that it is optimum to maximize production.

Another point to stress is the consistency of the results with the empirical arguments made by Douglas (1988) which is that impurity levels should be controlled in order to avoid build-up of inerts in the system that eventually makes the process inoperable. This was accomplished when we chose to control the inert (methane) concentration leaving the mixer (controlled variable Y29 above).

The final evaluation and selection of the control structure involves the selection of sets of controlled variables with acceptable loss, such as those shown in Table 3.13. These are then analyzed to see if they are adequate with respect to the expected dynamic control performance (input-output controllability). This, in addition to maximum throughput case and design of the regulatory layer, will be the focus of part II of the series where a dynamic analysis is used.

No constraint on the stabilizer column condenser temperature was included. In practice one should avoid the cryogenic temperature on the overhead methane product from the stabilizer column by allowing for a larger benzene contents. However, the flow rate of this distillate stream is very small so this would not change the results of this paper.

3.7 Conclusions

This chapter has discussed the selection of controlled variables for the HDA process using the self-optimizing control procedure. The large number of variable combinations makes it a challenging problem, and a local (linear) analysis based on the SVD of the linearized model of the plant was used to select good candidate sets for the unconstrained controlled variables. Specifically, 16 candidate sets were found to be suitable to select from. Aspen Plus^{TM} proved to be a valuable tool for the evaluation of self-optimizing control structures for large-scale processes.

3.8 Appendix

This appendix outlines the steps taken to compute the steady-state linear matrix G and the Hessian J_{uu} of the unconstrained inputs as well as the optimal variation for the candidate variables $span(c_i)$.

Optimization of the entire plant in Aspen Plus^{TM} was used to identify the active constraints. For the local analysis (calculation of $\Delta c_{opt}(d)$, G, and J_{uu}), several auxiliary blocks were used, including a Calculator block to compute the value of the cost function; Design Specification blocks were used to close feedback loops for the active constraints; and a Sensitivity block was used to perform auxiliary computations. Finally, Aspen Plus^{TM} was used to compute the "nonlinear" loss imposed by keeping the selected sets of controlled variables constant at their setpoints.

3.8.1 Calculation of the linear matrix G and the Hessian J_{uu}

G and J_{uu} are calculated with respect to the nominal optimal operating point, i.e. for $d = 0$. The matrix G is calculated by the usual approximation:

$$\frac{\partial c_i(u)}{\partial u_j} = \lim_{h \to 0} \frac{c(u + e_j h) - c(u)}{h_j} \tag{3.20}$$

where $i = 1...n_c$ is the index set of candidate variables, $j = 1...n_u$ is the index set of unconstrained inputs, h is the vector of increments for each input u_j, and $e_j = [000...1...0]$ is the zero vector except for the j-element which is 1.

In Aspen Plus^{TM}, $c(u)$ and $c(u + e_j h)$ are evaluated by adding the step $e_j h$ to the vector u for each input j in a Calculator block and then taken the resulting vectors to a MatLab^{TM} code that numerically calculates the terms $G_{ij} = \frac{\partial c_i(u)}{\partial u_j}$.

The Hessian J_{uu} is evaluate similarly. The following simple approximation was used:

$$\frac{\partial^2 J(u)}{\partial u_j^2}|_i = \lim_{h \to 0} \frac{J(u + E_{ii}h + E_{jj}h) - J(u + E_{ii}h) - J(u + E_{jj}h) + J(u)}{[hh^T]_{ij}} \tag{3.21}$$

where E_{ij} is the zero matrix except for the ij-element which is 1. The several functions of J in the denominator of (3.21) are evaluated in a Calculator block in Aspen Plus^{TM} and taken to MatLab^{TM} for the numerical calculation of $H_{ij} = \frac{\partial^2 J(u)}{\partial u_j^2}|_i$.

3.8.2 Optimal variation for the candidate variables

The optimal variation for the candidate variables ($span(c_i)$) is used to scale the linear matrix G obtained by linearizing the nonlinear model of the process. In this work, we used direct calculations from the nonlinear model of the HDA process in Aspen Plus^{TM}.

For each candidate controlled variable c_i, we obtain its maximum optimal variation $\Delta c_{i,opt}(d)$ due to variation in disturbances. From the nonlinear model, we compute

the optimal parameters (inputs and outputs) for various conditions (disturbances and operating points). This yields a "lookup" table of optimal parameter values as a function of the operating conditions. From this, we identify:

$$\Delta c_{i,opt}(d) = \max_{j \in D}(|c_{i,opt}^{j} - c_{i,opt}^{nom}|) \tag{3.22}$$

where D is the set of disturbances, $c_{i,opt}^{j}$ is the optimal value of c_i due to disturbance j and $c_{i,opt}^{nom}$ is the nominal optimal value of c_i.

For each candidate controlled variable c_i, we obtain its expected implementation error n_i (sum of measurement error and control error). Then, we scale the candidate controlled variables such that for each variable i the sum of the magnitudes of $\Delta c_{i,opt}(d)$ and the implementation error n_i is similar, which corresponds to selecting the scaling:

$$span(c_i) = \Delta c_{i,opt}(d) + n_i \tag{3.23}$$

Then, the scaling matrix S_1 can be computed as $S_1 = diag\{\frac{1}{span(c_i)}\}$. All data were retrieved from nonlinear simulations in Aspen Plus^{TM} and the calculations were performed in a dedicated MatLab^{TM} code.

Chapter 4

Application of Plantwide Control to the HDA Process. II - Regulatory Control

Based on the paper submitted for publication in
Industrial Engineering Chemistry Research

This chapter describes the design of a control structure for a large-scale process, the HDA plant. Steady-state "top-down" analysis and optimization of the process (Araujo *et al.*, 2006) was used to select 16 sets of candidate "self-optimizing" primary (economic) variables. In this chapter, we focus on the remaining "bottom-up" steps dealing with deciding where in the plant the production rate should be set; design of the regulatory control layer; design of the configuration of the supervisory control layer; and nonlinear dynamic simulations to validate the proposed control structure. Emphases is given to the systematic design of the regulatory control layer for it constitutes the backbone on which the optimal operation of higher layer relies on. In order to carry out the analysis, steady-state and dynamic models are necessary and Aspen Plus^{TM} and Aspen Dynamics^{TM} are used extensively. The final control structure is robust and yields good dynamic performance.

4.1 Synopsis

In a previous chapter, we applied the top-down part of the plantwide design procedure of Skogestad (2004*a*) (Table 4.1) to the HDA process. The present chapter deals with the bottom-up part, where the following steps are considered:

- Step 4: Selection of the production rate manipulator.

- Step 5: Structure of the regulatory control layer.

- Step 6: Structure of the supervisory control layer.

- Step 7: Decision on use and possibly structure of optimization layer (RTO).

- Step 8: Validation of the proposed control structure.

One of the main issues in the design of the regulatory control layer is to ensure "stable" and smooth operation. By "stable" we mean not only the mathematical stabilization of unstable modes (e.g., related to control of level loops) but also that the regulatory layer should prevent the plant from drifting too far away from its nominal operating point and that it should be designed such that the supervisory layer (or the operators) can handle the effect of disturbances on the primary outputs ($y_1 = c$).

We choose a decentralized supervisory control layer design since, as seen later, this layer appears to be non-interacting and also suitable for the HDA process where the active constraints remain constant despite of the set of disturbances considered (see Araujo *et al.* (2006)). We base the design of the regulatory control layer on steady-state as well as dynamic considerations and use more detailed measures for evaluating controllability of the linearized model of the process such as the existence of right half plane transmission zeros (RHP zeros) and relative gain array (RGA) related methods.

The resulting control structure of the HDA plant is then tested by conducting nonlinear dynamic simulation in Aspen Dynamics^{TM} for various disturbances in order to evaluate the final performance.

Previous work on the regulatory control structure for the HDA process includes Luyben (2002), the original work by Brognaux (1992), and more recently Qiu and Krishnaswamy (2003) and Konda *et al.* (2005*a*). However, no systematic quantitative procedure has been applied to date.

In this chapter, we use a slightly modified version of the steady-state and dynamic models given in Luyben (2002) to design the entire control structure of the HDA process. Luyben (2002) structure is then compared with the one proposed in this chapter using our nominal optimal steady-state operating point.

4.2 Overview of a plantwide control structure design procedure

In practice, a control system is usually divided into several layers, separated by time scale (see Figure 4.1). The layers are linked by the controlled variables, whereby the set points are computed by the upper layer and implemented by the lower layer.

Control structure design is also known as plantwide control and deals with the structural decisions that must be made to design a control structure for, in our case, a complete chemical plant. The decisions involve the following main tasks:

1. Selection of manipulated variables ("inputs");

2. Selection of controlled variables ("outputs"; variables with set points);

3. Selection of (extra) measurements (for control purposes including stabilization);

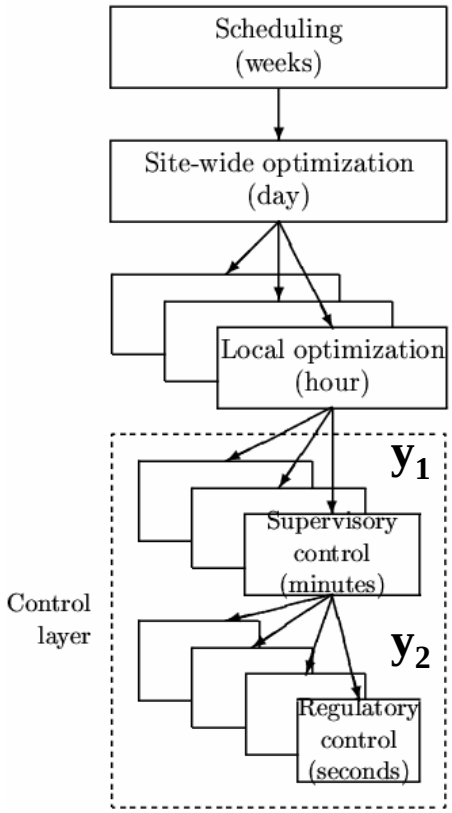

Figure 4.1: *Typical control hierarchy in a chemical plant.*

4. Selection of control configuration (the structure of the overall controller that interconnects the controlled, manipulated and measured variables);

5. Selection of controller type (control law specification, e.g. PID, decoupler, LQG, etc.).

The tasks above can be translated into a systematic plantwide procedure for control structure design as summarized in Table 4.1 extracted from Skogestad (2004*a*). The procedure has two main points:

I. *Top-down analysis*, including definition of operational objectives and consideration of degrees of freedom available to meet these (tasks 1 and 2 above; steps 1-4 in Table 4.1).

II. *Bottom-up design* of the control system, starting with the stabilizing control layer (tasks 3, 4 and 5 above; steps 5-8 in Table 4.1).

Steps 1-3 are thoroughly discussed in Araujo *et al.* (2006) and actually applied to the primary variable selection of the HDA process.

Table 4.1: *Plantwide control structure design procedure.*

Step
(I) Top-down analysis
1. Definition of operational objectives: Identify operational constraints, and preferably identify a scalar cost function J to be minimized. *2. Manipulated variables u and degrees of freedom:* Identify dynamic and steady-state degrees of freedom (DOF). *3. Primary controlled variables:* Which (primary) variables c should we control? - Control active constraints. - Remaining DOFs: control variables for which constant set points give small (economic) loss when disturbances occur (self-optimizing control). *4. Production rate:* Where should the production rate be set? This is a very important choice as it determines the structure of remaining inventory control system.
(II) Bottom-up design (with given primary controlled c and manipulated u variables)
5. Regulatory control layer: *Purpose*: "Stabilize" the plant using low-complexity controllers (single-loop PID controllers) such that a) the plant does not drift too far away from its nominal operating point and b) the supervisory layer (or the operators) can handle the effect of disturbances on the primary outputs ($y_1 = c$). *Main structural issue*: - Selection of secondary controlled variables (measurements) y_2. - Pairing of these y_2 with manipulated variables u_2. *6. Supervisory control layer:* *Purpose*: Keep (primary) controlled outputs $y_1 = c$ at optimal set points c_s, using as degrees of freedom (inputs) the set points $y_{2,sp}$ for the regulatory layer and any unused manipulated variables u_1. *Main structural issue*: - Decentralized (single-loop) control: a) May use simple PI or PID controllers; b) Structural issue: choose input-output pairing. - Multivariable control (usually with explicit handling of constraints (MPC)). Structural issue: Size of each multivariable application. *7. Optimization layer:* *Purpose*: Identify active constraints and compute optimal set points c_s for controlled variables. *Main structural issue*: Do we need real-time optimization (RTO)? *8. Validation:* Nonlinear dynamic simulation of the plant.

4.2.1 Production rate manipulator

The decision on where to place the production rate manipulator is closely related to where in the process there are bottlenecks that limit the flow of mass and energy. In addition, the decision directly affects the way total inventory (liquid or gas) of individual units are controlled across the process, namely [(Buckley, 1964) and (Price *et al.*, 1994)] (see Figure 4.2):

- Using outflow downstream of the location where the production rate is set, and
- Using inflow upstream of this location.

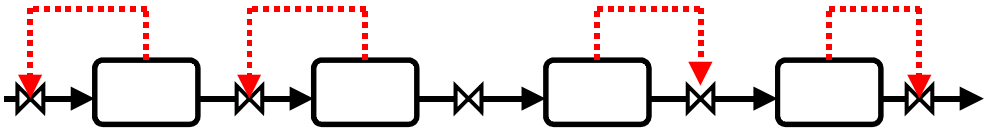

Figure 4.2: *General representation of inventory control (with production rate set inside the plant).*

We distinguish between two main modes of operation:

- **Mode I: Given throughput**. This mode of operation occurs when (a) the feed rate is given (or limited) or (b) the production rate is given (or limited, e.g. by market conditions). The operational goal is then to minimize utility (energy) consumption, that is, to maximize efficiency.

- **Mode II: Maximum throughput**. This mode of operation occurs when the product prices and market conditions are such that it is optimal to maximize throughput.

The production rate is commonly assumed to be set at the inlet to the plant, with outflows used for level control. This is reasonable for Mode I with given feed rate. However, during operation the feed rate is usually a degree of freedom and very often the economic conditions are such that it is optimal to maximize production (Mode II). As feed rate is increased, one eventually reaches a constraint (a bottleneck) where further increase is not feasible. To maximize production, we must have maximum flow through the bottleneck unit at all times. This gives the following rule for Mode II: *Determine the main bottleneck in the plant by identifying the maximum achievable feed rate for various disturbances. To maximize the flow through the bottleneck, the production rate should preferably be set at this location.* To avoid reconfiguration, the same production rate manipulator should be used also in Mode I.

However, one should be careful when applying this rule. First, other considerations may be important, such as the control of the individual units (e.g. distillation column) which may be affected by whether inflow or outflow is used for level control (Luyben *et al.*, 1998). Second, stabilization of the unit may require the "active" use of some flow variable, and thus prevent one from maximizing the flow at the bottleneck (this turns out to be the case for the HDA plant). Third, the bottleneck may move depending on the disturbances. In any case, the control systems should be such that close to optimal operation (that is, close to maximum bottleneck flow) can be achieved.

4.2.2 Regulatory control layer

We define the regulatory control system as the layer in the control hierarchy which has operation as its main purpose, and which normally contains the control loops that must be in service in order for the supervisory layer (operators) to be able to

operate the plant in an efficient manner. The main objective of this layer is generally to facilitate smooth operation and not to optimize objectives related to profit, which is done at higher layers. Usually, this is a decentralized control system which keeps a set of measurements y_2 at given set points. This is a cascaded control system where the values of these set points are determined by the higher layers in the control hierarchy (see Figure 4.1). In addition, this layer should allow for "fast" control, such that acceptable control is achieved using "slow" control in the layer above. Also, it should avoid "drift" so the system stays within its linear region which allows the use of linear controllers (Skogestad and Postlethwaite, 2005).

4.2.3 Selection of measurements y_2 and pairing with inputs u_2

Typically, the variables y_2 to be controlled in this layer are pressures, levels, and selected temperatures. A major structural issue in the design of the regulatory control layer is the selection of controlled variables y_2 and corresponding manipulations u_2. The following guidelines may be useful:

Selection of measurements y_2:

1. y_2 should be easy to measure.

2. Avoid "unreliable" measurements because the regulatory control layer should not fail.

3. y_2 should have good controllability, that is favorable dynamics for control: avoid variables y_2 with large (effective) delay.

4. y_2 should be located "close" to the manipulated variable u_2 (as a consequence of rule 3, because for good controllability we want a small effective delay).

5. The (scaled) gain from u_2 to y_2 should be large.

Note: Items 2 and 3 normally exclude compositions as secondary controlled variables y_2.

Selection of input u_2 (to be paired with y_2):

6. Select u_2 so that controllability for y_2 is good, that is u_2 has a "large" and "direct" effect on y_2. Here "large" means that the gain is large, and "direct" means good dynamics with no inverse response and a small effective delay.

7. Avoid using variables u_2 that may saturate.

8. Avoid variables u_2 where (frequent) changes are undesirable, for example, because they disturb other parts of the process.

Indirect control of primary variables - possible intermediate layer

Often, the self-optimizing controlled variables (both the ones related to active constraints and the unconstrained degrees of freedom) are compositions which are often unreliable and delayed. Therefore, in addition to the regulatory control layer, we sometimes need to include an intermediate layer between the supervisory and regulatory control layers for "indirect control" of the primary variables y_1. This is to ensure that the (near) optimal operation of the process can be "maintained" in case of failure of any of the primary (composition) loops. Since the time scale for the composition control layer is long, the variables y_1' for this intermediate layer can be selected using the "maximum (scaled) gain rule" based on steady-state considerations (Skogestad and Postlethwaite, 2005). For simplicity, we want to avoid the intermediate layer, so the preferred situation is that indirect composition control is achieved with constant y_2 and u_1 (where u_1 are the remaining unused inputs after closing the regulatory layer).

4.2.4 Supervisory control layer

The purpose of the supervisor control layer is to keep the (primary) controlled outputs y_1 at their optimal set points y_{1s}, using as degrees of freedom the set points $y'_{1,sp}/y_{2,sp}$ in the composition control/regulatory layer and any unused manipulated inputs. The variables to control at this layer can be determined by the self-optimizing control technique. The main issue about this layer is to decide on whether to use a decentralized or a multivariable control configuration, e.g. MPC. For the purpose of this chapter, we assume the discussion around the decentralized configuration alternative only. Decentralized single-loop configuration is the simplest and it is preferred for non-interacting process and cases where active constraints remain constant. Advantages with decentralized control are:

+ Tuning may be done on-line;

+ None or minimal model requirements;

+ Easy to fix and change.

On the other hand, the disadvantages are:

- Need to determine pairing;

- Performance loss compared to multivariable control;

- Complicated logic required for reconfiguration when active constraints move.

The decision on how to pair inputs ($y_{2,sp}$ and u_1) and outputs c is often done based on process insight. In more difficult cases a RGA-analysis may be useful, and the rule is pair such that the resulting transfer matrix is close to identity matrix at the crossover expected frequency, provided the element is not negative at steady-state. For a more detailed analysis one should also consider disturbances and compute the closed-loop disturbance gain (CLDG) (Skogestad and Postlethwaite, 2005).

4.2.5 Optimization layer (RTO)

The purpose of the optimization is to identify the active constraints and recompute optimal set points c_s for controlled variables. The main structural issue is to decide if it is necessary to use real-time optimization (RTO). Real-time optimization is costly in the sense that it requires a detailed steady-state model to be maintained and continuously updated. If the active constraints do not change and we are able to find good self-optimizing controlled variables, then RTO gives little benefit and should not be used.

4.2.6 Validation

Finally, after having determined a plantwide control structure, it may be necessary to validate the structure, for example, using nonlinear dynamic simulation of the plant.

4.3 Control structure design of the HDA process

4.3.1 HDA process description

In the HDA process, fresh toluene (pure) and hydrogen (97% hydrogen and 3% methane) are mixed with recycled toluene and hydrogen (Figure 4.3). This reactant mixture is first preheated in a feed-effluent heat exchanger (FEHE) using the reactor effluent stream and then to the reaction temperature in a furnace before being fed to an adiabatic plug-flow reactor.

A main reaction and a side reaction take place in the reactor as follows:

$$Toluene + H_2 \rightarrow Benzene + Methane \tag{4.1}$$

$$2\ Benzene \rightleftharpoons Diphenyl + H_2 \tag{4.2}$$

The reactor effluent is quenched by a portion of the recycle separator liquid flow to prevent coking, and further cooled in the FEHE and cooler before being fed to the vapor-liquid separator. Part of flow from the compressor discharge containing unconverted hydrogen and methane is purged to avoid accumulation of methane within the process while the remainder is recycled back to the process. The liquid from the separator is processed in the separation section consisting of three distillation columns. The stabilizer column removes hydrogen and methane as overhead product, and benzene is the desired product in the benzene column distillate. Finally, in the toluene column toluene is separated from diphenyl as distillate and recycled back to the process.

The dynamic model of the HDA process used in this chapter is the same one as developed by Luyben (2002). A schematic flowsheet of the Aspen Dynamics^{TM} model without the control loops is depicted in Figure 4.3. The stream table for the nominally optimal operating point taken from Araujo *et al.* (2006) is shown in Table 5.1.

Note that the reactor-recycle section and the distillation section are almost decoupled from an operational point of view. The design of the control structure for each section is therefore performed separately.

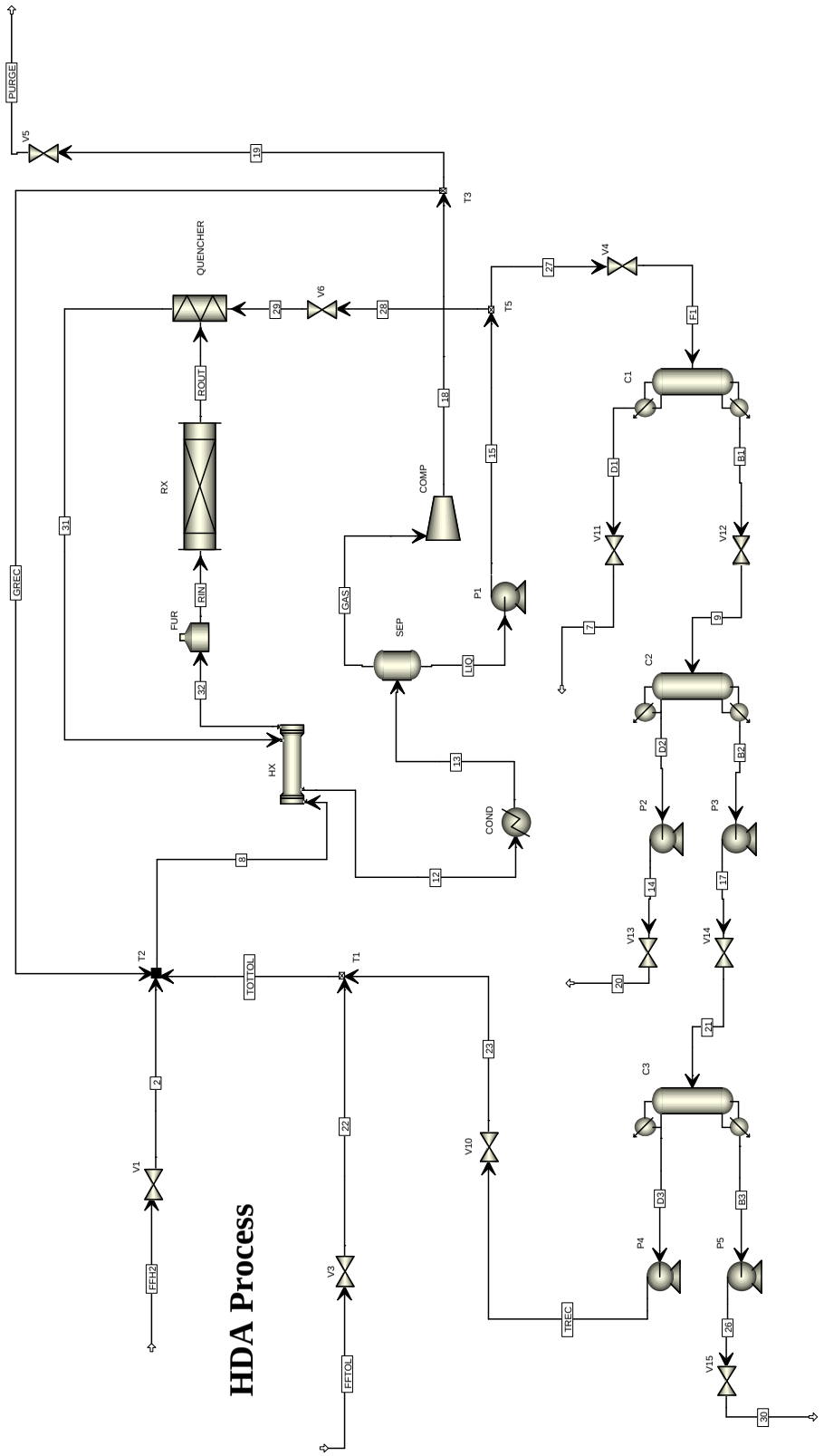

Figure 4.3: *HDA Aspen Dynamics*^{TM} *process flowsheet.*

Table 4.2: *Stream table for the nominally optimal operating point for the HDA process. See Figure 4.3 for the stream names.*

Stream	2	7	8	9	12	13	14	15	17	18	19	20	21	22	23	26	27	28	29	30
Mole Flow [lbmol/h]																				
Hydrogen	433.37	1.0841	1809.1	0	1519.4	1519.4	0	1.7618	0	1517.7	141.9	0	0	0	0	0	1.0841	0.6777	0.6777	0
Methane	13.403	14.438	2910.1	0	3219	3219	0	23.464	0	3195.5	298.78	0	0	0	0	0	14.438	9.0258	9.0258	0
Benzene	0	0.0016	45.023	276.36	498.76	498.76	276.33	449.13	0.0329	49.631	4.6405	276.33	0.0329	0	0.0329	0	276.36	172.77	172.77	0
Toluene	0	0	316.8	15.946	26.948	26.948	0.0831	25.914	15.862	1.0342	0.0967	0.0831	15.862	300	15.859	0.0038	15.946	9.9684	9.9684	0.0038
Diphenyl	0	0	0.0101	9.43	15.328	15.328	0	15.325	9.43	0.0031	0.0003	0	9.43	0	0.0073	9.4227	9.43	5.8951	5.8951	9.4227
Mole Fraction																				
Hydrogen	0.97	0.0698	0.3561	0	0.2878	0.2878	0	0.0034	0	0.3186	0.3186	0	0	0	0	0	0.0034	0.0034	0.0034	0
Methane	0.03	0.9301	0.5727	0	0.6097	0.6097	0	0.0455	0	0.6708	0.6708	0	0	0	0	0	0.0455	0.0455	0.0455	0
Benzene	0	1E-04	0.0089	0.9159	0.0945	0.0945	0.9997	0.8711	0.0013	0.0104	0.0104	0.9997	0.0013	0	0.0021	0	0.8711	0.8711	0.8711	0
Toluene	0	0	0.0623	0.0528	0.0051	0.0051	0.0003	0.0503	0.6263	0.0002	0.0002	0.0003	0.6263	1	0.9975	0.0004	0.0503	0.0503	0.0503	0.0004
Diphenyl	0	0	2E-06	0.0313	0.0029	0.0029	0	0.0297	0.3724	6E-07	6E-07	0	0.3724	0	0.0005	0.9996	0.0297	0.0297	0.0297	0.9996
Total Flow [lbmol/h]	446.77	15.524	5081.1	301.74	5279.5	5279.5	276.41	515.6	25.325	4763.9	445.42	276.41	25.325	300	15.899	9.4264	317.26	198.33	198.33	9.4264
Temperature [^{o}F]	100.11	-93.394	120.25	235.26	357.67	95	223.92	95.359	333	124.89	124.89	224.02	325.6	100.27	289.14	566.56	95.359	95.359	95.578	565.56
Pressure [psi]	555	50	530	31.714	477.4	477	80	530	84	555	555	50	30.75	555	555	82	530	530	487.4	32
Vapor Fraction	1	1	0.932	0.4557	1	0.9023	0	0	0	1	1	0	0.0337	0	0	0	0	0	0	0.005
Enthalpy [MBtu/h]	-0.3551	-0.4846	-88.217	9.8177	-68.617	-90.323	7.2579	10.044	0.8809	-99.2	-9.2752	7.2579	0.8809	1.8353	0.2276	0.7991	6.1802	3.8635	3.8635	0.7991

Stream	31	32	B1	B2	B3	D1	D2	D3	F1	FFH2	FFTOL	GAS	GREC	LIQ	PURGE	RIN	ROUT	TOTTOL	TREC
Mole Flow [lbmol/h]																			
Hydrogen	1519.4	1809.1	0	0	0	1.0841	0	0	1.0841	433.37	0	1517.7	1375.8	1.7618	141.9	1809.1	1518.8	0	0
Methane	3219	2910.1	0.0003	0	0	14.438	0	0	14.438	13.403	0	3195.5	2896.7	23.464	298.78	2910.1	3210	0	0
Benzene	498.76	45.023	276.36	0.0329	0	0.0016	276.33	0.0329	276.36	0	0	49.631	44.99	449.13	4.6405	45.023	325.99	0.0329	0.0329
Toluene	26.948	316.8	15.946	15.862	0.0038	0	0.0831	15.859	15.946	0	300	1.0342	0.9375	25.914	0.0967	316.8	16.98	315.86	15.859
Diphenyl	15.328	0.0101	9.43	9.43	9.4227	0	0	0.0073	9.43	0	0	0.0031	0.0028	15.325	0.0003	0.0101	9.4331	0.0073	0.0073
Mole Fraction																			
Hydrogen	0.2878	0.3561	0	0	0	0.0698	0	0	0.0034	0.97	0	0.3186	0.3186	0.0034	0.3186	0.3561	0.2989	0	0
Methane	0.6097	0.5727	1E-06	0	0	0.9301	0	0	0.0455	0.03	0	0.6708	0.6708	0.0455	0.6708	0.5727	0.6317	0	0
Benzene	0.0945	0.0089	0.9159	0.0013	0	1E-04	0.9997	0.0021	0.8711	0	0	0.0104	0.0104	0.8711	0.0104	0.0089	0.0642	0.0001	0.0021
Toluene	0.0051	0.0623	0.0528	0.6263	0.0004	0	0.0003	0.9975	0.0503	0	1	0.0002	0.0002	0.0503	0.0002	0.0623	0.0033	0.9999	0.9975
Diphenyl	0.0029	2E-06	0.0313	0.3724	0.9996	0	0	0.0005	0.0297	0	0	6E-07	6E-07	0.0297	6E-07	2E-06	0.0019	2E-05	0.0005
Total Flow [lbmol/h]	5279.5	5081.1	301.74	25.325	9.4264	15.524	276.41	15.899	317.26	446.77	300	4763.9	4318.5	515.6	445.42	5081.1	5081.1	315.9	15.899
Temperature [^{o}F]	1150	1004.8	371.4	332.65	565.54	-83.814	223.52	283.61	97.982	100	100	94.979	124.89	94.979	123.85	1201.2	1277.2	110.72	288.76
Pressure [psi]	487.4	510	154	34	32	150	30	30	160	605	605	476	555	476	505	500	496	555	675
Vapor Fraction	1	1	0	0	0	1	0	0	0.0293	1	0	1	1	0	1	1	1	0	0
Enthalpy [MBtu/h]	-7.2542	-26.854	9.8177	0.8801	0.7981	-0.4846	7.2521	0.2222	6.1802	-0.3551	1.8353	-100.36	-89.925	10.033	-9.2752	-11.118	-11.118	2.0629	0.2276

4.3.2 Selection of primary controlled variables (Mode I)

Araujo *et al.* (2006) report that there are 20 manipulated variables available for control, 7 of which have a dynamic effect only since there are 7 liquid levels with no steady-state effect that need to be controlled. This leaves 13 degrees of freedom at steady-state. Moreover in Mode I (with given feed rate), 5 constraints are optimally active for all operating points (defined by 12 different disturbances), namely:

1. Quencher outlet temperature $T_{quencher} = 1150^o$F (upper bound).
2. Separator temperature $T_{sep} = 95^o$F (lower bound).
3. Fresh toluene feed rate $F_{tol} = 300$lbmol/h (upper bound).
4. Reactor inlet pressure $P_{rin} = 500$psi (upper bound).
5. Hydrogen to aromatic ratio in reactor inlet $rH_2 = 5$ (lower bound).

In addition, for the distillation columns it was decided to control compositions (Araujo *et al.*, 2006). The decision on controlling benzene mole fraction in stabilizer distillate $x^{stab}_{D,ben}$ was based on the acceptable loss of benzene in this stream. However, small values of $x^{stab}_{D,ben}$ lead to cryogenic overhead conditions in the stabilizer column and in practice one should avoid this by allowing for a larger benzene contents. Therefore in this chapter, we control the condenser temperature T^{stab}_1 at its lowest possible level, $T^{stab}_1 = 77^o$F. Note that the flow rate of this distillate stream is very small so this does not change the economics of the process. We then end up with the following controlled variables:

6. Condenser temperature at stabilizer column $T^{stab}_1 = 77^o$F (lower bound).
7. Methane mole fraction in stabilizer bottoms $x^{stab}_{B,met} = 10^{-6}$ ("optimal" value).
8. Benzene mole fraction in benzene column distillate $x^{bc}_{D,ben} = 0.9997$ (lower bound).
9. Benzene mole fraction in benzene column bottoms $x^{bc}_{B,ben} = 0.0013$ ("optimal" value).
10. Diphenyl mole fraction in toluene column distillate $x^{tc}_{D,dip} = 0.0005$ ("optimal" value).
11. Toluene mole fraction in toluene column bottoms $x^{tc}_{B,tol} = 0.0004$ ("optimal" value).

As the benzene column distillate is essentially composed by benzene and toluene only, we control in practice the toluene mole fraction in the benzene column distillate $x^{bc}_{D,tol}$ instead of $x^{bc}_{D,ben}$ because of measurement accuracy. We also add that except for this active constraint (lower bound), control of the compositions is not important

because the trade-off makes the optimum flat (Araujo *et al.*, 2006). In practice, temperature control will be acceptable for the other products.

The "optimal" values for the distillation columns were found as a trade-off between maximizing the recovery of valuable component and minimizing energy consumption (Araujo *et al.*, 2006).

The remaining number of unconstrained steady-state degrees of freedom is 2 ($13 - 11 = 2$). The first best 10 sets of self-optimizing control variables with the minimum loss are given in Table 4.3 (Araujo *et al.*, 2006). Note that all the best candidates involve compositions.

Table 4.3: *Candidate sets of controlled variables with small losses (Mode I).*

Set	Variables	Average loss$^{(*)}$ [k$/year]
I	Mixer outlet inert (methane) mole fraction ($x_{mix,met}$)	
	Quencher outlet toluene mole fraction ($x_{quen,tol}$)	15.39
II	Mixer outlet inert (methane) mole fraction ($x_{mix,met}$)	
	Toluene conversion at reactor outlet ($c_{rout,tol}$)	26.55
III	Mixer outlet inert (methane) mole fraction ($x_{mix,met}$)	
	Separator liquid benzene mole fraction ($x_{sepliq,ben}$)	31.39
IV	Mixer outlet inert (methane) mole fraction ($x_{mix,met}$)	
	Separator liquid toluene mole fraction ($x_{sepliq,tol}$)	40.40
V	Mixer outlet inert (methane) mole fraction ($x_{mix,met}$)	
	Separator overhead vapor benzene mole fraction ($x_{sepvap,ben}$)	51.75
VI	Mixer outlet inert (methane) mole fraction ($x_{mix,met}$)	
	Gas recycle benzene mole fraction ($x_{gasrec,ben}$)	58.18
VII	Mixer outlet inert (methane) mole fraction ($x_{mix,met}$)	
	Quencher outlet benzene mole fraction ($x_{quen,ben}$)	63.46
VIII	Mixer outlet inert (methane) mole fraction ($x_{mix,met}$)	
	Separator liquid diphenyl mole fraction ($x_{sepliq,dip}$)	66.97
IX	Mixer outlet inert (methane) mole fraction ($x_{mix,met}$)	
	Mixer outlet benzene mole fraction ($x_{mix,ben}$)	72.59
X	Mixer outlet inert (methane) mole fraction ($x_{mix,met}$)	
	Quencher outlet diphenyl mole fraction ($x_{quen,dip}$)	77.54

$^{(*)}$ The average loss is calculated with each variable in the set kept at its nominal optimal set point and taking into account also its implementation error.

4.3.3 Maximum throughput (Mode II)

As mentioned, we consider two modes of operation:

- **Mode I: Given feed rate (F_{tol}).** The optimal operation for this case is described in Araujo *et al.* (2006) and the main results were given in the previous Section.

- **Mode II: Maximum throughput.** From an economic point of view, it is optimal to increase the production rate F_{ben} as much as possible because the prices are such that the profit J increases almost linearly with F_{ben}. However, as discussed in detail below, other process constraints result in bottlenecks that prevent increasing F_{ben} above a certain maximum.

In addition to the process constraints already considered by Araujo *et al.* (2006), we also introduce maximum capacities for the compressor power (+20% compared to nominal), furnace heat duty (+50%), and distillation columns heat duties (+50%). To find the maximum throughput (Mode II) we use the available (maximum) toluene feed rate as a degree of freedom and reoptimize the process (using the profit J from Mode I). The results are summarized in Table 4.4 and the profit J as a function of F_{tol} is shown in Figure 4.4.

Table 4.4: *Re-optimizing with variable toluene feed rate F_{tol}.*

Variable	Nominal	Maximum	Reached at F_{tol} (lbmol/h)
Compressor power (hp)	454.39	545.27 (+20%)	380 (+27%)
Furnace heat duty (MBtu)	16.26	24.39 (+50%)	393 (+31%)[1]
Cooler heat duty (MBtu)	21.57	32.36 (+50%)	410 (+37%)[1,2]
Reactor outlet temperature (^{o}F)	1277	1300	420 (+40%)[1,2,3]
Distillation heat duties		(+50%)	Up to 450 (+50%)[4]

[1] Bottleneck: With compression power at maximum.
[2] Disregarding maximum furnace heat duty.
[3] Disregarding maximum cooler heat duty.
[4] The constraints on the heat duties of the distillation columns (reboiler and condenser) were not reached for F_{tol} up to 450 lbmol/h.

Note that the active constraints from the nominal case ($T_{quencher}$, T_{sep}, $P_{reactor}$, and rH_2) were found to be also active when increasing F_{tol}.

From Table 4.4, we see that the optimal compressor power reaches its maximum (+20%) when the feed rate is increased by 27%. This does not constitute a bottleneck for the process as the toluene feed rate can be further increased by increasing the reactor temperature to counteract for the loss in toluene conversion caused by the constraint on compression power. However, as the toluene feed rate is further increased from 27% to 31%, the maximum constraint on the furnace heat duty Q_{fur} is reached. This is the real bottleneck as a further increase in F_{tol} with Q_{fur} at its maximum, causes infeasible operation. This may be explained because an increase in feed rate with

a fixed furnace heat duty results in a decrease in the reactor temperature, reducing conversion of toluene, which leads to a build-up of toluene that eventually overflows at the benzene column sump and toluene column reflux drum. There is a possibility of counteracting the reduced overall conversion in the reactor by using the remaining unconstrained degree of freedom or "backing off" from one of the economically optimum constraints. However, since maximum conversion is already favored by the economics (and the system is already optimal), none of these options can be used. Therefore, the reactor-recycle system becomes a bottleneck when the constraint on the furnace heat duty is reached. We must then have $Q_{fur} = Q_{fur,max}$ for optimal operation and production rate should be set at this location.

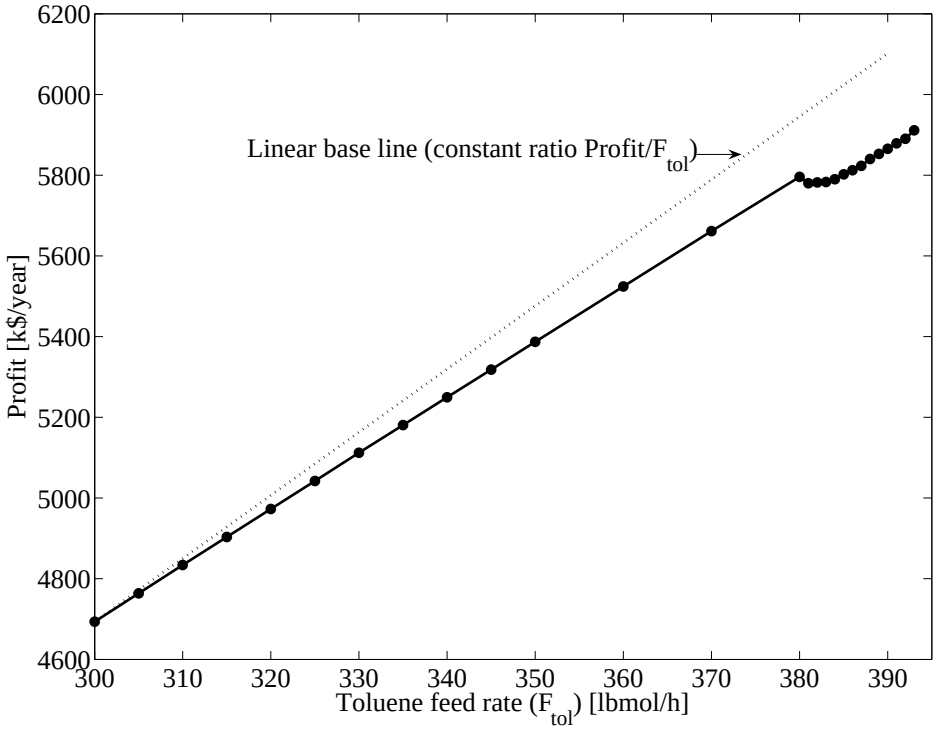

Figure 4.4: *Optimization of the HDA process with variable toluene feed rate. The compressor power reaches its maximum at $F_{tol} = 380$ lbmol/h and the furnace neat duty becomes a bottleneck at $F_{tol} = 393$ lbmol/h.*

We are then left with one unconstrained degree of freedom and we must find a self-optimizing controlled variable for it. With given feed rate (Mode I), we find that mixer outlet inert (methane) molde fraction $x_{mix,met}$ is present in all candidate sets (see Table 4.3) and in order to minimize reconfiguration of loops when switching from one mode of operation to another (from Mode I to Mode II and converse), it would be desirable to select $x_{mix,met}$ as the self-optimizing controlled variable. Fortunately, the loss by keeping $x_{mix,met}$ at its nominally optimal set point in Mode II is acceptable as shown

in Table 4.5. Thus, we decide to select $x_{mix,met}$ as the unconstrained "self-optimizing" controlled variables also in Mode II.

Table 4.5: *Mode II - Maximum production rate (Mode II): Loss by selecting $x_{mix,met}$ as the unconstrained "self-optimizing" controlled variables.*

Case	Description	Optimal		Loss$^{(*)}$
		$x_{mix,met}$	Profit [k$/year]	[k$/year]
Nominal	$F_{tol} = 393$ lbmol/h	0.5555	5931.2	0
D1	Fresh gas feed rate methane mole fraction from 0.03 to 0.08	0.5254	6316.4	175.8
D2	Hydrogen to aromatics ratio in reactor inlet from 5.0 to 5.5	0.4943	6249.6	329.0
D3	Reactor inlet pressure [psi] from 500 to 507	0.5643	6198.7	181.0
D4	Quencher outlet temperature [^{o}F] from 1150 to 1170	0.5381	6371.5	190.4
D5	Product purity in the benzene column distillate from 0.9997 to 0.9980	0.5202	6531.1	277.3
n_y	Implementation error of 0.0001 in $x_{mix,met}$	0.5556	5977.5	46.3

$^{(*)}$ Loss with fixed $x_{mix,met} = 0.5555$ (nominal optimum).

4.3.4 Selection of throughput manipulator

In Mode II, the bottleneck is the furnace heat duty, and optimally the production rate should be set here so that $Q_{fur} = Q_{fur,max}$. However, the reactor is unstable and the furnace heat duty is the most favorable input for closing a stabilizing temperature loop. We must accept some "back off" from the maximum furnace heat duty to avoid saturation in this stabilizing loop. Therefore, we decide to locate the throughput manipulator at the main feed rate (toluene) both in Mode I and Mode II. In Mode II, we use a duty controller that keeps the furnace heat duty at a given value (back off) below its maximum.

4.3.5 Structure of the regulatory control layer

The main objective of this layer is to provide sufficient quality of control to enable a trained operator to keep the plant running safely without the use of the higher layers in the control system. The regulatory control layer should be designed such that it is independent of the mode of operation.

Stabilization of unstable modes (including liquid levels)

In the reaction section, a temperature must be controlled to stabilize the reactor operation. As mentioned, the input with the most direct effect on the reactor temperature is the furnace heat duty (Q_{fur}). We choose to control the reactor inlet temperature (T_{rin}) because Q_{fur} has a direct effect on T_{rin} (with a small effective delay). In addition, there is a lower limit of 1150^oF for this temperature, which may become active in other cases.

The levels in the separator and the reboiler sumps and reflux drums of the distillation columns need to be stabilized. Since the throughput manipulator is at the feed, we use the liquid flow out of the separator to control its level. For the distillation columns we assume LV configuration which means that the reboiler sump and reflux drum levels are controlled by distillate and bottoms rate, respectively. The exception is the reflux drum level of the stabilizer that is controlled by the condenser heat duty.

Avoiding drift I: Pressure control

In addition to stabilizing unstable modes, the regulatory control layer has as a primary objective to prevent the plant from drifting away from its desired operating point on the short time scale. Pressure dynamics are generally very fast, so pressure drift is avoided by controlling pressure at selected locations in the plant. First, pressure should be controlled somewhere in the reactor recycle loop. The obvious choice is the reactor inlet pressure P_{rin} which is an active constraint and must be controlled at its nominal optimal set point for optimal operation. There are three manipulated variables that can effectively be used to controlled P_{rin}, namely fresh gas feed F_{hyd}, compressor power W_s, and purge flow rate F_{purge}. One could also consider cooler heat duty Q_{cool} but since the separator temperature T_{sep} must be also controlled (active constraint) and Q_{cool} has a direct effect on T_{sep}, we decided not to consider Q_{cool} as an alternative. Furthermore, since pressure control should be fast, F_{hyd} and W_s are not good choices. First, excessive movement of F_{hyd} will likely upset the plant too much since F_{hyd} directly affects the mass balance of the process. Second, the compressor is an expensive and delicate piece of equipment, so compressor power W_s is usually avoided as a manipulated variable, at least on a fast time scale. This leaves F_{purge} as the choice for controlling P_{rin}.

The pressures in the distillation columns need also be controlled and we use condenser heat duty as manipulated variables. An exception is made for the stabilizer where distillate rate (vapor) is used instead.

Avoiding drift II: Temperature loops

Temperature measurements are are fast and reliable, so temperature loops are frequently closed to avoid drift.

Since the operation of the separator has a large impact on both the gas recycle loop and the separation section, its temperature should be controlled. Moreover, this temperature has been identified as an active constraint. Therefore, a temperature loop is placed in the separator. The choice for the manipulated variable in this case is the cooler heat duty.

In addition, the quencher outlet temperature $T_{quencher}$ (also an active constraint) must be controlled to prevent coke formation upstream to the quencher. We use the flow rate of the cold liquid stream from the separator as the manipulated variable.

The composition control in the distillation columns is usually slow because of measurement delays and interactions. Thus, temperatures should also be controlled in the distillation columns to avoid drift on the fast time scale. However, it is not clear which stages to select for temperature control and this calls for a more detailed analysis based on self-optimizing control considerations. The idea is to select a temperature location at a given stage in the distillation column T_j so to minimize the offset in the composition of important products when disturbances occur. To find the best location, we use the maximum gain rule that maximizes the gain of the linearized model G from $u = Q_{reb}$ to $y = T_j$ (Skogestad and Postlethwaite, 2005). For dynamic reasons, we should also avoid locations where the temperature slope is small (Hori and Skogestad, 2006). The results are shown in Figure 4.5.

For the stabilizer, Figure 4.5a shows that the best choice from a steady-state point of view would be to control temperature around stage 5 since the scaled gain is higher at this location. However, as the temperature slope at this stage is very small, this may give difficult control problems dynamically, so we decide to use stage 3 (T_3^{stab}) instead.

The benzene and toluene columns are essentially binary columns and we expect the scaled gain and temperature slope to have their peaks at the same section. This is confirmed by Figures 4.5b and c. Therefore, for the benzene column we control temperature at stage 20 (T_{20}^{bc}), and for the toluene column at stage 5 (T_5^{tc}).

Avoiding drift III: Flow control

To reduce drift caused by pressure changes, but also to avoid nonlinearity in control valves, we use flow controllers for toluene feed rate F_{tol} and hydrogen feed rate F_{hyd}.

Possible "intermediate" regulatory layer

The primary controlled variables that we want to control for economic reasons are given in Section 4.3.2. We here focus on the reactor-recycle system as the distillation column units are not critical for the economics in this case (first, because the loss for composition change is small (Araujo *et al.*, 2006) and second, because they are not bottlenecks (see Section 4.3.3). The question here is: Do we need any intermediate regulatory layer, or will control of the secondary controlled variables y_2 indirectly result in "acceptable"

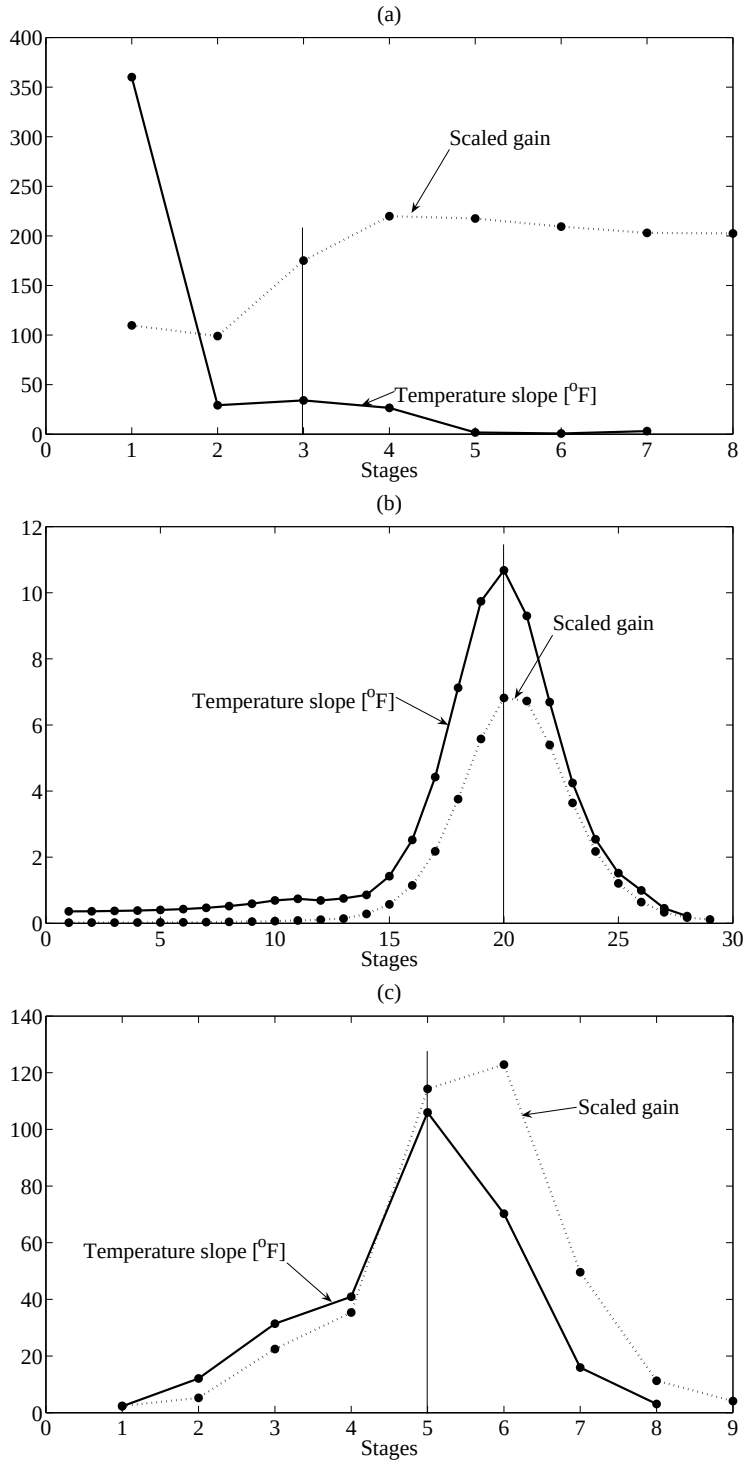

Figure 4.5: *Temperature slope (solid line) and scaled gain (dotted line) for distillation columns. Temperature should be controlled at a location where both are sufficiently large. (a) Results for stabilizer; (b) Results for benzene column; (c) Results for toluene column.*

control of the primary controlled variables y_1? If we compare the variables controlled in the regulatory control layer (designed so far) with the primary controlled variables, then we still need to control 3 compositions in Mode I (rH_2,$x_{mix,met}$, and $x_{quen,tol}$) and 2 compositions in Mode II (rH_2 and $x_{mix,met}$). The composition control will be slow because of measurement delays, so, as mentioned in Section 4.2.3, we may introduce an intermediate layer where we control the extra variables y_1' which are easier to control on the intermediate time scale. The degrees of freedom (manipulated variables u_1') are F_{hyd}, $T_{rin,sp}$, and W_s. In Mode II, W_s is fixed at its maximum and is therefore not available, and also in Mode I we choose not use W_s at this relatively fast time scale.

Once more, the maximum gain rule (Skogestad and Postlethwaite, 2005) is used to decide which variables should be controlled. We chose not use W_s at the intermediate time scale. The candidate controlled variables y_1' are chosen to be temperatures, flows, and pressures in the reaction section (compositions are ruled out for obvious reasons) as well as the three manipulated variables themselves. The result of the maximum gain rule analysis is seen in Table 4.6 for Mode I.

Table 4.6: *Local analysis for possible "intermediate" regulatory control: Maximum (scaled) singular rule of best sets of candidate controlled variables (W_s is assumed constant).*

Set	Controlled variables	$\underline{\sigma}(S_1 G J_{uu}^{-1/2})$ ·1000
I	FEHE hot side outlet temperature ($T_{fehe,hs}$) Fresh gas feed rate (F_{hyd})	0.4939
II	FEHE hot side outlet temperature ($T_{fehe,hs}$) Mixer outlet flow rate (F_{mix})	0.4937
III	FEHE hot side outlet temperature ($T_{fehe,hs}$) Separator vapor outlet flow rate ($F_{sep,vap}$)	0.4929
IV	FEHE hot side outlet temperature ($T_{fehe,hs}$) Quencher outlet flow rate (F_{quen})	0.4923
V	Reactor outlet temperature (T_{rout}) Fresh gas feed rate (F_{hyd})	0.4911
VI	Reactor outlet temperature (T_{rout}) Mixer outlet flow rate (F_{mix})	0.4909
VII	Furnace outlet temperature (T_{rin}) Fresh gas feed rate (F_{hyd})	0.4907
VIII	Furnace outlet temperature (T_{rin}) Mixer outlet flow rate (F_{mix})	0.4906
IX	Reactor outlet temperature (T_{rout}) Separator vapor outlet flow rate ($F_{sep,vap}$)	0.4900
X	Furnace outlet temperature (T_{rin}) Separator vapor outlet flow rate ($F_{sep,vap}$)	0.4895

As seen from Table 4.6, the economic loss by controlling $u_1' = \{F_{hyd}, T_{rin,sp}, W_s\}$

(Set VII) is almost the same as for the best set in the table (Set I). Thus, we decide that there is no benefit of an additional "intermediate" layer for indirect composition control in this case.

Summary on the regulatory control layer

In summary, we have decided to close the following regulatory loops in the reactor-recycle section (Modes I and II):

RgRR1. Flow control of hydrogen feed rate F_{hyd}.

RgRR2. Reactor inlet pressure P_{rin} with purge flow F_{purge}.

RgRR3. Flow control of toluene feed rate F_{tol}.

RgRR4. Quencher outlet temperature $T_{quencher}$ with cooling flow from separator $F_{sep,liq}$.

RgRR5. Reactor inlet temperature T_{rin} with furnace heat duty Q_{fur}.

RgRR6. Separator temperature T_{sep} with cooler heat duty Q_{cool}.

RgRR7. Separator level using its liquid outlet flow rate to the distillation section.

As for the distillation section, we have decided for the following regulatory control structure (Modes I and II):

RgDC1. Stabilizer pressure P_{stab} with distillate flow rate D_{stab}.

RgDC2. Benzene column pressure P_{bc} with condenser heat duty Q^{bc}_{cond}.

RgDC3. Toluene column pressure P_{tc} with condenser heat duty Q^{tc}_{cond}.

RgDC4. Temperature at stage 3 T^{stab}_3 with reboiler heat duty Q^{stab}_{reb} in the stabilizer.

RgDC5. Temperature at stage 20 T^{bc}_{20} with reboiler heat duty Q^{bc}_{reb} in the benzene column.

RgDC6. Temperature at stage 5 T^{tc}_5 with reflux rate L_{tc} in the benzene column.

RgDC7. Reflux drum level with condenser heat duty Q^{stab}_{cond} in the stabilizer.

RgDC8. Reboiler sump level with bottoms flow rate B_{stab} in the stabilizer.

RgDC9. Reflux drum level with distillate flow rate D_{bc} in the benzene column.

RgDC10. Reboiler sump level with bottoms flow rate B_{bc} in the benzene column.

RgDC11. Reflux drum level with distillate flow rate D_{tc} in the toluene column.

RgDC12. Reboiler sump level with bottoms flow rate B_{tc} in the toluene column.

4.3.6 Structure of the supervisory control layer

The production rate is set at the toluene feed rate. In Mode I it is fixed and in Mode II it is adjusted to give the desired maximum furnace duty.

The aim of the supervisory control layer is to keep the active constraints and unconstrained (self-optimizing) controlled variables at constant set points. For the unconstrained controlled variables, we select in Mode I to control Set I in Table 4.3, i.e. mixer outlet inert (methane) mole fraction ($x_{mix,met}$) and quencher outlet toluene mole fraction ($x_{quen,tol}$). In Mode II, the compression power W_s is not available as a degree of freedom, and we only control $x_{mix,met}$.

We here consider in detail Mode I. With the regulatory control in place, there are still 9 composition loops (3 compositions in the reactor-recycle section and 2 in each distillation column) to be closed, and we will proceed with a more detailed analysis based on RGA methods which requires a linear model of the process and for this we use the linearization capabilities of Aspen Dynamics^{TM}. A linearization script defining controlled and manipulated variables can be easily written in Aspen Dynamics^{TM} and the linear state-space model with constant matrices A, B, C, and D generated by the code are exported to MatLab^{TM} to be used in the linear analysis.

We start with the distillation columns taken one at the time. The steady-state RGA matrix tells us in all cases to use the expected pairing where reflux controls the top product. For the stabilizer, $u = [L_{stab}\ T^{stab}_{3,sp}]$ and $y = [T^{stab}_{1}\ x^{stab}_{B,met}]$ and the RGA matrix

$$\Lambda_{stab}(0) = \begin{bmatrix} 0.9844 & 0.0156 \\ 0.0156 & 0.9844 \end{bmatrix}$$

suggests to pair reflux rate (L_{stab}) with condenser temperature (T^{stab}_{1}) and the set point of the temperature controller at stage 3 ($T^{stab}_{3,sp}$) with methane mole fraction in bottoms ($x^{stab}_{B,met}$).

The steady-state RGA matrix for the benzene column (with $u = [L_{bc}\ T^{bc}_{20,sp}]$ and $y = [x^{bc}_{D,tol}\ x^{bc}_{B,ben}]$)

$$\Lambda_{bc}(0) = \begin{bmatrix} 1.8457 & -0.8457 \\ -0.8457 & 1.8457 \end{bmatrix}$$

indicates the pairing should be reflux rate (L_{bc}) with benzene mole fraction in distillate ($x^{bc}_{D,tol}$) and the set point of the temperature controller at stage 20 ($T^{bc}_{20,sp}$) with benzene mole fraction in bottoms ($x^{bc}_{B,ben}$).

As for the toluene column, since the stream of interest is the distillate (recycle of toluene to the process), we choose to use reflux rate (L_{tc}) to control the temperature at stage 5 (T^{tc}_{5}). This gives a steady-state RGA matrix (with $u = [Q^{tc}_{reb}\ T^{tc}_{5,sp}]$ and $y = [x^{tc}_{B,tol}\ x^{tc}_{D,dip}]$)

$$\Lambda_{tc}(0) = \begin{bmatrix} 1.3187 & -0.3187 \\ -0.3187 & 1.3187 \end{bmatrix}$$

and the chosen pairing is reboiler heat duty (Q^{tc}_{reb}) with toluene mole fraction in bottoms ($x^{tc}_{B,tol}$) and the set point of the temperature controller at stage 5 ($T^{tc}_{5,sp}$) with diphenyl mole fraction in distillate ($x^{tc}_{D,dip}$).

For the reactor-recycle section, a control configuration for the remaining 3×3 partially controlled system (here denoted $\hat{g}_{3\times3}$) with the available manipulations

$$u = \{T_{rin,sp}; W_s; F_{hyd,sp}\} \tag{4.3}$$

and controlled variables

$$y = \{rH_2; x_{mix,met}; x_{quen,tol}\} \tag{4.4}$$

need to be designed, where $T_{rin,sp}$ is the set point of the temperature controller at the reactor inlet, $F_{hyd,sp}$ is the set point of the hydrogen feed rate flow controller, $x_{mix,met}$ is the methane mole fractions at mixer outlet and $x_{quen,tol}$ is the toluene mole fraction at quencher outlet.

To check the controllability of the 3×3 system ($\hat{g}_{3\times3}$), we obtain the zeros, and found two pairs of RHP-zeros ($250\pm908i$ and $588\pm346i$ rad/h), but these are located quite far into the right-half plane (corresponding to an effective delay at about $\frac{1}{250}\text{h} = 0.24\text{min}$) and will not cause any performance limitations. We also found that the RHP-zeros were moved closer to the origin (becoming more restrictive) by loosening the control (using lower gains) in the regulatory loops. This indicates that we have paired on negative steady-state gains in the lower loops (Cui and Jacobsen, 2002), but this is not a problem as long as the regulatory loops do not fail (e.g., saturate) and are sufficiently fast.

At first sight, it seems reasonable to pair $F_{hyd,sp}$ with rH_2 (hydrogen to aromatic ratio at reactor inlet) since we might expect $F_{hyd,sp}$ to have a large and direct effect on rH_2. However, a more detailed steady-state RGA analysis of $\hat{g}_{3\times3}$ where

$$\Lambda_{reac}(0) = \begin{bmatrix} -0.3736 & \underline{1.1774} & 0.1962 \\ 0.5032 & -0.1439 & \underline{0.6407} \\ \underline{0.8704} & -0.0335 & 0.1631 \end{bmatrix}$$

suggests this should be avoided due to pairing on negative steady-state RGA elements. To avoid pairing on negative RGA elements, we must pair $T_{rin,sp}$ with $x_{quen,tol}$; W_s with rH_2; and $F_{hyd,sp}$ with $x_{mix,met}$. Figure 4.6 shows that the RGA number ($||\Lambda(\hat{g}_{3\times3}) - I_3||_{sum}$) as a function of frequency with these pairings, and we find that the dynamic interactions are also small.

Summary on the supervisory control layer

In summary, we close the following supervisory control loops in the reactor-recycle section (Mode I):

> SpRR1. Toluene mole fraction at quencher outlet $x_{quen,tol}$ with set point of the reactor temperature controller $T_{rin,sp}$.

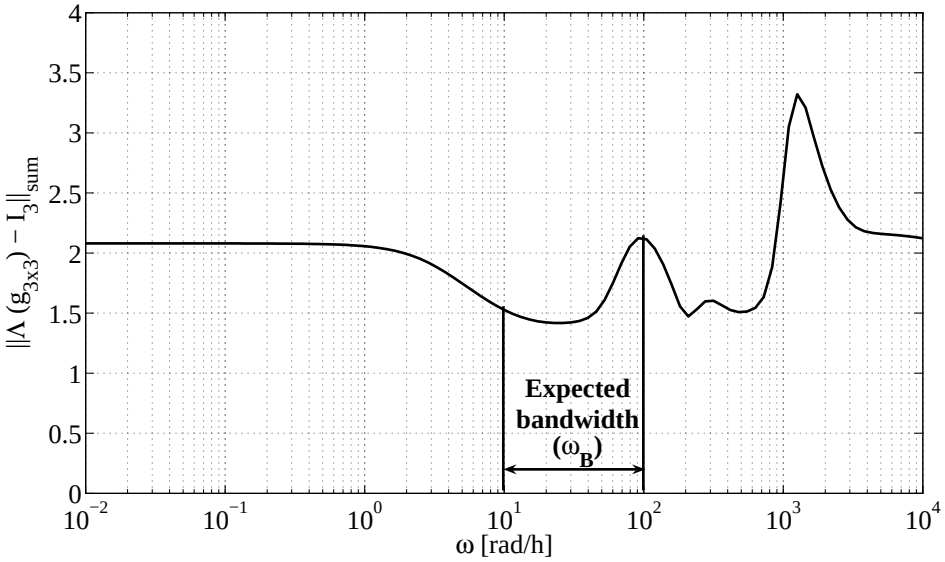

Figure 4.6: *RGA number as a function of frequency for $\hat{g}_{3\times3}$ with pairing given by $T_{rin,sp}$ - $x_{quen,tol}$; W_s - rH_2; and $F_{hyd,sp}$ - $x_{mix,met}$.*

SpRR2. Methane mole fraction at mixer outlet $x_{mix,met}$ with set point of the hydrogen feed rate flow controller $F_{hyd,sp}$.

SpRR3. Hydrogen to aromatic ratio at reactor inlet rH_2 with compressor power W_s.

In addition, in the distillation section we close the following supervisory loops (Modes I and II):

SpDC1. Toluene mole fraction in bottoms $x^{tc}_{B,tol}$ with reboiler heat duty Q^{tc}_{reb} in the toluene column.

SpDC2. Benzene mole fraction in bottoms $x^{bc}_{B,ben}$ with the set point of the temperature controller at stage 20 $T^{bc}_{20,sp}$ in the benzene column.

SpDC3. Toluene mole fraction in distillate $x^{bc}_{D,tol}$ with reflux rate L_{bc} in the benzene column.

SpDC4. Methane mole fraction in bottoms $x^{stab}_{B,met}$ with the set point of the temperature controller at stage 3 $T^{stab}_{3,sp}$ in the stabilizer.

SpDC5. Diphenyl mole fraction in distillate $x^{tc}_{D,dip}$ with the set point of the temperature controller at stage 5 $T^{tc}_{5,sp}$ in the toluene column.

SpDC6. Condenser temperature T^{stab}_{1} with reflux rate L_{stab} in the stabilizer.

Switching between Mode I and Mode II

For Mode I, the strategy is to keep the toluene feed rate F_{tol} constant at its nominally optimal set point. For Mode II, F_{tol} controls the furnace heat duty $Q_{fur,sp} = Q_{fur,max} - Q_{fur,bkoff}$ (non-optimal strategy), where $Q_{fur,bkoff}$ is a back-off value (input resetting) imposed to the furnace heat duty so that it can handle disturbances in the reactor temperature T_{rin} without causing the reactor operation to becoming unstable. This back-off value must be decided based on the expected disturbances for the reactor temperature control loop.

Switching from Mode I to Mode II is accomplished through the following logic steps:

1. Break the loop between W_s and rH_2 and fix the compressor power W_s at its maximum.
2. Use $F_{hyd,sp}$ to control rH_2 (to assure active constraint control).
3. Use $T_{rin,sp}$ to control $x_{mix,met}$ and change the set point of $x_{mix,met}$ from its nominally optimal value in Mode I (0.5724) by its nominally optimal value in Mode II (0.5555).
4. Use $F_{tol,sp}$ to control Q_{fur} (production rate manipulation).
5. Tune the loops with the parameters listed in Tables 4.7 and 4.8. Note that only the loops $F_{hyd,sp}$ - rH_2 and $F_{tol,sp}$ - Q_{fur} need to be retuned.

Controller tuning

The lower layer loops selected above are closed and tuned one at the time in a sequential manner (starting with the fastest loops). Aspen Dynamics^{TM} has an open loop test capability that was used to determine a first-order plus delay model from u to y. Based on the model parameters, we used the SIMC tuning rules (Skogestad, 2004*b*) to design the PI-controllers:

$$K_c = \frac{1}{k}\frac{\tau}{\tau_c + \theta}, \quad \tau_I = \min[\tau, 4(\tau_c + \theta)] \tag{4.5}$$

where k, τ, and θ are the gain, time constant, and effective time delay, respectively. In our case, we choose $\tau_c = 3\theta$ to give smooth control with acceptable performance in terms of disturbance rejection.

The controllers parameters, gain K_c and integral time τ_I, are given in Tables 4.7 and 4.8 for the reactor-recycle section and distillation section, respectively. See also Figures 4.7 and 4.8 for the controller tag.

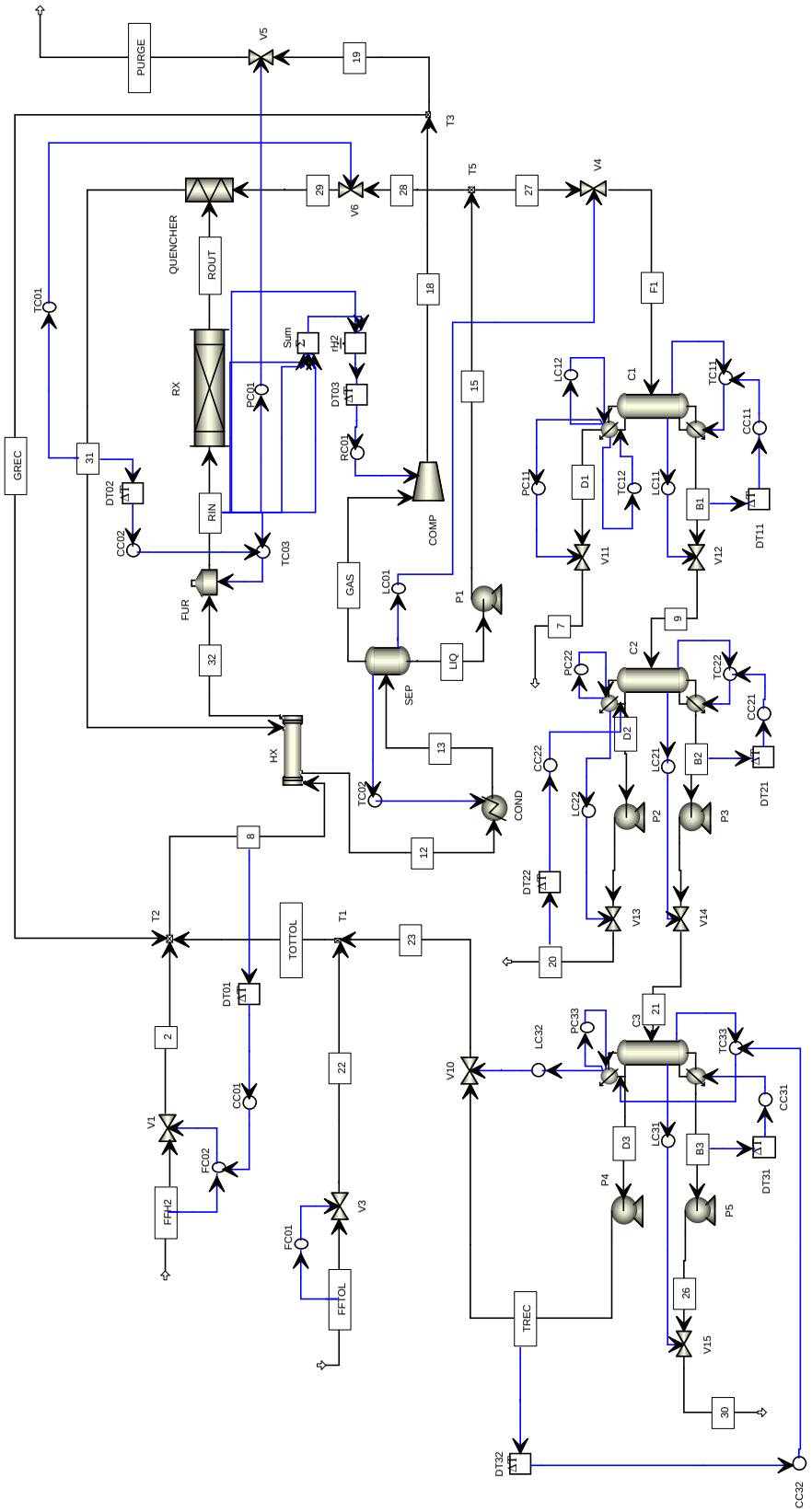

Figure 4.7: *Mode I: HDA Aspen Dynamics^{TM} process flowsheet with controllers installed.*

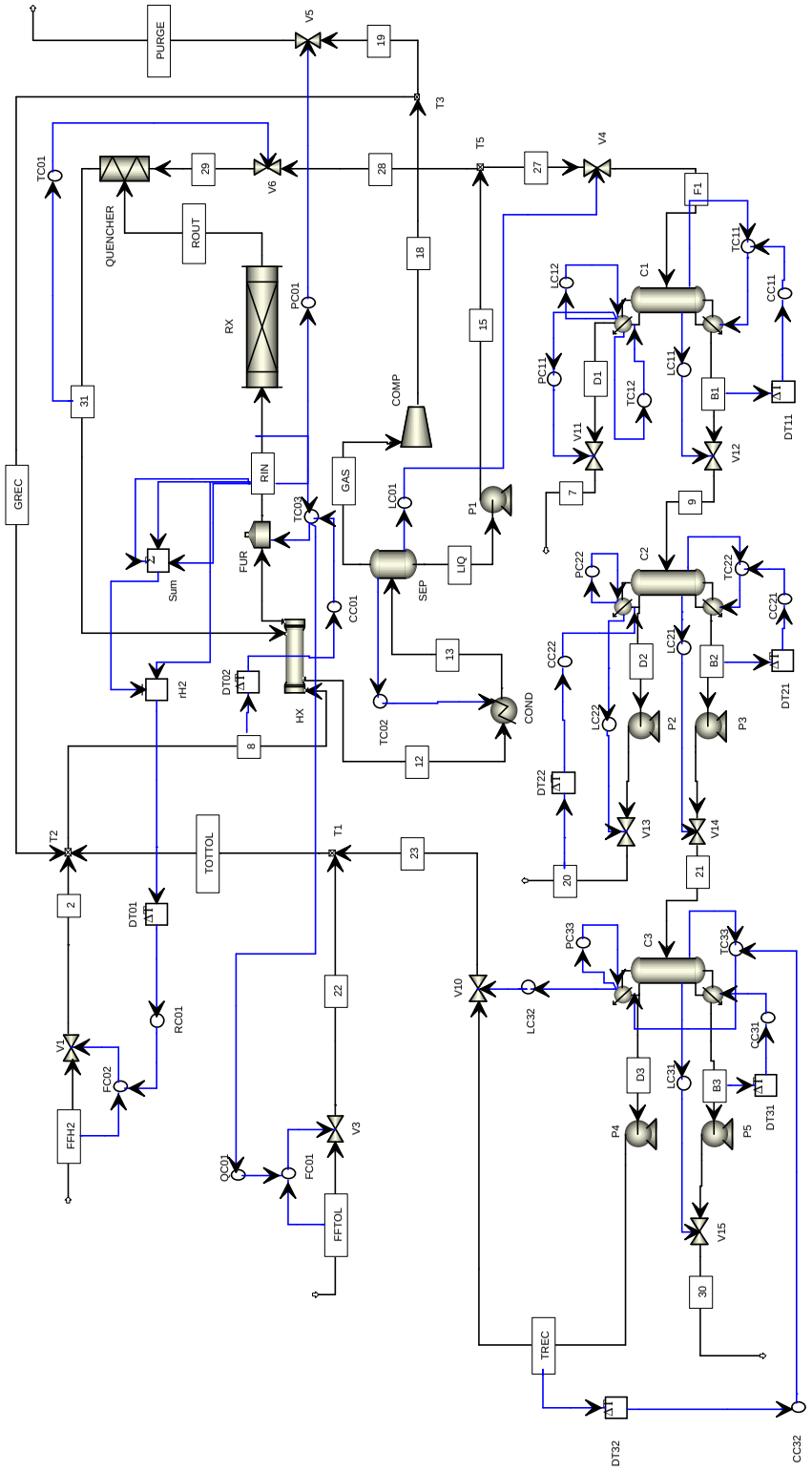

Figure 4.8: *Mode II: HDA Aspen Dynamics™ process flowsheet with controllers installed.*

Table 4.7: *Tuning parameters for the reactor-recycle section (Modes I and II).*

		Loop		PI-controller parameters	
No.	Input	Output	Tag[a]	K_c (%/%)	τ_I (min)
RgRR1	V_1	F_{hyd}	FC02	3.08	0.65
RgRR2	V_5	P_{rin}	PC01	144.7	0.80
RgRR3	V_3	F_{tol}	FC01	3.13	0.57
RgRR4	V_6	$T_{quencher}$	TC01	34.98	0.47
RgRR5	Q_{fur}	T_{rin}	TC03	9.83	0.67
RgRR6	Q_{cool}	T_{sep}	TC02	1.36	0.80
RgRR7	M_{sep}	$F_{sep,liq}$	LC01	2	-
SpRR1[b]	$T_{rin,sp}$	$x_{quen,tol}$	CC02	0.69	2.93
SpRR2	$F_{hyd,sp}$	$x_{mix,met}$	CC01	0.54	12.48
SpRR3	W_s	rH_2	RC01	0.27	2.86
SpRR2[c]	$T_{rin,sp}$	$x_{mix,met}$	CC01	0.54	12.48
SpRR3[c]	$F_{hyd,sp}$	rH_2	RC01	0.07	49.55
SpRR4[c]	$F_{tol,sp}$	Q_{fur}	QC01	1	100

[a] See tags in Figures 4.7 and 4.8.
[b] This loop is only activated in Mode I.
[c] This loop is only activated in Mode II.

4.3.7 Structure of the optimization layer

Since we obtained a design that takes care of important disturbances (self-optimizing control structure) with acceptable loss, on-line optimization is not needed.

4.4 Dynamic simulations

In this section, we compare the control structure designed in this study with the one proposed by Luyben (2002) for Mode I of operation. They are both based on the same underlying Aspen model but Luyben (2002) consider a different steady-state operating point. However, the best control structure should not depend on the operating point. In order to have a consistent basis for comparison, we use the steady-state considered in this chapter but maintain the original tuning settings determined by Luyben (2002). Figures 4.9 through 4.12 compares the results for the disturbances in Table 5.15.

From Figures 4.9 - 4.12, we can see that the structure of Luyben (2002) is not optimal (or even feasible) in some cases, since the hydrogen-to-aromatic ratio at reactor inlet rH_2 and product purity $x^{bc}_{D,ben}$, which are active constraints, are not controlled. Moreover, Luyben (2002) does not consider using compressor power W_s as a degree

Table 4.8: *Tuning parameters for the distillation section (Modes I and II).*

		Loop		PI-controller parameters	
No.	Input	Output	Tag[a]	K_c (%/%)	τ_I (min)
RgDC1	V_{11}	P_{stab}	PC11	122.02	0.80
RgDC2	Q^{tc}_{cond}	P_{tc}	PC33	56.30	0.80
RgDC3	Q^{bc}_{cond}	P_{bc}	PC22	21.047	0.80
RgDC4	Q^{stab}_{reb}	T^{stab}_{3}	TC11	1.23	0.80
RgDC5	L_{tc}	T^{tc}_{5}	TC33	110.44	1.12
RgDC6	Q^{bc}_{reb}	T^{bc}_{20}	TC22	5.82	4.8
RgDC7	M^{stab}_{D}	Q^{stab}_{cond}	LC11	2	-
RgDC8	M^{stab}_{B}	B_{stab}	LC12	2	-
RgDC9	M^{bc}_{D}	D_{bc}	LC21	20	-
RgDC10	M^{bc}_{B}	B_{bc}	LC22	2	-
RgDC11	M^{tc}_{D}	D_{tc}	LC31	2	-
RgDC12	M^{tc}_{B}	B_{tc}	LC32	20	-
SpDC1	Q^{tc}_{reb}	$x^{tc}_{B,tol}$	CC31	40.96	16.19
SpDC2	$T^{bc}_{20,sp}$	$x^{bc}_{B,ben}$	CC21	6.69	4.56
SpDC3	L_{bc}	$x^{bc}_{D,tol}$	CC22	432.64	25.60
SpDC4	$T^{stab}_{3,sp}$	$x^{stab}_{B,met}$	CC11	5611.33	1.74
SpDC5	$T^{tc}_{5,sp}$	$x^{tc}_{D,dip}$	CC32	56.95	52.61
SpDC6	L_{stab}	T^{stab}_{1}	TC12	4243.41	0.8

[a] See tags in Figures 4.7 and 4.8.

Table 4.9: *Disturbances for dynamic simulations of the HDA process.*

	Variable	Nominal(*)	Disturbance (Δ)
Dyn1	Toluene feed rate (F_{tol})	300 lbmol/h	+30 lbmol/h (+10%)
Dyn2	Toluene feed rate (F_{tol})	300 lbmol/h	-30 lbmol/h (-10%)
Dyn3	Methane mole fraction in hydrogen feed rate (x_{met})	0.03	+0.05
Dyn4	Quencher outlet temperature ($T_{quencher}$)	1150^{o}F	+20^{o}F

(*) This refers to the optimal nominal considered in this work.

of freedom in contrast with our control structure that makes use of W_s for long term control. However, in general, the dynamic responses of the two control structures are similar with essentially the same settling time (about 4 hours) and with small oscillations.

For Mode II of operation, we found that a back-off in furnace heat duty (Q_{fur}) of 98% takes care of most disturbances without saturation of Q_{fur}. The simulation results for disturbances Dyn3 and Dyn4 are depicted in Figures 4.13 - 4.14. We can see that the responses are not as good as those of Mode I of operation but they are still satisfactory if we consider that practically no retune from Mode I was done.

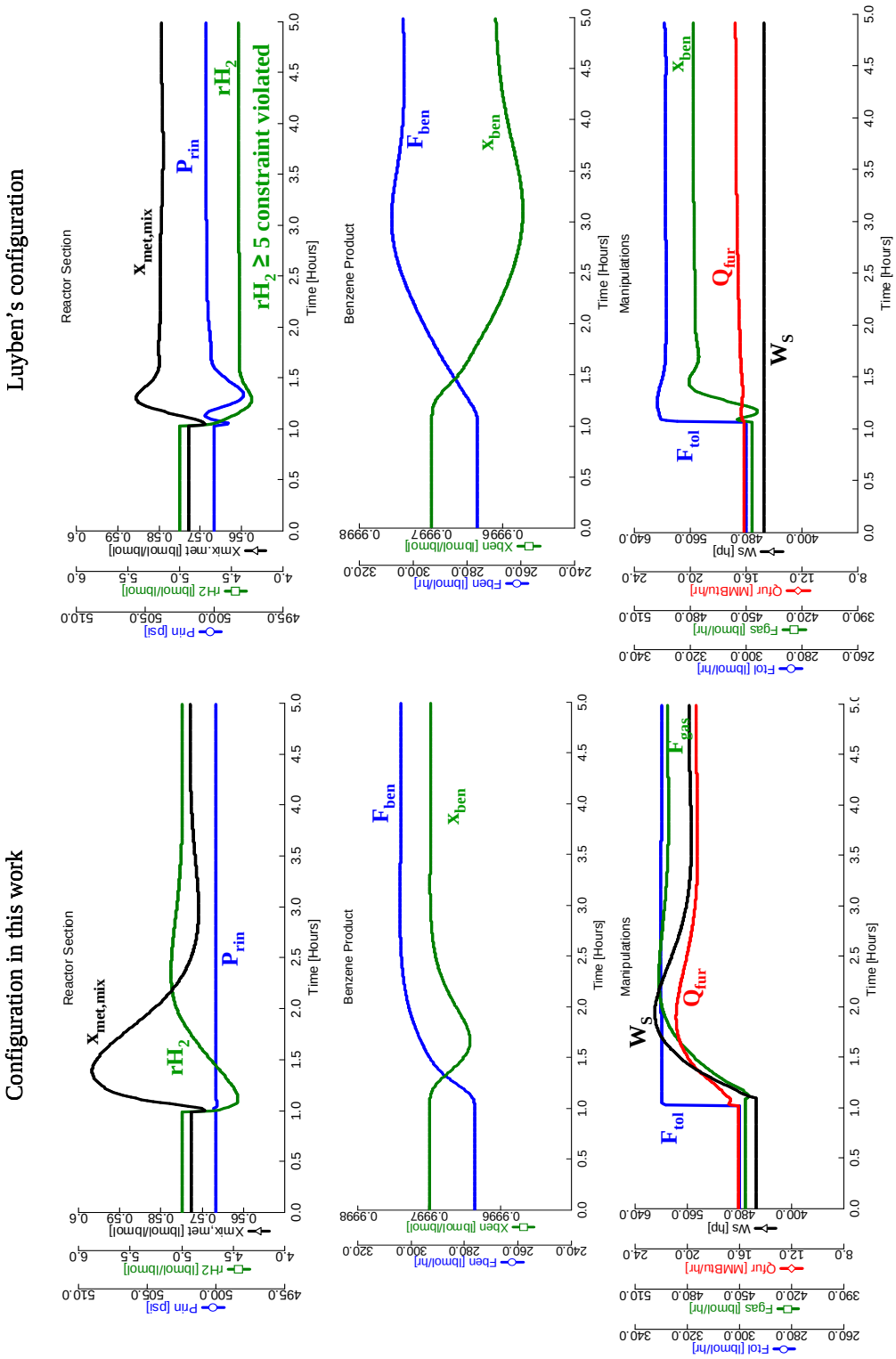

Figure 4.9: *Mode I: Dynamic response of selected variables for disturbance Dyn1: +10% increase in F_{tol}.*

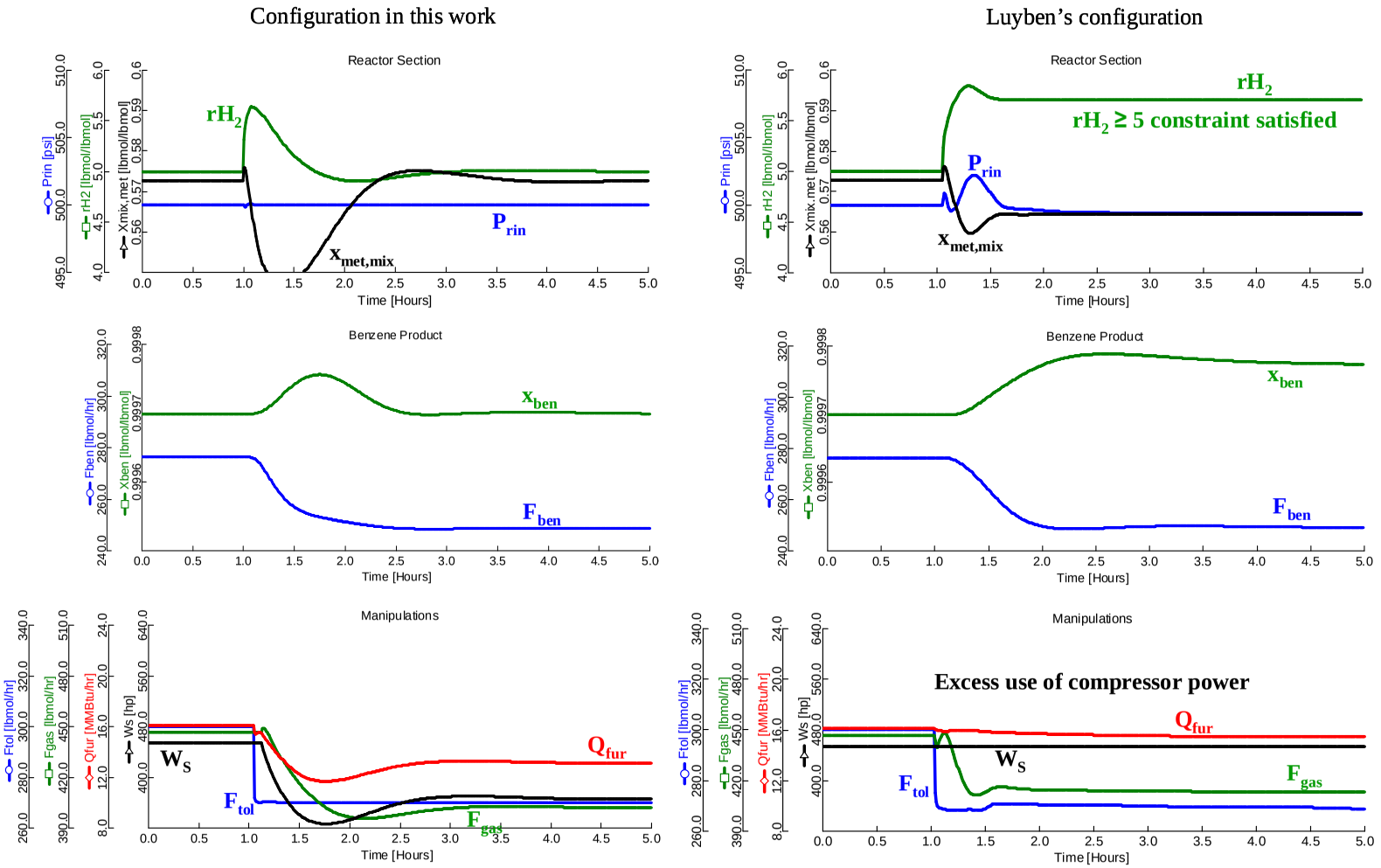

Figure 4.10: *Mode I: Dynamic response of selected variables for disturbance Dyn2: -10% increase in* F_{tol}.

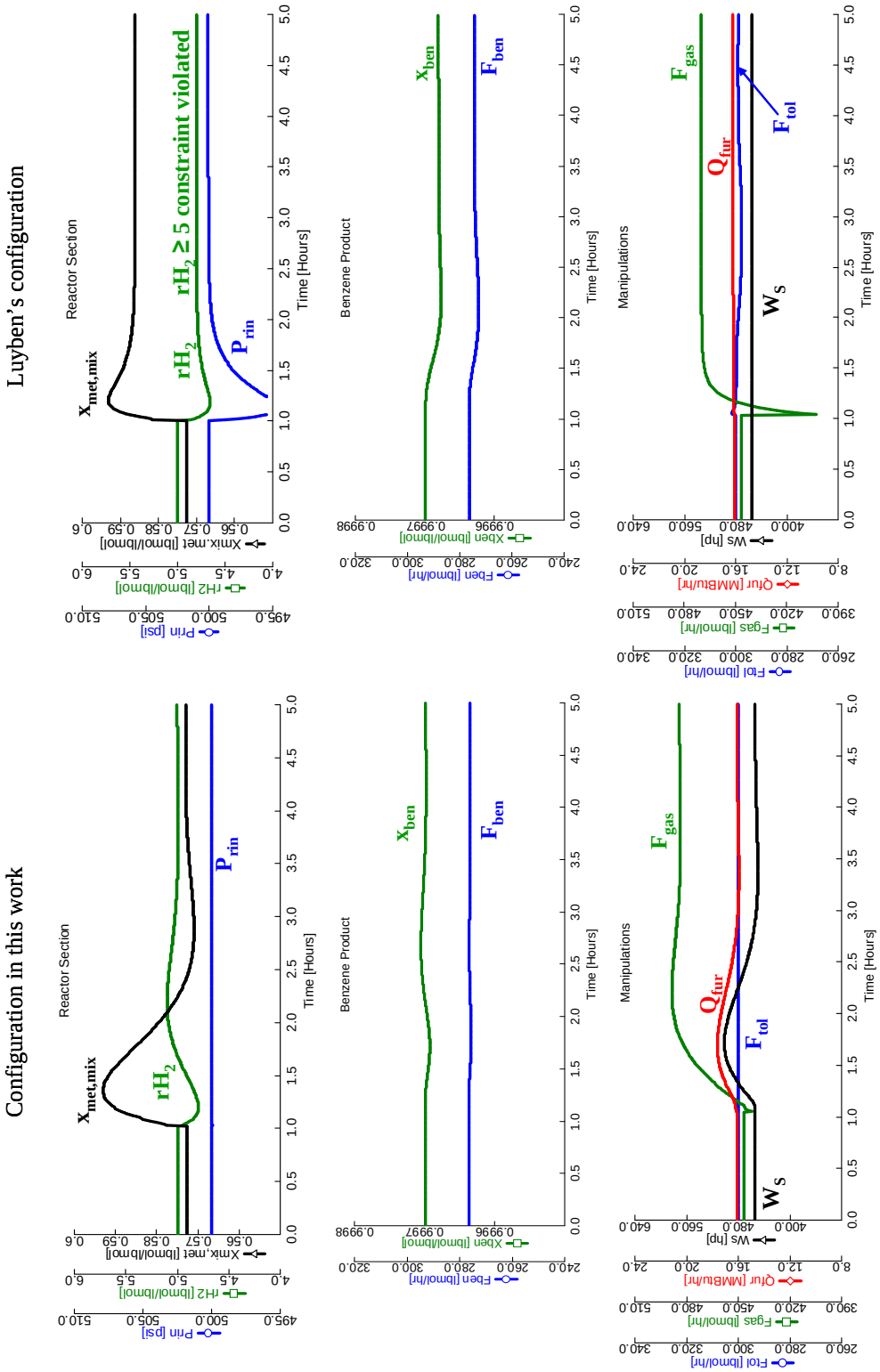

Figure 4.11: *Mode I: Dynamic response of selected variables for disturbance Dym3: +0.05 increase in* x_{met}.

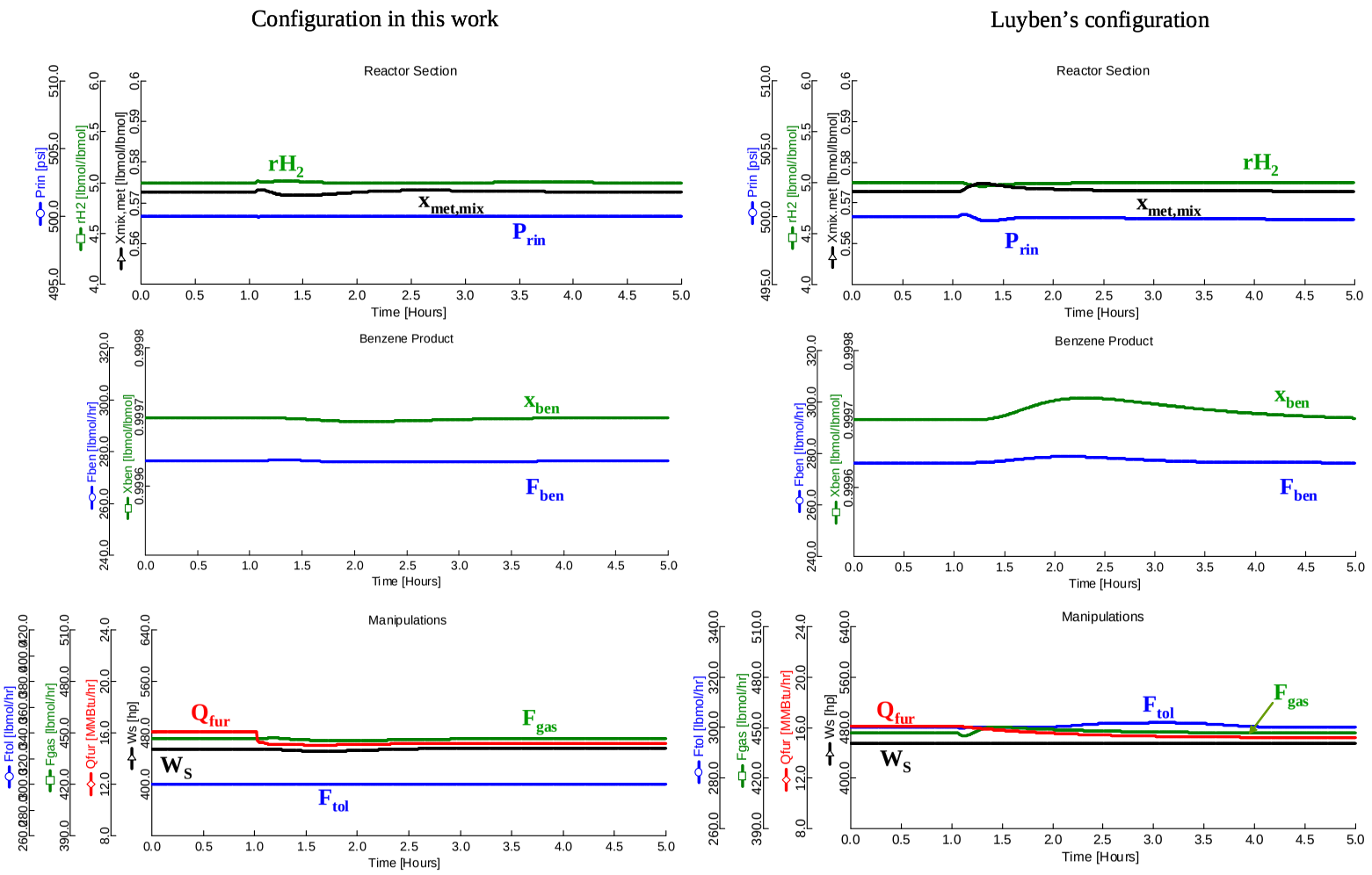

Figure 4.12: *Mode I: Dynamic response of selected variables for disturbance Dyn4: +20°F increase in* $T_{quencher}$.

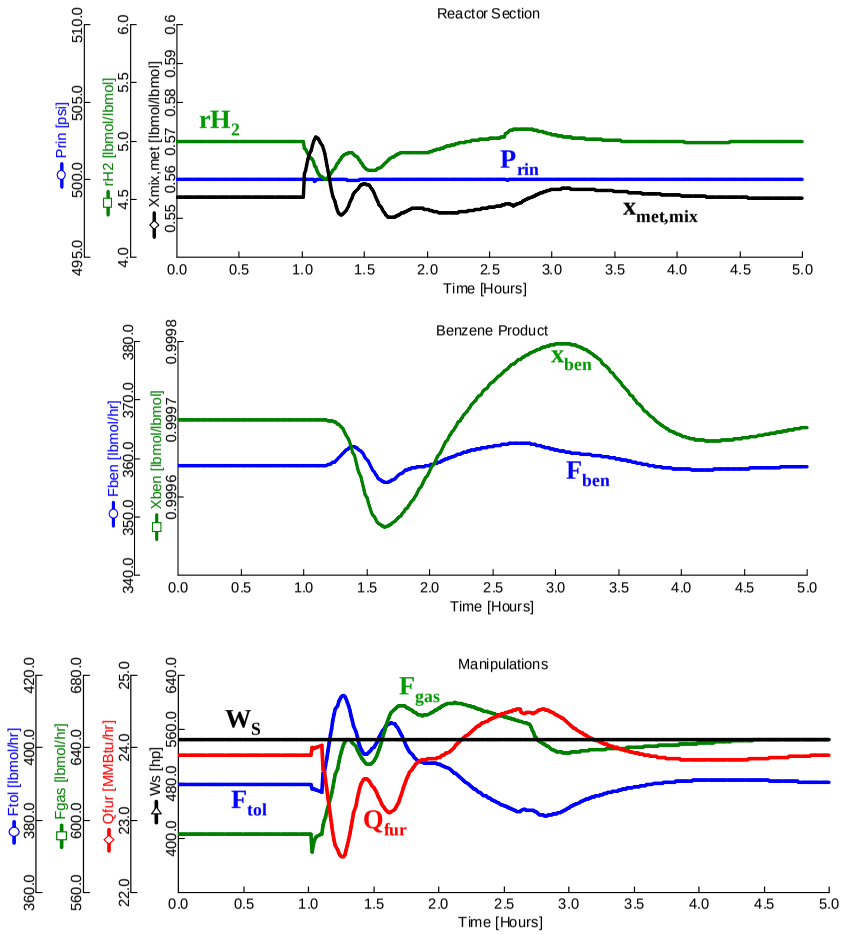

Figure 4.13: *Mode II (this work): Dynamic response of selected variables for disturbance Dyn3: +0.05 increase in x_{met}.*

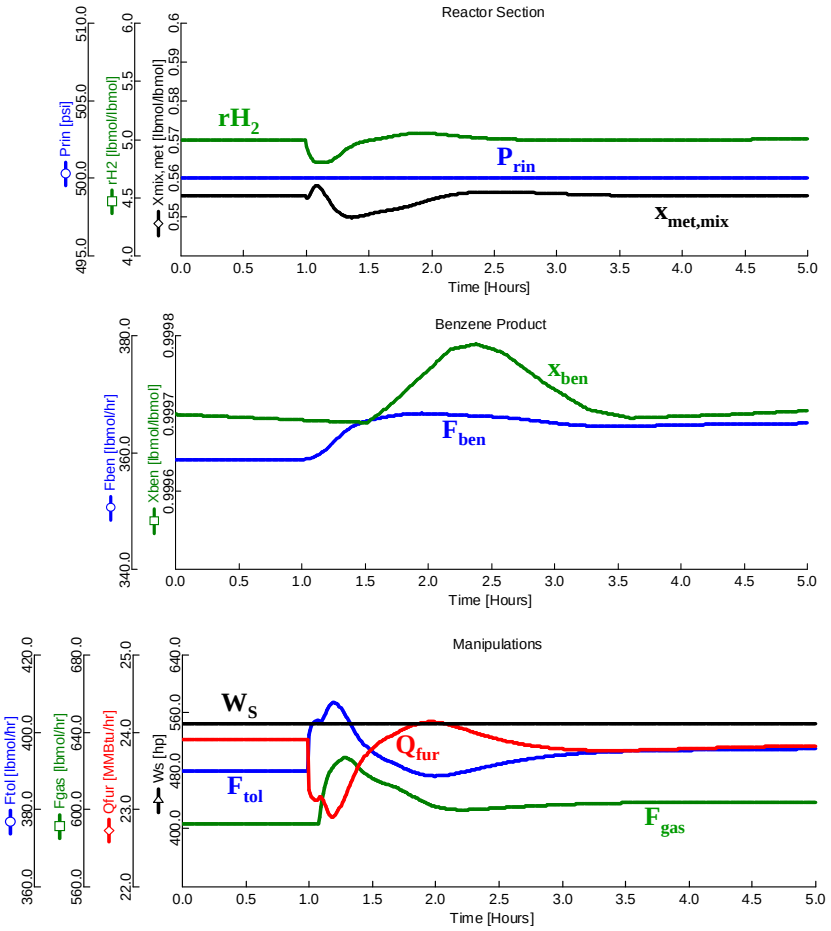

Figure 4.14: *Mode II (this work): Dynamic response of selected variables for disturbance Dyn4: +20°F increase in $T_{quencher}$.*

4.5 Conclusion

This chapter has discussed the control structure design of the HDA process using the design procedure given by Skogestad (2004*a*) with emphasis on the regulatory control layer. For this process, the bottleneck for maximum production rate (Mode II) was found to be the furnace heat duty Q_{fur}. However, this heat duty is needed to stabilizer the reactor, so the throughput manipulator was selected as the toluene feed rate F_{tol}. The final regulatory control layer shows good dynamic responses, as seen from the simulation results. The reason for this is that the systematic procedure ensures that the process does not drift away from its nominally optimal operating point (both Mode I and II). Note that no "intermediate" control layer was introduced in the hierarchy which contributed to the low complexity of the overall control structure.

Chapter 5

Control structure design for the ammonia synthesis process

Based on the paper submitted for publication in
Computers and Chemical Engineering

This paper discusses the application of the plantwide control design procedure of Skogestad (2004*a*) to the ammonia synthesis process. Three modes of operation are considered: (I) Given feed rate, (IIa) Maximum throughput, and (IIb) "Optimized" throughput. Two control structures, one for Mode I and another for Mode IIb, are proposed. In Mode I, it is proposed to keep constant purge rate and compressor powers. There is no bottleneck in the process, and thus there is no Mode IIa of operation. In Mode IIb, the compressors are at their maximum capacity and it is proposed to adjust the feed rate such that the inert concentration is constant. The final control structures result in good dynamic performance.

5.1 Synopsis

There are hundreds of references on the ammonia synthesis process that discuss the various aspects of its operation and design but none addresses the issue of control structure design in a systematic manner. In this chapter, we consider the application of the plantwide control structure design procedure of Skogestad (2004*a*) to an ammonia synthesis process. We start with a top-down analysis of the process where we define the operational objectives (identification of a scalar cost function and operational constraints) and identify the dynamic and steady-state (economic) degrees of freedom. This is followed by the identification of the most important disturbances to the process. Based on all of this information, we proceed by selecting the controlled variables that gives optimal operation [variables that are active at their constraints, (Maarleveld and Rijnsdorp, 1970)] and use the self-optimizing control technique (Skogestad, 2000) to decide for the remaining unconstrained controlled variables so that near-optimal operation is achieved without the need to re-optimize when disturbances occur.

One important issue in the plantwide control procedure is the definition on where in the plant the production rate should be set. We distinguish between 3 modes of operation:

- **Mode I: Given throughput**. This mode of operation occurs when (a) the feed rate is given (or limited) or (b) the production rate is given (or limited, e.g. by market conditions). The operational goal is then to minimize utility (energy) consumption, that is, to maximize efficiency.
- **Mode II: Throughput as a degree of freedom**. We here have two cases:
  - **Mode IIa: Maximum throughput**. This mode encompasses feasibility issues and the maximum throughput does not depend on cost data. It occurs when the product prices are sufficiently high and feed is available.
  - **Mode IIb: "Optimized" throughput**. In some cases, it is not economically optimal to maximize throughput, even if feed is available. This happens if the profit reaches a maximum, for example, because purge streams increase sharply at high feed rates.

The mode in which a given process will operate depends on market conditions and in which way the plant responds to increasing production rate.

The bottom-up design aims at defining the structure of the regulatory and supervisory control layers. The optimization (RTO) layer is not considered in this chapter since we assume that near-optimal operation is satisfactory as long as the loss between the truly optimal and the near-optimal (with constant set point policy for the unconstrained variables) is acceptable. The main purpose of the regulatory control layer is "stabilization" such that the plant does not drift too far away from its nominal operating point and it also should make the operation of the supervisory control layer smooth such that disturbances on the primary outputs can be handle effectively. The most important issue in the design of the regulatory layer is the selection of good secondary controlled variables and the pairing of these with the inputs at this layer.

With the regulatory layer in place, we then proceed to the design of the supervisory control layer. The purpose of this layer is to keep the primary (economic) controlled variables at their optimal set points using as degrees of freedom (inputs) the set points for the regulatory layer and any unused input at the supervisory layer. The main decisions involved in this layer are related to configuration of the control system, that is, the use of decentralized or multivariable (MPC) control.

A validation step is also included in the procedure in order to evaluate the effectiveness of the proposed control structure against disturbances using dynamic simulation.

For the ammonia plant, we will apply this procedure from a practical perspective in order to illustrate its applicability to actual industrial plants.

We do not consider the reaction section of the process. However, for Modes IIa and IIb (feed rate is a degree of freedom), we assume that there is available capacity in the synthesis gas section.

5.2 The ammonia synthesis process

We here consider the ammonia synthesis process given in Figure 5.1, for which the stream table results corresponding to the nominally optimal operating point is given in Table 5.1.

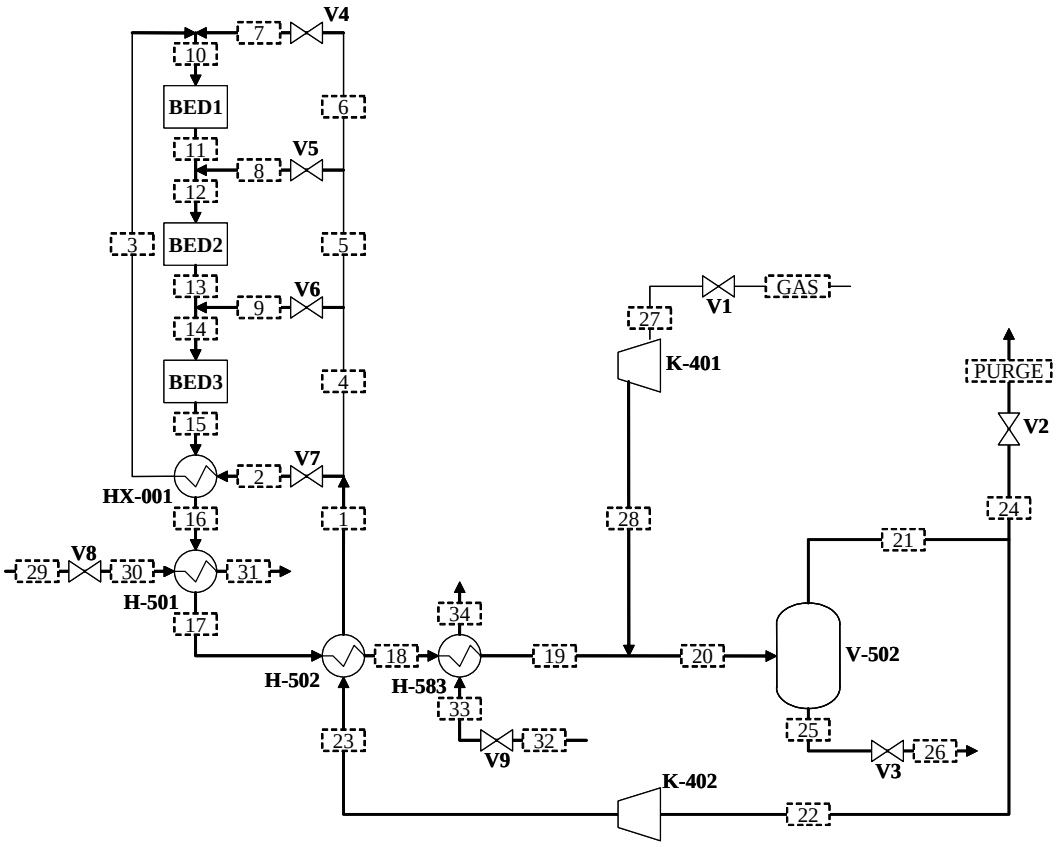

Figure 5.1: *Ammonia synthesis flowsheet.*

Table 5.1: *Stream table for the nominally optimal operating point for the ammonia synthesis process. See Figure 5.1 for the stream names.*

Stream	1	2	3	4	5	6	7	8	9	10	11	12	13	14	15	16	17	18
Temperature (°C)	231.7	231.8	340.1	231.7	231.7	231.7	231.8	231.8	231.8	306.3	456.2	420.1	452.1	423.9	449.3	394.4	296.9	107.6
Pressure (bar)	203.194	204.957	203.96	206.957	206.957	206.957	203.957	202.957	201.857	203.957	202.957	202.957	201.857	201.857	200.757	199.76	198.76	197.76
Vapor Frac	1	1	1	1	1	1	1	1	1	1	1	1	1	1	1	1	1	1
Mole Flow (kmol/h)	40573.8	20449.2	20449.2	5152.87	5639.75	9331.97	9331.97	5639.75	5152.87	29781.2	27046.4	32686.1	32002	37154.8	36531.7	36531.6	36531.6	36531.6
Mass Flow (kg/h)	412598	207950	207950	52400	57351.2	94897.6	94897.6	57351.2	52400	302848	302848	360199	360199	412599	412599	412598	412598	412598
Enthalpy (Mkcal/h)	-22.911	-11.547	5.95	-2.91	-3.185	-5.27	-5.27	-3.185	-2.91	0.68	0.68	-2.504	-2.504	-5.414	-5.414	-22.912	-53.546	-112.78
Mole Flow (kmol/h)																		
Hydrogen	25329.8	12766.2	12766.2	3216.88	3520.84	5825.84	5825.84	3520.84	3216.88	18592	14489.8	18010.7	16984.4	20201.3	19266.5	19266.5	19266.5	19266.5
Nitrogen	7432.32	3745.89	3745.89	943.904	1033.09	1709.43	1709.43	1033.09	943.904	5455.32	4087.92	5121.01	4778.92	5722.82	5411.25	5411.23	5411.23	5411.23
Methane	1341.71	676.221	676.219	170.397	186.497	308.593	308.593	186.497	170.397	984.812	984.812	1171.31	1171.31	1341.71	1341.71	1341.7	1341.7	1341.7
Argon	943.356	475.452	475.45	119.806	131.127	216.972	216.972	131.127	119.806	692.422	692.422	823.549	823.549	943.355	943.355	943.351	943.351	943.351
Ammonia	5526.63	2785.42	2785.48	701.882	768.202	1271.13	1271.13	768.202	701.882	4056.61	6791.41	7559.61	8243.79	8945.68	9568.82	9568.82	9568.82	9568.82
Water	0	0	0	0	0	0	0	0	0	0	0	0	0	0	0	0	0	0
Mole Frac																		
Hydrogen	0.624	0.624	0.624	0.624	0.624	0.624	0.624	0.624	0.624	0.624	0.536	0.551	0.531	0.544	0.527	0.527	0.527	0.527
Nitrogen	0.183	0.183	0.183	0.183	0.183	0.183	0.183	0.183	0.183	0.183	0.151	0.157	0.149	0.154	0.148	0.148	0.148	0.148
Methane	0.033	0.033	0.033	0.033	0.033	0.033	0.033	0.033	0.033	0.033	0.036	0.036	0.037	0.036	0.037	0.037	0.037	0.037
Argon	0.023	0.023	0.023	0.023	0.023	0.023	0.023	0.023	0.023	0.023	0.026	0.025	0.026	0.025	0.026	0.026	0.026	0.026
Ammonia	0.136	0.136	0.136	0.136	0.136	0.136	0.136	0.136	0.136	0.136	0.251	0.231	0.258	0.241	0.262	0.262	0.262	0.262
Water	0	0	0	0	0	0	0	0	0	0	0	0	0	0	0	0	0	0

Stream	19	20	21	22	23	24	25	26	27	28	29	30	31	32	33	34	FEED	PURGE
Temperature (°C)	27.1	40.5	40.4	40.4	48	40.4	40.4	40.5	17	304.2	15	15.1	144.7	15	15.1	82.9	17	40.2
Pressure (bar)	196.76	196.284	195.284	195.284	207.957	195.284	195.284	190.284	23.1	196.284	10	5	4	10	5	4	23.1	190.284
Vapor Frac	0.81	0.907	1	1	1	1	0	0.001	1	1	0	0	0.456	0	0	0	1	1
Mole Flow (kmol/h)	36531.6	44750.2	40578	40573.8	40573.8	4.257	4172.14	4172.14	8218.57	8218.57	4440.68	4440.68	4440.68	38855.9	38855.9	38855.9	8218.57	4.257
Mass Flow (kg/h)	412598	483598	412641	412598	412598	43.294	70956.9	70956.9	71000	71000	80000	80000	80000	700000	700000	700000	71000	43.294
Enthalpy (Mkcal/h)	-164.1	-148.04	-84.485	-84.477	-82.14	-0.009	-63.552	-63.552	-0.961	16.065	-306.04	-306.04	-275.4	-2677.8	-2677.8	-2626.5	-0.96	-0.009
Mole Flow (kmol/h)																		
Hydrogen	19266.5	25390.2	25332.4	25329.8	25329.8	2.658	57.707	57.707	6123.66	6123.66	0	0	0	0	0	0	6123.66	2.658
Nitrogen	5411.23	7454.37	7433.11	7432.33	7432.32	0.78	21.261	21.261	2043.14	2043.14	0	0	0	0	0	0	2043.14	0.78
Methane	1341.7	1368.82	1341.85	1341.71	1341.71	0.141	26.97	26.97	27.121	27.121	0	0	0	0	0	0	27.121	0.141
Argon	943.351	968.007	943.46	943.361	943.356	0.099	24.547	24.547	24.656	24.656	0	0	0	0	0	0	24.656	0.099
Ammonia	9568.82	9568.82	5527.16	5526.58	5526.63	0.58	4041.66	4041.66	0	0	0	0	0	0	0	0	0	0.58
Water	0	0	0	0	0	0	0	0	0	0	4440.68	4440.68	4440.68	38855.9	38855.9	38855.9	0	0
Mole Frac																		
Hydrogen	0.527	0.567	0.624	0.624	0.624	0.624	0.014	0.014	0.745	0.745	0	0	0	0	0	0	0.745	0.624
Nitrogen	0.148	0.167	0.183	0.183	0.183	0.183	0.005	0.005	0.249	0.249	0	0	0	0	0	0	0.249	0.183
Methane	0.037	0.031	0.033	0.033	0.033	0.033	0.006	0.006	0.003	0.003	0	0	0	0	0	0	0.003	0.033
Argon	0.026	0.022	0.023	0.023	0.023	0.023	0.006	0.006	0.003	0.003	0	0	0	0	0	0	0.003	0.023
Ammonia	0.262	0.214	0.136	0.136	0.136	0.136	0.969	0.969	0	0	0	0	0	0	0	0	0	0.136
Water	0	0	0	0	0	0	0	0	0	0	1	1	1	1	1	1	0	0

Hydrogen and nitrogen are fed to the process at the molar ratio of 3:1 along with a small concentration of inerts (methane and argon). In the synthesis reactor, the following exothermic equilibrium reaction (5.1) take place:

$$N_2 + 3H_2 \rightleftharpoons 2NH_3 \tag{5.1}$$

We assume that the reaction kinetics are described by the Temkin-Pyzhev kinetics (Froment and Bischoff, 1990, p. 433) in (5.2):

$$r_{NH_3} = \frac{2f}{\rho_{cat}} \left(k_1 \frac{p_{N_2} p_{H_2}^{1.5}}{p_{NH_3}} - k_{-1} \frac{p_{NH_3}}{p_{H_2}^{1.5}} \right), \quad \left[\frac{kmol\ NH_3}{kg\ cat \cdot h} \right] \tag{5.2}$$

with the partial pressure p_i in [bar] and the catalyst bulk density ρ_{cat} in [kg/m^3]. The pre-exponential factors of the forward and reverse paths are, respectively:

$$k_1 = 1.79 \cdot 10^4 e^{-\frac{87{,}090}{RT}}, \quad k_{-1} = 2.75 \cdot 10^{16} e^{-\frac{198{,}464}{RT}} \tag{5.3}$$

where T is the temperature in $[K]$. The multiplier factor f is used to correct for the catalyst activity, and we use the value of $f = 4.75$ as given in Morud and Skogestad (1998).

The simplified reactor model is shown in Figure 5.1. It consists of three adiabatic catalytic reactors (beds) in series with interstage cooling and preheating of the feed with the reactor effluent. The interstage cooling is provided by direct mixing of cold reactor feed with the respective inlet flow to each bed. The beds are modeled in Aspen Plus^{TM} by means of its built-in catalytic plug-flow reactor model. This is clearly a simplified model as, e.g. no radial distribution is assumed. However, it is believed to be acceptable for our purposes.

The reactor effluent is quenched in a series of three heat exchangers where the first one (H-501) uses the hot gases from the reactor to generate low pressure steam. The second heat exchanger (H-502) pre-heats the reactor feed, while the third one (H-583) provides cooling for the condensation of ammonia in the separator (V-502).

The ammonia product, which is about 97%w/w ammonia, leaves the process as a liquid stream through the separator bottom. A small flow is purged from the separator to prevent accumulation of inerts (methane and argon) in the system.

Next, we apply the control structure design procedure of Skogestad (2004*a*) to the ammonia synthesis process just described, starting with the degree of freedom analysis.

5.3 Top-down analysis

5.3.1 Degree of freedom (DOF) analysis

The ammonia synthesis in Figure 5.1 has 10 manipulated variables (Table 5.2) and 11 candidate measurements (Table 6.2).

Table 5.2: *List of manipulable variables.*

	Manipulated variable	Status in this work
U1	Gas feed rate F_{gas} [kg/h]	Steady state DOF
U2	Purge flow rate F_{purge} [kg/h]	Steady state DOF
U3	Feed compressor power W_{K-401} [kW]	Steady state DOF
U4	Recycle compressor power W_{K-402} [kW]	Steady state DOF
U5	Interstage cooling flow rate to first bed F_{bed1} [kg/h]	Not used
U6	Interstage cooling flow rate to second bed F_{bed2} [kg/h]	Not used
U7	Interstage cooling flow rate to third bed F_{bed3} [kg/h]	Not used
U8	Condensate flow rate to H-501 F_{cond} [kg/h]	Not used
U9	Cooling water flow rate to H-583 F_{cool} [kg/h]	Not used
U10	Product flow rate F_{prod} [kg/h]	Dynamic only (level control)

Table 5.3: *Steady-state degrees of freedom analysis for the ammonia synthesis plant.*

Process unit	No. of units	DOF/unit	DOF
External feed streams	1	1	1
Splitters (Purge)$^{(*)}$	1	1	1
Compressors (K-401 and K-402)	2	1	2
Adiabatic flashes$^{(**)}$ (V-502)	1	0	0
Gas phase reactors$^{(**)}$	3	0	0
Heat exchangers$^{(***)}$ (H-501 and H-583)	2	1	2
Total			**6**

$^{(*)}$ Cold shots for reactors are not used.
$^{(**)}$ Assuming no adjustable valves for pressure control (assume fully open valve before separator).
$^{(***)}$ We will see later that its is optimal to keep maximum cooling.

Based on the steady-state degree of freedom analysis described in (Skogestad, 2002), we consider six steady-state degrees of freedom for optimization as given in Table 5.3.

Note that we do not consider the interstage cooling flow rates to the beds as steady-state degrees of freedom and thus manipulated variables U5 to U7 are not available. This is in accordance with the industrial practice. Moreover, we can anticipate that maximum cooling is optimal in heat exchangers H-501 and H-583 (active constraints) since a small temperature in the separator (V-502) favors more ammonia recovery and less power consumption in the recycle compressor (K-402). This leaves 4 steady-state degrees of freedom for optimization. In addition, there is one dynamic degree of freedom for controlling the liquid level in the separator, namely F_{prod}.

Table 6.2 lists the 11 candidate controlled variables considered in this study. With 4 steady-state degrees of freedom and 11 candidate measurements, there are $\binom{11}{4} = \frac{11!}{4!7!} = 660$ possible ways of selecting the control structure.

Table 5.4: *Selected candidate controlled variables.*

Y1	Gas feed rate F_{gas} [kg/h]
Y2	Reactor inlet pressure P_{rin} [bar]
Y3	Feed compressor power W_{K-401} [kW]
Y4	Recycle compressor power W_{K-402} [kW]
Y5	Product purity x_{NH_3}
Y6	Purge flow rate F_{purge} [kg/h]
Y7	Mole fraction of hydrogen $y_{H_2,purge}$ in the purge stream
Y8	Mole fraction of nitrogen $y_{N_2,purge}$ in the purge stream
Y9	Mole fraction of ammonia $y_{NH_3,purge}$ in the purge stream
Y10	Mole fraction of argon $y_{Ar,purge}$ in the purge stream
Y11	Mole fraction of methane $y_{CH_4,purge}$ in the purge stream

5.3.2 Definition of optimal operation

The operational objective to be maximized is given by the profit P below:

$$P = \$_{prod}(x_{NH_3}F_{prod}) + \$_{purge}F_{purge} + \$_{steam}F_{steam} - \$_{gas}F_{gas} - \$_{ws}(W_{K-401} + W_{K-402}) \quad (5.4)$$

where x_{NH_3} is the product purity and F_{steam} is the steam generation in [kg/h]. Note that P is the operational profit and does not include other fixed costs or capital costs.

The prices are $\$_{prod} = 0.200\$/kg$, $\$_{purge} = 0.010\$/kg$, $\$_{steam} = 0.017\$/kg$, $\$_{gas} = 0.080\$/kg$, and $\$_{ws} = 0.040\$/kJ$.

The constraints on operation are:

$$P_{rin} \leq 250\ bar \quad (5.5)$$
$$W_{K-401} \leq 25000\ kW \quad (5.6)$$
$$W_{K-402} \leq 3500\ kW \quad (5.7)$$
$$F_{cond} \leq 80000\ kg/h \quad (5.8)$$
$$F_{cool} \leq 700000\ kg/h \quad (5.9)$$

Nominally, we have F_{gas} = 71000 kg/h, P_{rin} = 203 bar, W_{K-401} = 19800 kW, W_{K-402} = 2718 kW, and the molar feed compositions y_{H_2} = 0.7450, y_{N_2} = 0.2486, y_{CH_4} = 0.0033, and y_{AR} = 0.0030, as given in Table 5.1.

We now proceed the self-optimizing control analysis for the cases with given feed rate and variable feed rate, separately.

5.3.3 Operation with given feed rate

Identification of important disturbances

For the case with given gas feed rate F_{gas}, we consider the disturbances listed in Table 6.3.

Table 5.5: *Disturbances to the process operation for Mode I.*

No.	Description	Nominal	Disturbance
D1	Gas feed rate [kg/h]	71000	+15%
D2	Gas feed rate [kg/h]	71000	-15%
D3	Split fraction to the first bed	0.230	+0.1*
D4	Split fraction to the second bed	0.139	+0.1*
D5	Split fraction to the third bed	0.127	+0.1*
D6	Mole fraction of CH_4 in the gas feed	0.0033	+0.0030**
D7	Mole fraction of Ar in the gas feed	0.0030	+0.0030**

(*) The split fraction to the feed effluent heat exchanger is reduced by the same amount.
(**) Mole fraction of H_2 in the gas feed is reduced by the same amount.

Optimization

With a given gas feed rate F_{gas}, there are 5 steady-state degrees of freedom for optimization, namely F_{purge}, W_{K-401}, W_{K-402}, F_{cond}, and F_{cool}. Figure 5.2 gives the results of the optimizations conducted in Aspen Plus^{TM} for the nominal operating point and for the 7 disturbances described in Table 6.3. As it can be seen, the profit is weakly dependent on the disturbances, except for disturbances D1 and D2 that have a large effect on the profit P. However, note that the fact that a disturbance has a small

effect on the profit does *not* means it can be discarded when selecting the controlled variables.

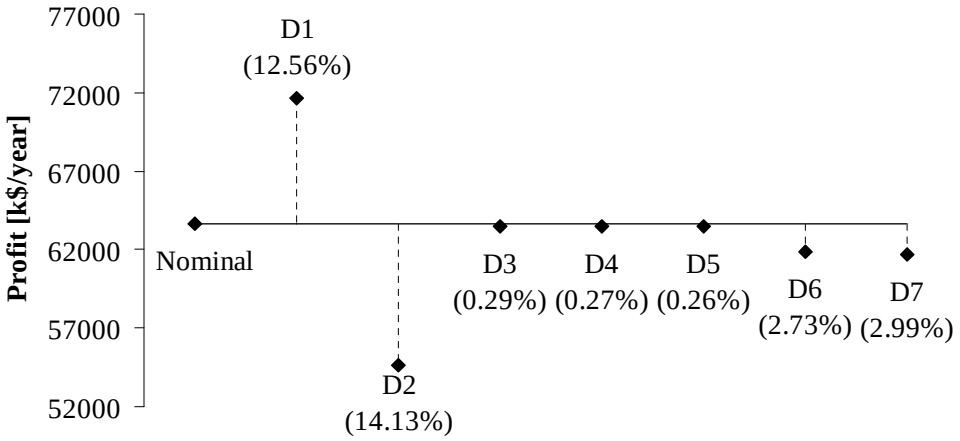

Figure 5.2: *Effect of disturbances (see Table 6.3) on optimal operation for Mode I. Percentages in parentheses are the changes with respect to the nominally optimum.*

As already mentioned, two constraints were found active for all disturbances, namely F_{cond} and F_{cool} are at their upper bounds. This leaves $5-2=3$ unconstrained degrees of freedom (W_{K-401}, W_{K-402}, and F_{purge}) and we will later use self-optimizing control to select the corresponding controlled variables.

Identification of candidate controlled variables - local analysis

Because of the large number of candidate structures, we first pre-screen using a local (linear) analysis as described in Skogestad and Postlethwaite (2005). The objective is to find the set of 3 unconstrained controlled variables that gives the maximum value of the minimum singular value $\underline{\sigma}(S_1 G J_{uu}^{-1/2})$, where S_1 is the matrix of scalings for the candidate measurements $S_1 = diag\{\frac{1}{span(Y_i)}\}$. $span(Y_i)$ is the variation of each candidate controlled variable Y_i due to variation in disturbances and implementation error n_i:

$$span(Y_i) = \Delta Y_{i,opt} + n_i = \sum_j \left| \frac{\partial Y_i}{\partial d_j} \right| \Delta d_j + n_i \tag{5.10}$$

G is the steady-state gain matrix of the process from the unconstrained degrees of freedom (manipulations u_1) to the candidate controlled variables in Table 6.2 (variables Y2 to Y11); J_{uu} is the Hessian of the profit function. In Table 5.6, we give the optimal variation and implementation error for the candidate controlled variables in Table 6.2. A branch-and-bound algorithm (Cao *et al.*, 1998*a*) is used to obtain the candidate sets

of controlled variables. The results for the ten sets with largest $\underline{\sigma}(S_1 G J_{uu}^{-1/2})$ are shown in Table 5.7.

Table 5.6: *Optimal variation for the candidate controlled variables for Mode I.*

	Description	Nominal	$\Delta Y_{i,opt}(d)$	n_i	$span(Y_i)$
Y2	Reactor inlet pressure P_{rin} [bar]	203	35	5	40
Y3	Feed compressor power W_{K-401} [kW]	19800	5200	1000	6200
Y4	Recycle compressor power W_{K-402} [kW]	2718	782	100	882
Y5	Product purity x_{NH_3}	0.969	0.015	0.01	0.025
Y6	Purge flow rate F_{purge} [kg/h]	43.29	673	5	678
Y7	Mole fraction of hydrogen $y_{H_2,purge}$ in the purge stream	0.624	0.069	0.05	0.119
Y8	Mole fraction of nitrogen $y_{N_2,purge}$ in the purge stream	0.183	0.044	0.03	0.074
Y9	Mole fraction of ammonia $y_{NH_3,purge}$ in the purge stream	0.136	0.016	0.03	0.046
Y10	Mole fraction of argon $y_{Ar,purge}$ in the purge stream	0.023	0.023	0.002	0.025
Y11	Mole fraction of methane $y_{CH_4,purge}$ in the purge stream	0.033	0.028	0.003	0.031

As we can see from Table 5.7, it is desirable to keep the purge flow rate (candidate controlled variable Y6) fixed at its nominally optimal set point. The other 2 controlled variables may be "freely" chosen among any of the 10 sets in Table 5.7 because $\underline{\sigma}(S_1 G_{3\times 3} J_{uu}^{-1/2})$ is essentially the same. As an attractive option, we choose to keep the variables in Set S_9^I (feed compressor power W_{K-401}, recycle compressor power W_{K-402}, and purge flow rate F_{purge}) at their nominally optimal set point since this reduces significantly the complexity of the control structure.

Evaluation of loss

We now evaluate in more detail the loss caused by keeping each controlled variable in Set S_9^I, corresponding to Mode I of operation, at its nominally optimal set point. The

Table 5.7: *Local analysis (Mode I): Minimum singular values for the ten best sets of unconstrained controlled variables.*

Set	Variables			$\underline{\sigma}(S_1 G_{3\times3} J_{uu}^{-1/2})$
S_1^I	Y6	Y8	Y2	0.07652
S_2^I	Y6	Y11	Y4	0.07534
S_3^I	Y6	Y3	Y10	0.07512
S_4^I	Y6	Y3	Y2	0.07502
S_5^I	Y6	Y3	Y7	0.07501
S_6^I	Y6	Y3	Y9	0.07491
S_7^I	Y6	Y8	Y3	0.07490
S_8^I	Y6	Y3	Y5	0.07489
S_9^I	Y6	Y3	Y4	0.07485
S_{10}^I	Y6	Y2	Y9	0.07478

results are shown in Table 6.4.

Table 5.8: *Loss by keeping the variables in Set S_9^I in Table 5.7 at their nominally optimal set points for Mode I.*

Disturbance	Optimal profit [k$/year]	Profit with S_9^I [k$/year]	Loss [k$/year]
D1	71616	71228	388
D2	54631	53734	897
D3	63437	63203	234
D4	63450	63198	252
D5	63458	63191	267
D6	61886	61400	485
D7	61723	61603	120
Average			378

As the average loss is considered acceptable, we confirm that Set S_9^I an acceptable set of primary controlled variables for the case with given gas feed rate (Mode I).

5.3.4 Operation with variable feed rate

Maximum throughput

From an economic point of view, it is optimal to increase the production rate F_{prod}. With the given feed rate as a parameter, we optimize the profit P in (5.4) with the same constraints (5.5) - (5.9). The results are given in Figure 5.3.

When $F_{gas} = 71850$ kg/h, the constraint (5.7) on the recycle compressor power (W_{K-402}) becomes active and remains active as the feed is increased. When $F_{gas} =$

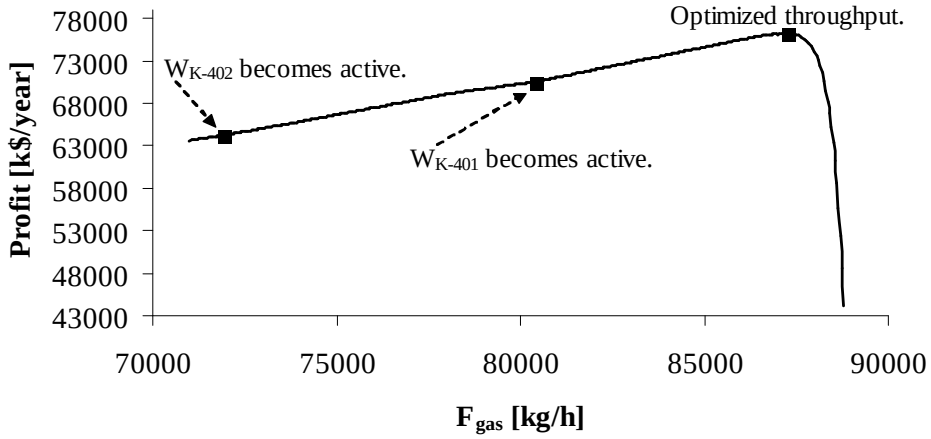

Figure 5.3: *Optimization of the ammonia plant with variable gas feed rate* F_{gas}.

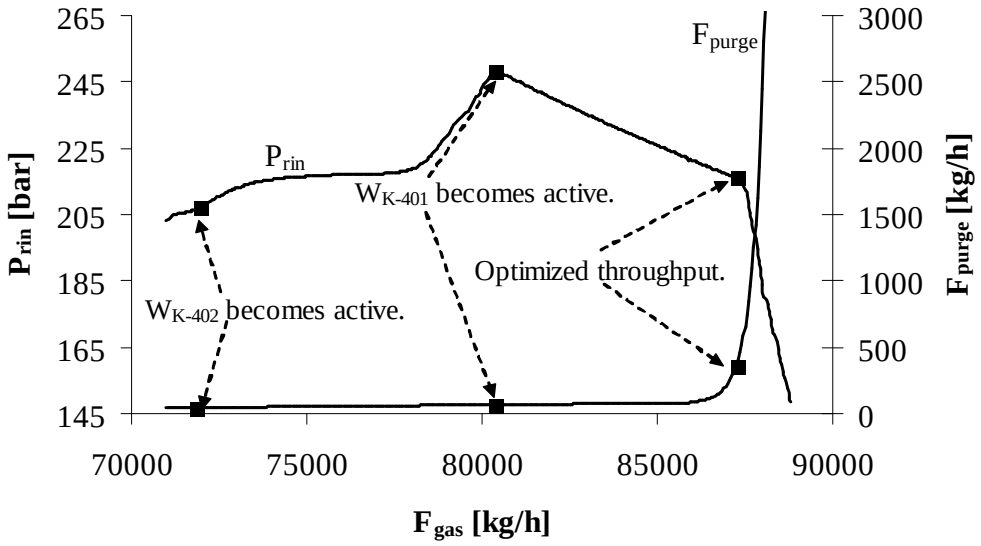

Figure 5.4: *Optimal reactor inlet pressure* P_{rin} *and purge flow rate* F_{purge} *as a function of gas feed rate* F_{gas}.

80400 kg/h, constraint (5.6) on the feed compressor power (W_{K-401}) becomes active and also remains active. Around $F_{gas} = 87250$ kg/h, the profit reaches its maximum and then it starts falling sharply. The reason for the drop is the reduction in pressure which reduces the conversion and results in a sharp increase in the purge flow rate (see Figure 5.4). Note that the degrees of freedom corresponding to condensate flow rate to H-501 F_{cond} and cooling water flow rate to H-583 F_{cool} were found to be active throughout the optimizations.

Note that there is no bottleneck and thus no maximum throughput (Mode II) for this case study. The reason is that the feed may be purged and there is no limit on the purge rate.

On the other hand, there is an "optimized" throughput (Mode IIb) corresponding to an "economic" bottleneck where $\frac{\partial P}{\partial F_{gas}} = 0$ and further increase in F_{gas} leads to non-optimal economic operation.

Optimization (Mode IIb)

We now evaluate the optimal operation with the gas feed rate as a degree of freedom and the two compressors at their constraints, i.e. $W_{K-401} = 25000$ kW and $W_{K-401} = 3500$ kW, respectively. There are two remaining degrees of freedom for optimization, namely the gas feed rate F_{gas} and the purge flow rate F_{purge} and we perform the optimizations for the disturbances listed in Table 5.9 below. The results are shown in Figure 5.5.

Table 5.9: *Disturbances to the process operation for Mode IIb.*

No.	Description	Nominal	Disturbance
D3	Split fraction to the first bed	0.230	+0.1*
D4	Split fraction to the second bed	0.139	+0.1*
D5	Split fraction to the third bed	0.127	+0.1*
D6	Mole fraction of CH_4 in the gas feed	0.0033	+0.003**
D7	Mole fraction of Ar in the gas feed	0.0030	+0.003**
D8	Feed compressor power W_{K-401} [kW]	25000	+1000
D9	Recycle compressor power W_{K-402} [kW]	3500	+100

(*) The split fraction to the feed effluent heat exchanger is reduced by the same amount.
(**) Mole fraction of H_2 in the gas feed is reduced by the same amount.

Identification of candidate controlled variables - local analysis

We use a linear analysis, similar to the one conducted in the Section 5.3.3, to pre-screen the candidate controlled variables in Table 6.2.

The optimal variation and implementation error are given in Table 5.10 and the ten best sets with largest $\underline{\sigma}(S_1 G J_{uu}^{-1/2})$ are shown in Table 5.11.

Table 5.10: *Total span summary for the candidate controlled variables for Mode IIb.*

	Description	Nominal	$\Delta Y_{i,opt}(d)$	n_i	$span(Y_i)$
Y1	Gas feed rate F_{gas} [kg/h]	87250	1570	1700	3315
Y2	Reactor inlet pressure P_{rin} [bar]	226	68	5	73
Y5	Product purity x_{NH_3}	0.968	0.019	0.01	0.029
Y6	Purge flow rate F_{purge} [kg/h]	366	22348	36.6	22384.5
Y7	Mole fraction of hydrogen $y_{H_2,purge}$ in the purge stream	0.603	0.068	0.05	0.118
Y8	Mole fraction of nitrogen $y_{N_2,purge}$ in the purge stream	0.174	0.040	0.03	0.070
Y9	Mole fraction of ammonia $y_{NH_3,purge}$ in the purge stream	0.172	0.019	0.03	0.049
Y10	Mole fraction of argon $y_{Ar,purge}$ in the purge stream	0.022	0.027	0.002	0.029
Y11	Mole fraction of methane $y_{CH_4,purge}$ in the purge stream	0.029	0.025	0.003	0.028

Table 5.11: *Local analysis (Mode IIb): Minimum singular values for the ten best sets of unconstrained controlled variables.*

Set	Variables		$\underline{\sigma}(S_1 G_{2\times 2} J_{uu}^{-1/2})$
S_1^{IIb}	Y2	Y11	0.07011
S_2^{IIb}	Y2	Y10	0.06809
S_3^{IIb}	Y2	Y8	0.06510
S_4^{IIb}	Y2	Y9	0.06391
S_5^{IIb}	Y2	Y7	0.05913
S_6^{IIb}	Y7	Y8	0.05022
S_7^{IIb}	Y7	Y10	0.04599
S_8^{IIb}	Y7	Y11	0.04172
S_9^{IIb}	Y9	Y5	0.03987
S_{10}^{IIb}	Y10	Y11	0.03429

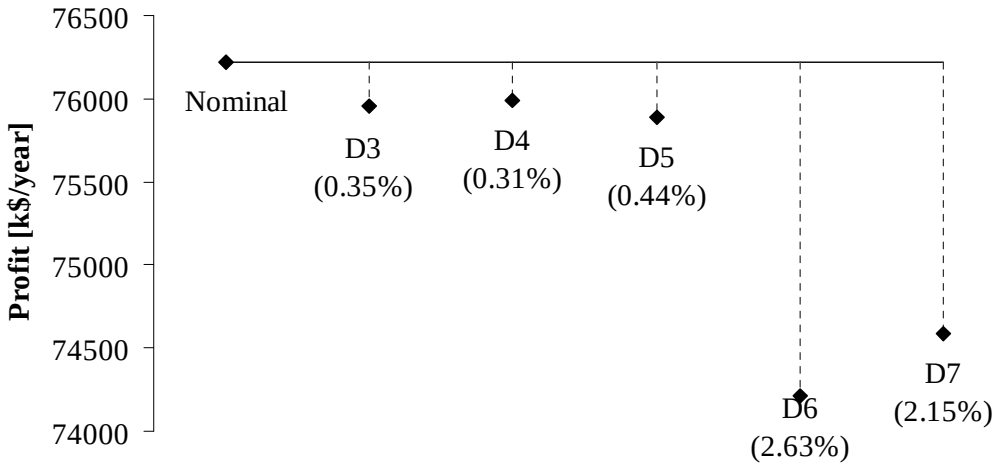

Figure 5.5: *Effect of disturbances (see Table 5.9) on optimal operation for Mode IIb. Percentages in parentheses are the changes with respect to the nominally optimum.*

From Table 5.11, we see that the five best sets involve control of reactor pressure (Y2), which is easy to control. The other controlled variable (Y7 - Y11) is a composition. The lowest minimum singular value is for methane (Y11) and we consider this in more detail in the following.

Evaluation of loss (Mode IIb)

The loss is calculated is calculated for set S_1^{IIb} and given in Table 5.12 for various disturbances.

Table 5.12: *Loss by keeping the variables in Set S_1^{IIb} in Table 5.11 at their nominal optimal set points for Mode IIb.*

Disturbance	Optimal		With S_1^{IIb}		Loss
	Feed rate [kg/h]	Profit [k$/year]	Feed rate [kg/h]	Profit [k$/year]	[k$/year]
D3	87595	75955	87759	75421	534
D4	87502	75986	87832	75410	576
D5	87663	75887	87715	75334	553
D6	89490	74216	91563	73564	652
D7	89114	74583	90892	73971	612
D8	89529	78675	88263	77990	685
D9	90752	79258	89536	78627	631
Average					606

As the average loss for Mode IIb is acceptable, we confirm Set S_1^{IIb} in Table 5.11 as the selected set of primary controlled variables.

5.4 Bottom-up design

5.4.1 Structure of the regulatory control layer (Modes I and IIb)

The unstable mode associated with the separator level is stabilized using its outlet liquid flow rate with a P-controller. Moreover, as discussed in Morud and Skogestad (1998), the reactor is normally unstable and sustained oscillations in the reactor outlet temperature may appear as a consequence of a reduction in reactor inlet pressure or temperature. They suggested to control the temperature at the inlet of the first bed using the quench flow rate before the first bed to overcome this instability. Although our model does not seem to have this feature, probably because of no radial variation of dispersion, we here follow this suggestion and close a temperature loop at this location.

To reduce drift caused by pressure changes, and also to avoid nonlinearity in control valves, we use flow controllers for the gas feed rate F_{gas} and purge flow rate F_{purge}.

The regulatory control layer is then designed as follows:

1. Flow control of gas feed rate F_{gas}.
2. Flow control of purge flow rate F_{purge}.
3. First-bed inlet temperature T_{bed1} with quench flow rate before the first bed F_{bed1}.
4. Separator level L_{sep} using its liquid outlet flow rate F_{prod}.

5.4.2 Structure of the supervisory control layer

Mode I: Keep the following at constant (optimal) values: feed compressor power W_{K-401}, recycle compressor power W_{K-402}, and purge flow rate $F_{purge,sp}$. These are all manipulated variables, so no additional control loops are needed.

Mode IIb: Keep the compressors (K-401 and K-402) are maximum power. With the two remaining inputs $u = \{F_{gas,sp},\ F_{purge,sp}\}$ we control $y = \{P_{rin},\ y_{CH_4,purge}\}$ at constant optimal set points. Suggested pairings are $F_{gas,sp}$ - P_{rin} and $F_{purge,sp}$ - $y_{CH_4,purge}$.

5.4.3 Switching between Mode I and Mode IIb

The transition between Modes I and IIb involves changing the set points for W_{K-401}, W_{K-402}, and T_{bed1} from the nominally optimal for Mode I to the maximum throughput set point in Mode IIb. In addition, we need to close two loops: $F_{gas,sp}$ - P_{rin} and $F_{purge,sp}$ - $y_{CH_4,purge}$.

5.4.4 Controller tuning

The regulatory loops selected above are closed and tuned one at the time in a sequential manner (starting with the fastest loops). Aspen Dynamics^{TM} has an open loop test capability that was used to determine a first-order plus delay model from u to y. Based on the model parameters, we used the SIMC tuning rules (Skogestad, 2004*b*) to design the PI-controllers:

$$K_c = \frac{1}{k}\frac{\tau}{\tau_c + \theta}, \quad \tau_I = \min[\tau, 4(\tau_c + \theta)] \tag{5.11}$$

where k, τ, and θ are the gain, time constant, and effective time delay, respectively. In our case, we choose $\tau_c = \theta$ to ensure robustness and small input variation.

The gain K_c and integral time τ_I for the regulatory controllers (Modes I and IIb) are given in Table 5.13, and for supervisory controllers (Mode IIb) in Table 5.14.

Table 5.13: *Tuning parameters for the regulatory loops (Modes I and IIb). Note that the Table is sorted by the time constant τ in ascending order.*

Tag(*)	Input	Output	Set point		PI-controller parameters	
			Mode I	Mode IIb	K_c (%/%)	τ_I (min)
FC1	V_1	F_{gas} [kg/h]	71000	87250(**)	6.75	0.39
FC2	V_2	F_{purge} [kg/h]	43	366(**)	5.05	0.60
TC1	V_4	T_{bed1} [^{o}C]	306	293	8.05	1.60
LC1	V_3	L_{sep} [m]	2.5	2.5	2.00	-

(*) See tags in Figure 5.6.

(**) Nominal value. Set point set by outer loop.

Table 5.14: *Tuning parameters for supervisory loops (Mode IIb).*

Tag(*)	Input	Output	Set point		PI-controller parameters	
			Mode I	Mode IIb	K_c (%/%)	τ_I (min)
PC1	$F_{gas,sp}$	P_{rin} [bar]	203	226	5.55	4.99
CC1	$F_{purge,sp}$	$y_{CH_4,purge}$	0.033	0.029	93.39	72.88

(*) See tags in Figure 5.7.

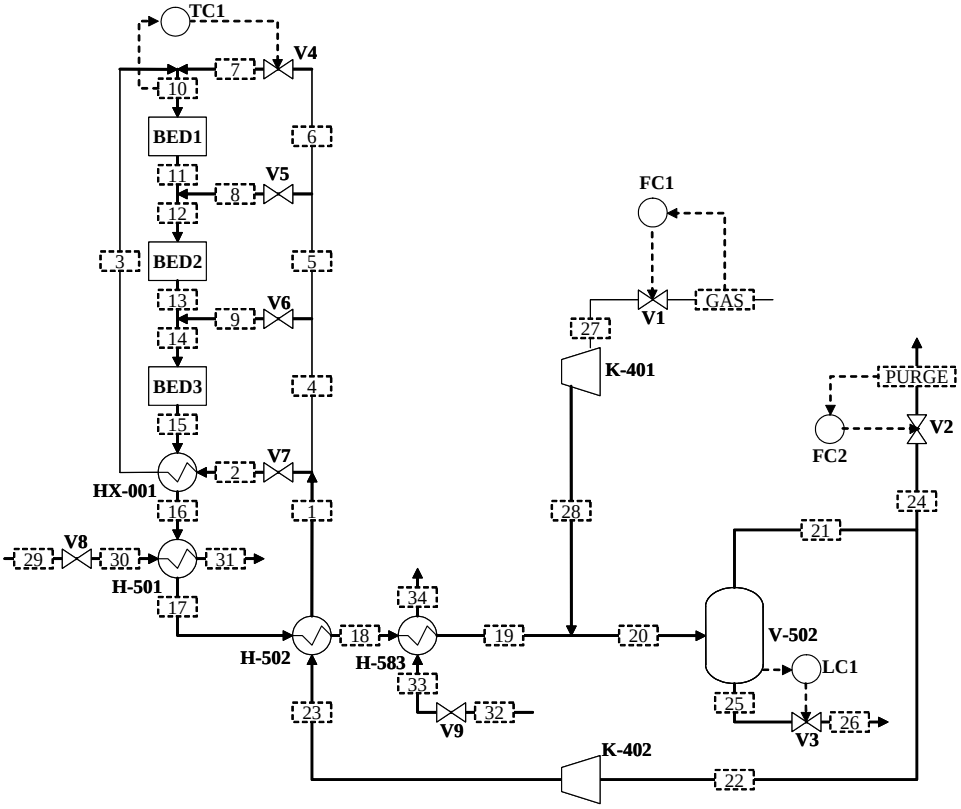

Figure 5.6: *Ammonia synthesis process flowsheet with controllers installed (Mode I).*

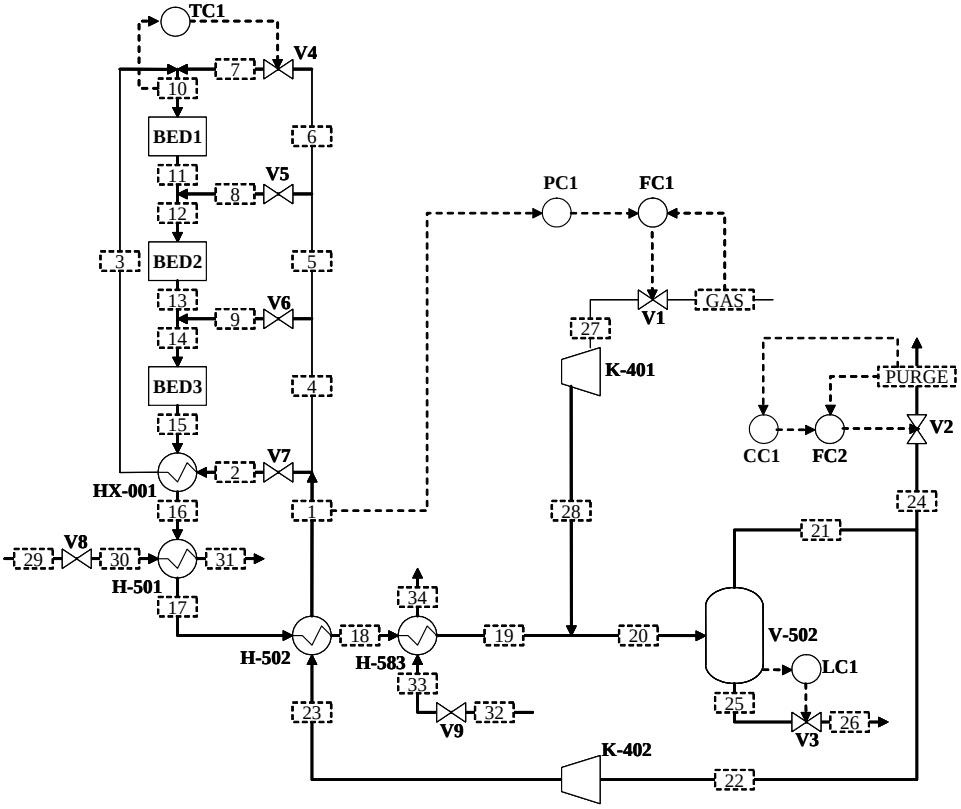

Figure 5.7: *Ammonia synthesis process flowsheet with controllers installed (Mode IIb).*

5.4.5 Dynamic simulations

In this section, we conduct dynamic simulation to evaluate the performance of the selected control structure. We will consider the disturbances listed in Table 5.15 for both Modes I and IIb. The responses are shown in Figures 6.6 to 5.15. Note that the disturbances are applied 1 hour after the beginning of each simulation run.

Table 5.15: *Disturbances to the effect of dynamic simulations for Modes I and IIb.*

No.	Description	Nominal		Disturbance
		Mode I	Mode IIb	
Dyn1	Mole fraction of CH_4 in the gas feed	0.0033	0.0033	$+0.0010^{(*)}$
Dyn2	Cooling water temperature in H-583 [^{o}C]	15	15	+5
Dyn3	Compressor power W_{K-401} [kW]	19800	25000	+5%
Dyn4	Gas feed rate F_{gas} [kg/h]	71000	$87250^{(**)}$	+5%

$^{(*)}$ Mole fraction of H_2 in the gas feed is reduced by the same amount.
$^{(**)}$ Gas feed rate disturbance for Mode IIb considered as measurement error.

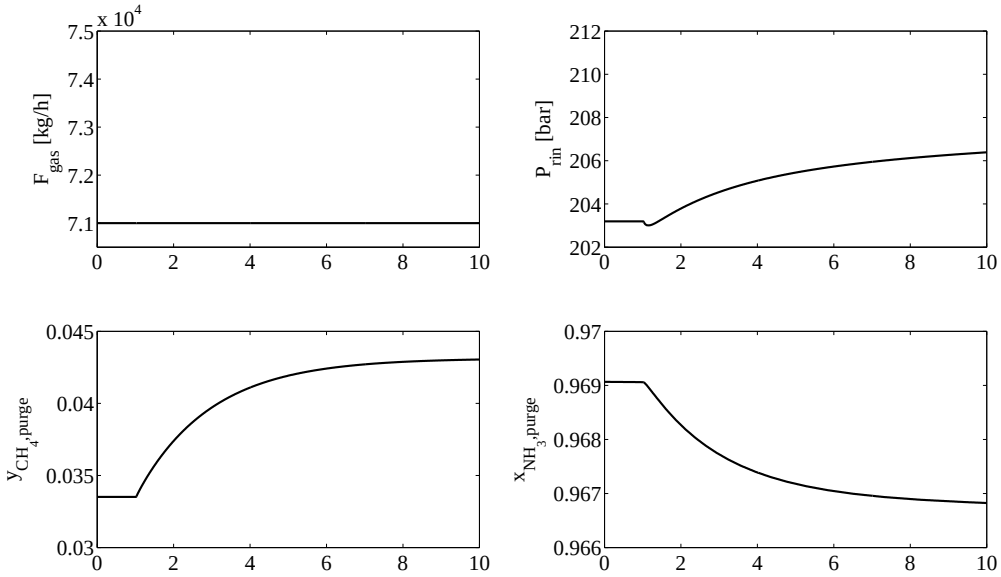

Figure 5.8: *Mode I - Dynamic response of selected variables for disturbance Dyn1.*

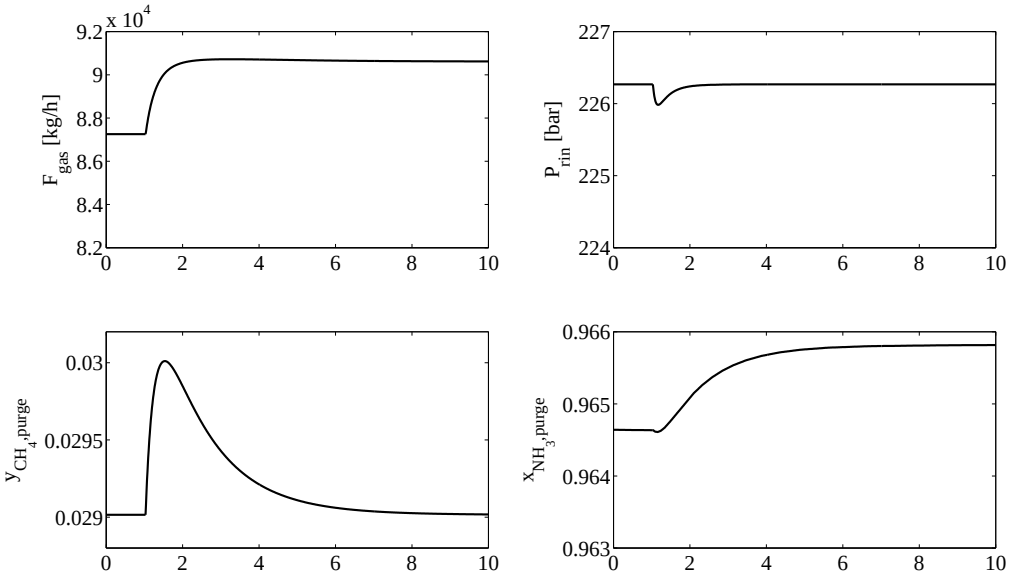

Figure 5.9: *Mode IIb - Dynamic response of selected variables for disturbance Dyn1.*

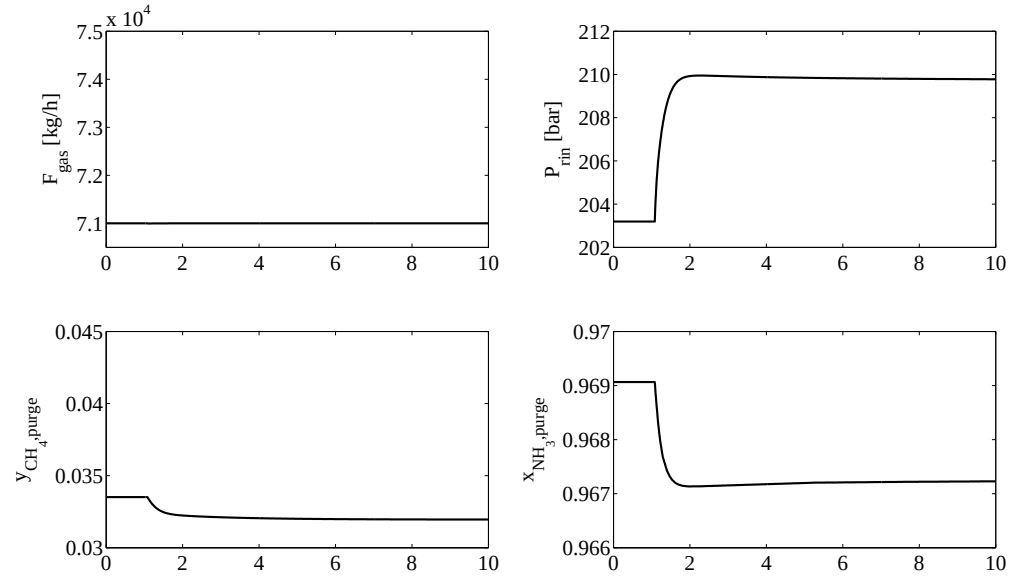

Figure 5.10: *Mode I - Dynamic response of selected variables for disturbance Dyn2.*

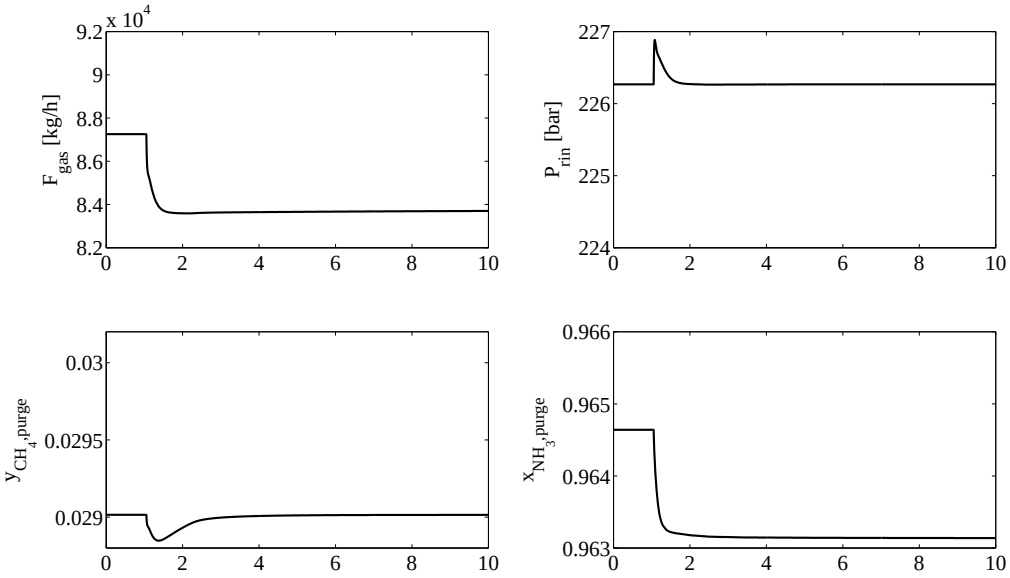

Figure 5.11: *Mode IIb - Dynamic response of selected variables for disturbance Dyn2.*

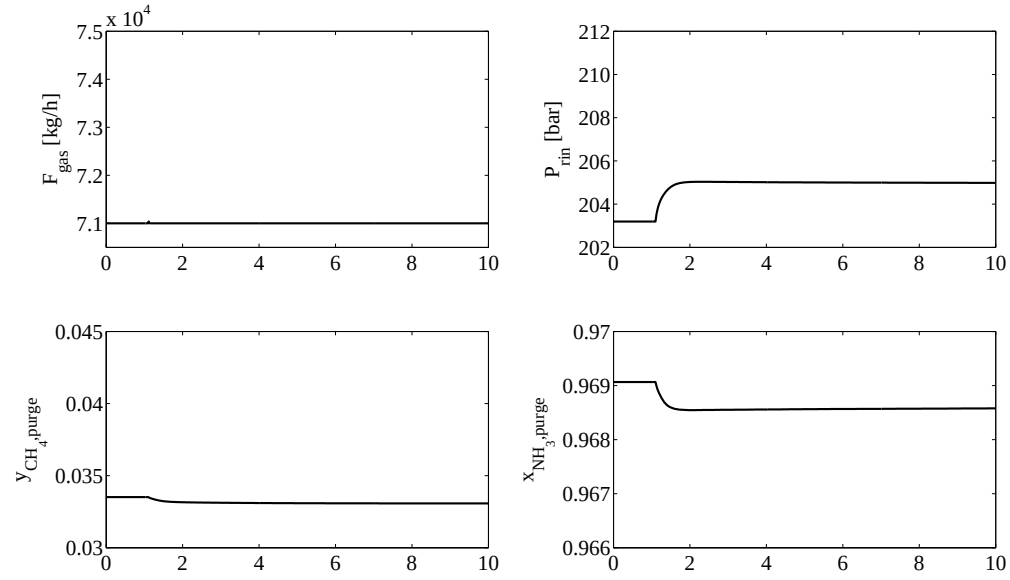

Figure 5.12: *Mode I - Dynamic response of selected variables for disturbance Dyn3.*

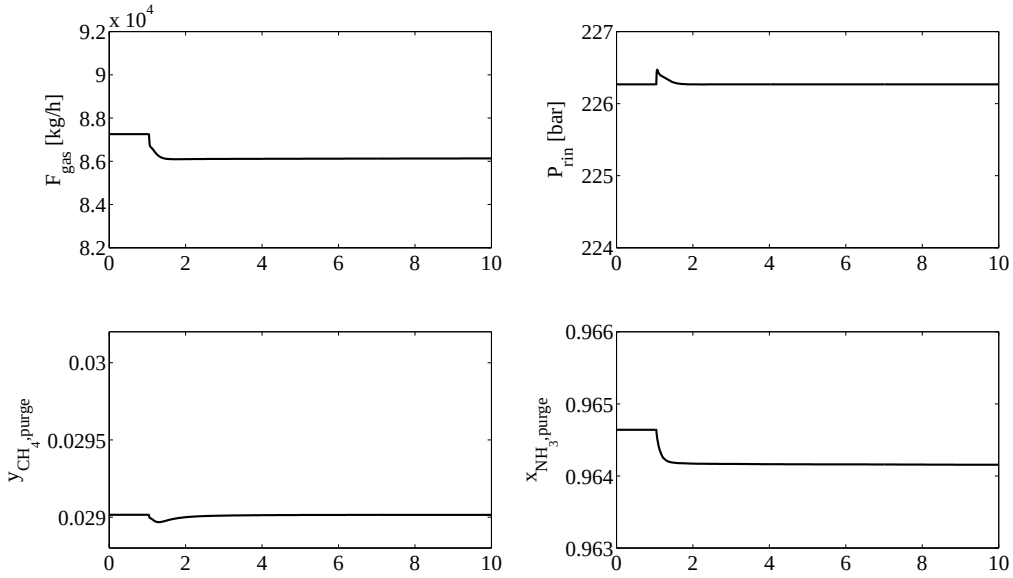

Figure 5.13: *Mode IIb - Dynamic response of selected variables for disturbance Dyn3.*

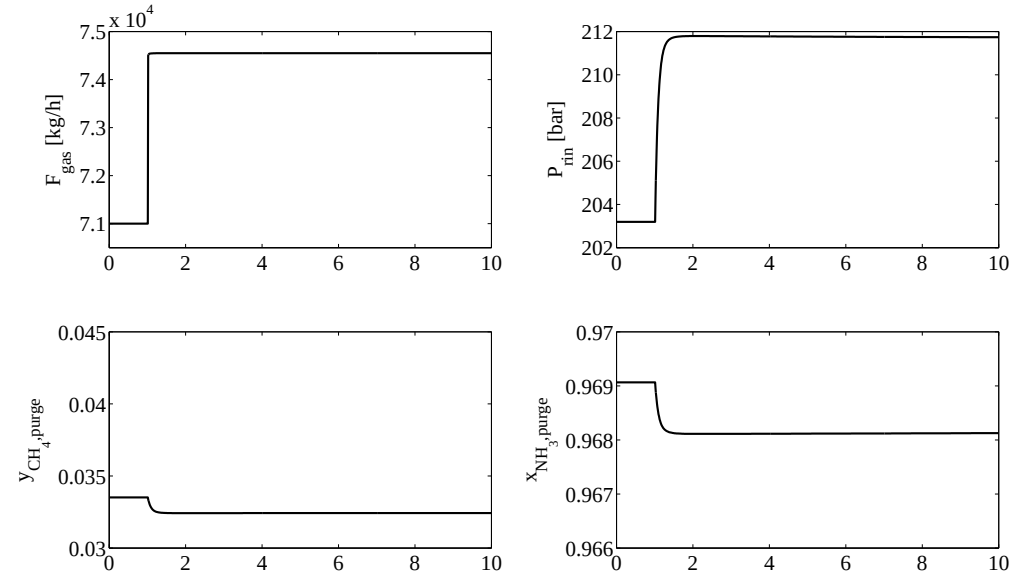

Figure 5.14: *Mode I - Dynamic response of selected variables for disturbance Dyn4.*

It can be seen from Figures 6.6 and 5.15 that the product purity does not change significantly in both modes of operation. The reason for this is that ammonia is satis-

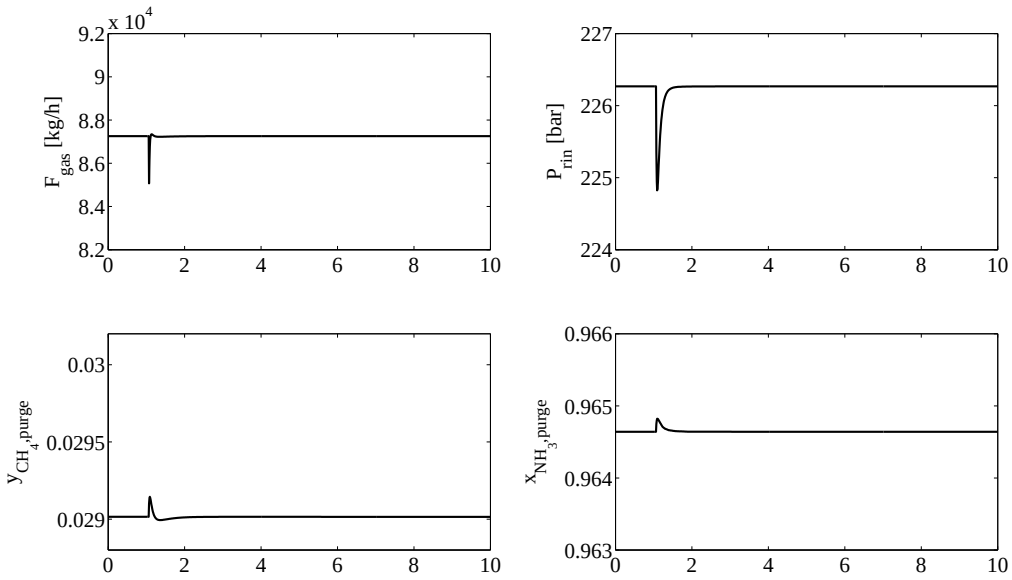

Figure 5.15: *Mode IIb - Dynamic response of selected variables for disturbance Dyn4.*

factorily separated from the other components at all conditions. Moreover, as discussed before, in Mode I the pressure of the system is allowed to fluctuate without causing the process to drift away from its nominally optimal operating condition. In Mode IIb, the pressure is tight controlled. In general, the dynamic responses for both modes are satisfactory with settling time of about 4 hours, except for disturbance Dyn1 which seems to be the most difficult disturbance. But this was expected since composition is usually slower than other variables like flow, pressure, and temperature.

5.5 Conclusion

This chapter discussed the application of the plantwide design procedure of Skogestad (2004*a*) to the ammonia synthesis process. It has been found that it is not economically attractive to operate the process beyond the production rate determined by the "economic" bottleneck corresponding to the maximum gas feed rate. By applying the self-optimizing technique of Skogestad (2000), we also found that it is (near) optimal to operate the supervisory control layer by keeping constant set point policy for the feed compressor power, recycle compressor power, and purge flow rate when the gas feed rate is given (Mode I), which corresponds to the practice currently adopted in industrial ammonia synthesis plants. In case of optimized throughput (Mode IIb), the pressure of the system and the mole fraction of CH_4 should be controlled to achieve (near) optimal operation. The regulatory layer is enhanced by controlling the reactor temperature so to avoid the deteriorating effects of oscillations caused by variations in the reactor inlet

conditions (temperature and/or pressure) (Morud and Skogestad, 1998).

Chapter 6

Time Scale Separation and the Link Between Open-loop and Closed-loop Dynamics

Based on the paper presented at the 16th European Symposium on computer Aided Process Engineering and 9th International Symposium on Process Systems Engineering, Garmisch-Partenkirchen, Germany, July 9-13, 2006

This chapter aims at combining two different approaches (Skogestad (2000) and Baldea and Daoutidis (2006)) into a method for control structure design for plants with large recycle. The self-optimizing approach (Skogestad, 2000) identifies the variables that must be controlled to achieve acceptable economic operation of the plant, but it gives no information on how fast these variables need to be controlled and how to design the control system. A detailed controllability and dynamic analysis is generally needed for this. One promising alternative is the singular perturbation framework proposed in Baldea and Daoutidis (2006) where one identifies potential controlled and manipulated variables on different time scales. The combined approaches have successfully been applied to a reactor-separator process with recycle and purge.

6.1 Synopsis

Time scale separation is an inherent property of many integrated process units and networks. The time scale multiplicity of the open loop dynamics (e.g., Baldea and Daoutidis (2006)) may warrant the use of multi-tiered control structures, and as such, a hierarchical decomposition based on time scales. A hierarchical decomposition of the control system arises from the generally separable layers of: (1) Optimal operation at a slower time scale ("supervisory control") and (2) Stabilization and disturbance rejection at a fast time scale ("regulatory control"). Within such a hierarchical framework:

a. The upper (slow) layer controls variables (CV's) that are more important from an overall (long time scale) point of view and are related to the operation of the entire

plant. Also, it has been shown that the degrees of freedom (MV's) available in the slow layer include, along with physical plant inputs, the set points (reference values, commands) for the lower layer, which leads naturally to cascaded control configurations.

b. The lower (fast) variables implements the set points given by the upper layer, using as degrees of freedom (MV's) the physical plant inputs (or the set points of an even faster layer below).

c. With a "reasonable" time scale separation, typically a factor of five or more in closed-loop response time, the stability (and performance) of the fast layer is not influenced by the slower upper layer (because it is well inside the bandwidth of the system).

d. The stability (and performance) of the slow layer depends on a suitable control system being implemented in the fast layer, but otherwise, assuming a "reasonable" time scale separation, it should not depend much on the specific controller settings used in the lower layer.

e. The lower layer should take care of fast (high-frequency) disturbances and keep the system reasonable close to its optimum in the fast time scale (between each set point update from the layer above).

The present work aims to elucidate the open-loop and closed-loop dynamic behavior of integrated plants and processes, with particular focus on reactor-separator networks, by employing the approaches of singular perturbation analysis and self-optimizing control. It has been found that the open-loop strategy by singular perturbation analysis in general imposes a time scale separation in the "regulatory" control layer as defined above.

6.2 Self-optimizing control

Self-optimizing control is defined as:

Self-optimizing control is when one can achieve an acceptable loss with constant set point values for the controlled variables without the need to re-optimize when disturbances occur (real time optimization).

To quantify this more precisely, we define the (economic) loss L as the difference between the actual value of a given cost function and the truly optimal value, that is to say,

$$L(u, d) = J(u, d) - J_{opt}(d) \tag{6.1}$$

Truly optimal operation corresponds to $L = 0$, but in general $L > 0$. A small value of the loss function L is desired as it implies that the plant is operating close to its optimum. The main issue here is not to find optimal set points, but rather to find the right variables to keep constant. The precise value of an "acceptable" loss must be selected on the basis of engineering and economic considerations.

In Skogestad (2000) it is recommended that a controlled variable c suitable for constant set point control (self-optimizing control) should have the following requirements:

R1. The optimal value of c should be insensitive to disturbances, i.e., $c_{opt}(d)$ depends only weakly on d.

R2. The value of c should be **sensitive** to changes in the manipulated variable u, i.e., the gain from u to y should be large.

R3. For cases with two or more controlled variables, the selected variables in c should not be closely correlated.

R4. The variable c should be easy to measure and control.

During optimization some constraints are found to be active in which case the variables they are related to must be selected as controlled outputs, since it is optimal to keep them constant at their set points (active constraint control). The remaining unconstrained degrees of freedom must be fulfilled by selecting the variables (or combination thereof) which yield the smallest loss L with the active constraints implemented.

6.3 Time scale separation by singular perturbation analysis

In Baldea and Daoutidis (2006) and Kumar and Daoutidis (2002) it has shown that the presence of material streams of vastly different magnitudes (such as purge streams or large recycle streams) leads to a time scale separation in the dynamics of integrated process networks, featuring a fast time scale, which is in the order of magnitude of the time constants of the individual process units, and one or several slow time scales, capturing the evolution of the network. Using singular perturbation arguments, it is proposed a method for the derivation of non-linear, non-stiff, reduced-order models of the dynamics in each time scale. This analysis also yields a rational classification of the available flow rates into groups of manipulated inputs that act upon and can be used to control the dynamics in each time scale. Specifically, the large flow rates should be used for distributed control at the unit level, in the fast time scale, while the small flow rates are to be used for addressing control objectives at the network level in the slower time scales.

In this approach it is assumed that a non-linear model of the process (usually comprising a reaction and separation section linked by a large recycle stream) is available. The principle of this method consists in rearranging and further decomposing the model according to its characteristic time scale separation found by considering the different orders of magnitude of its variables (flows). For a reactor-separator network with a large recycle flow compared with its throughput and small purge of inert components, three different time scales can be identified. In addition, during the rearrangement step two sort of inputs can be classified: those corresponding to "large" flow rates (u^l) and those corresponding to "small" flow rates (u^s).

The decomposition of the rearranged system is carried out based on the singular perturbation analysis. This step consists of finding the three equations which describe the system within the fast, intermediate, and slow time scales as well as revealing in a natural way which manipulated variables are to be used in each time scale: u^l is to manipulate the variables in the fast time scale, u^s is used to manipulate the variables in the intermediate time scale, and u_p (the purge flow rate) manipulates the small amount of feed impurity.

Thus, control objectives in each of the time scales can be addressed by using the manipulated inputs that are available and act upon the dynamics in the respective time scale, starting from the fastest. Specifically:

a. Large flow rates are available for addressing regulatory control objectives at the unit level, such as liquid level/holdup control, as well as for the rejection of fast disturbances. Similar control objectives for the units outside the recycle loop are to be addressed using the small flow rates u^s, as the large flow rates do not influence the evolution of these units. Typically, the above control objectives objectives are fulfilled using simple linear controllers, possibly with integral action, depending on the stringency of the control objectives.

b. The small flow rates u^s appear as the manipulated inputs available for controlling the "overall" network dynamics in the intermediate time scale. Control objectives at network level include the product purity, the stabilization of the total material holdup and setting the production rate. Very often, the number of available manipulated inputs u^s is exceeded by the number of network level control objectives. In this case, it is possible to use the set points y^l_{sp} of the controllers in the fast time scale as manipulated inputs in the intermediate time scale, which leads to cascaded control configurations. Such configurations are beneficial from the point of view of achieving a tighter coordination between the distributed and supervisory control levels.

c. The concentration of the impurities in the network evolves over a very slow time scale. Moreover, the presence of impurities in the feed stream, corroborated with the use of large recycle flow rates, can lead to the accumulation of the impurities in the recycle loop, with detrimental effects on the operation of the network and on the process economics. Therefore, the control of the impurity levels in the network is a key operational objective and it should be addressed in the slow time scale, using the flow rate of the purge stream u_p, as a manipulated input.

6.4 Case study on reactor-separator with recycle process

In this section, a case study on reactor-separator network is considered where the objective is to hierarchically decide on a control structure which inherits the time scale separation of the system in terms of its closed-loop characteristics. This process was

studied in Kumar and Daoutidis (2002), but for the present chapter the expressions for the flows F, L, P, and R and economic data were added.

6.4.1 The process

The process consists of a gas-phase reactor and a condenser-separator that are part of a recycle loop (see Figure 6.1). It is assumed that the recycle flow rate R is much larger than the feed flow rate F_o and that the feed stream contains a small amount of an inert, volatile impurity $y_{I,o}$ which is removed via a purge stream of small flow rate P. The objective is to ensure a stable operation while controlling the purity of the product x_B.

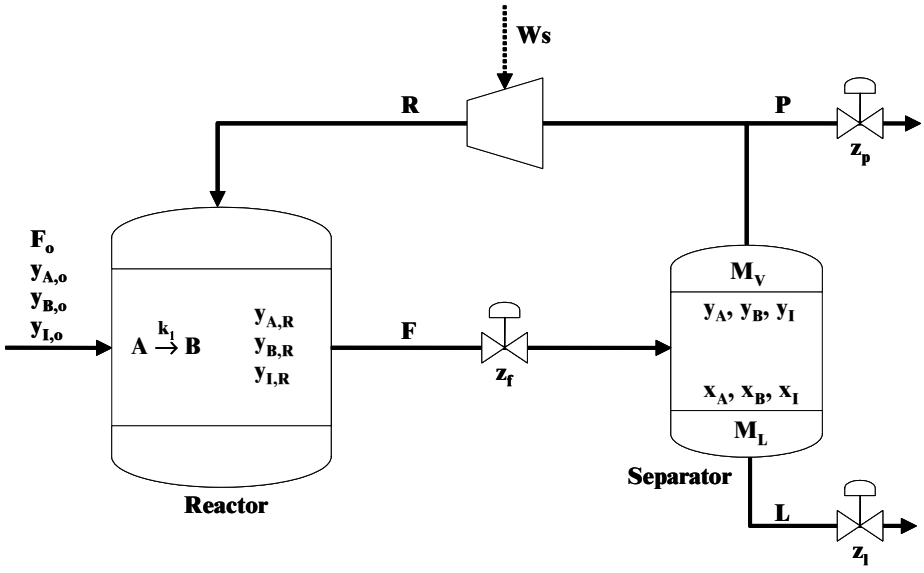

Figure 6.1: *Reactor-separator process.*

A first-order reaction takes place in the reactor, i.e. $A \xrightarrow{k_1} B$. In the condenser-separator, the interphase mole transfer rates for the components A, B, and I are governed by rate expressions of the form $N_j = K_j\alpha(y_j - \frac{P_j^S}{P}x_j)\frac{M_L}{\rho_L}$, where $K_j\alpha$ represents the mass transfer coefficient, y_j the mole fraction in the gas phase, x_j the mole fraction in the liquid phase, P_j^S the saturation vapor pressure of the component j, P the pressure in the condenser, and ρ_L the liquid density in the separator. A compressor drives the flow from the separator (lower pressure) to the reactor. Moreover, valves with openings z_f, z_l, and z_p allow the flow through F, L, and P, respectively. Assuming isothermal operation (meaning that the reactor and separator temperatures are perfectly controlled), the dynamic model of the system has the form given in Table 6.1.

Table 6.1: *Dynamic model of the reactor-separator with recycle network.*

Differential equations
$\frac{dM_R}{dt} = F_o + R - F$
$\frac{dy_{A,R}}{dt} = \frac{1}{M_R}[F_o(y_{A,o} - y_{A,R}) + R(y_A - y_{A,R}) - k_1 M_R y_{A,R}]$
$\frac{dy_{I,R}}{dt} = \frac{1}{M_R}[F_o(y_{I,o} - y_{I,R}) + R(y_I - y_{I,R})]$
$\frac{dM_V}{dt} = F - R - N - P$
$\frac{dy_A}{dt} = \frac{1}{M_V}[F(y_{A,R} - y_A) - N_A + y_A N]$
$\frac{dy_I}{dt} = \frac{1}{M_V}[F(y_{I,R} - y_I) - N_I + y_I N]$
$\frac{dM_L}{dt} = N - L$
$\frac{dx_A}{dt} = \frac{1}{M_L}[N_A - x_A N]$
$\frac{dx_I}{dt} = \frac{1}{M_L}[N_I - x_I N]$
Algebraic equations
$P_{reactor} = \frac{M_R R_{gas} T_{reactor}}{V_{reactor}}$
$P_{separator} = \frac{M_V R_{gas} T_{separator}}{(V_{separator} - \frac{M_L}{\rho_L})}$
$N_A = K_A \alpha \left(y_A - \frac{P_A^S}{P_{separator}} x_A \right) \frac{M_L}{\rho_L}$
$N_I = K_I \alpha \left(y_I - \frac{P_I^S}{P_{separator}} x_I \right) \frac{M_L}{\rho_L}$
$N_B = K_B \alpha \left[(1 - y_A - y_I) - \frac{P_B^S}{P_{separator}} (1 - x_A - x_I) \right] \frac{M_L}{\rho_L}$
$N = N_A + N_B + N_I$
$F = Cv_f z_f \sqrt{P_{reactor} - P_{separator}}$
$L = Cv_l z_l \sqrt{P_{separator} - P_{downstream}}$
$P = Cv_p z_p \sqrt{P_{separator} - P_{downstream}}$
$R = \frac{W_s}{\frac{1}{\epsilon} \frac{\gamma R_{gas} T_{separator}}{\gamma - 1} \left[(\frac{3P_{reactor,max}}{P_{separator}})^{\frac{\gamma-1}{\gamma}} - 1 \right]}$

Where:
- M_R, M_V, and M_L denote the molar holdups in the reactor and separator vapor and liquid phases, respectively.
- R_{gas} is the universal gas constant.
- $\gamma = \frac{C_P}{C_V}$ is assumed constant.
- Cv_f, Cv_l, and Cv_p are the valve constants.
- $P_{downstream}$ is the pressure downstream the system (assumed constant).
- ϵ is the compressor efficiency.
- $P_{reactor,max}$ is the maximum allowed pressure in the reactor.

6.4.2 Economic approach to the selection of controlled variables

Degree of freedom analysis

The open loop system has 3 degrees of freedom at steady state, namely the valve at the outlet of the reactor (z_F), the purge valve (z_P), and the compressor power (W_s). The valve at the separator outlet (z_L) has no steady state effect and is used solely to stabilize the process.

Table 6.2 lists the candidate controlled variables considered in this example. With 3 degrees of freedom and 18 candidate there are $\binom{18}{3} = \frac{18!}{3!15!} = 816$ possible ways of selecting the control configuration. We then determine whether there are active constraints during operation.

Table 6.2: *Selected candidate controlled variables.*

Y1	Reactor holdup	M_R
Y2	Vapor mole fraction of A in the reactor	$y_{A,R}$
Y3	Vapor mole fraction of I in the reactor	$y_{I,R}$
Y4	Vapor mole fraction of A in the separator	y_A
Y5	Vapor mole fraction of I in the separator	y_I
Y6	Liquid mole fraction of A in the separator	x_A
Y7	Liquid mole fraction of B in the separator	x_B
Y8	Liquid mole fraction of I in the separator	x_I
Y9	Reactor pressure	$P_{reactor}$
Y10	Separator pressure	$P_{separator}$
Y11	Flow out of the reactor	F
Y12	Liquid flow out of the separator	L
Y13	Purge flow	P
Y14	Recycle flow	R
Y15	Valve opening	z_F
Y16	Valve opening	z_L
Y17	Valve opening	z_P
Y18	Compressor power	W_S

Definition of optimal operation

The following profit is to be maximized:

$$(-J) = (p_L - p_P)L - p_W W_s \tag{6.2}$$

subject to

$$P_{reactor} \leq 2MPa$$
$$x_B \geq 0.8711$$
$$W_S \leq 20kW$$
$$z_F, z_P \in [0, 1]$$

where p_L, p_P, and p_W are the prices of the liquid product, purge (here assumed to be sold as fuel), and compressor power, respectively.

Identification of important disturbances

We will consider the disturbances listed in Table 6.3 below.

Table 6.3: *Disturbances to the process operation.*

No.	Disturbance
D1	20% increase in F_0
D2	10% reduction in F_0
D3	20% increase in $y_{I,o}$
D4	$y_{B,o} = 0.02$ with $y_{A,o} = 0.96$
D5	5% reduction in $K_{reaction}$
D6	10% reduction in $T_{reaction}$
D7	5% reduction in x_B
D8	5% increase in x_B

Optimization

Two constraints are active at the optimal through the optimizations (each of which corresponding to a different disturbance), namely the reactor pressure $P_{reactor}$ at its upper bound and the product purity x_b at its lower bound. These consume 2 degree of freedom since it is optimal to control them at their set point (Maarleveld and Rijnsdorp, 1970) leaving 1 unconstrained degree of freedom.

Unconstrained variables: Evaluation of the loss

To find the remaining controlled variable, it is evaluated the loss imposed by keeping selected variables constant when there are disturbances.

The candidate set is given in Table 6.2 with the exception of $P_{reactor}$ and x_B. Table 6.4 shows the results of the loss evaluation. We see that the smallest losses were found for the compressor power W_s which is then selected as the unconstrained controlled variable.

In summary, by the self-optimizing approach, the primary variables to be controlled are then $y = [P_{reactor}\ x_B\ W_S]$ with the manipulations $u = [z_F\ z_P\ W_S]$. In addition,

Table 6.4: *Loss evaluation for the selected candidates in Table 6.2.*

Candidate	D1	D2	D3	D4	D5	D6	D7	D8	Avg.
M_R	0.000	0.009	0.010	0.000	0.000	Inf$^{(*)}$	Inf	0.000	Inf
$y_{A,R}$	Inf	Inf	Inf	Inf	Inf	Inf	Inf	Inf	Inf
$y_{I,R}$	Inf	2.80	2.07	5.99	0.13	6.76	Inf	Inf	Inf
y_A	Inf	Inf	11.15	Inf	Inf	68.49	Inf	34.50	Inf
y_I	Inf	5.05	11.52	61.74	Inf	68.52	Inf	Inf	Inf
x_A	Inf	0.37	0.42	3.59	Inf	1.46	Inf	Inf	Inf
x_I	Inf	0.37	0.42	3.59	Inf	1.46	Inf	1.60	Inf
P_{sep}	574.63	5.04	11.51	Inf	Inf	Inf	Inf	Inf	Inf
F	6.65	1.96	0.49	0.27	1.34	0.01	4.06	0.95	1.97
L	Inf	Inf	Inf	Inf	Inf	69.37	Inf	Inf	Inf
P	Inf	Inf	Inf	Inf	Inf	Inf	Inf	Inf	Inf
R	6.33	1.96	0.47	0.21	1.34	0.01	4.06	1.09	1.93
z_F	5.95	2.12	0.54	0.15	1.14	0.05	0.85	0.31	1.39
z_L	Inf	Inf	Inf	Inf	Inf	69.26	Inf	Inf	Inf
z_P	Inf	Inf	Inf	Inf	Inf	Inf	Inf	Inf	Inf
W_S	2.88	1.89	0.37	0.78	1.07	0.11	1.64	0.86	1.20

$^{(*)}$ Inf means infeasible operation.

secondary controlled variables may be introduced to improve the dynamic behavior of the process. With these variables, a number of control configurations can be assigned and some of them will be assessed later in this chapter.

6.4.3 Selection of controlled variables by singular perturbation analysis

According to the hierarchical control structure design proposed by Baldea and Daoutidis (2006) based on the time scale separation of the system, the variables to be controlled and their respective manipulations are given in Table 6.5. It is important to note that no constraints are imposed in the variables in contrast with the self-optimizing control approach.

Previously in Baldea and Daoutidis (2006) economics were not considered and the structure they found leads to infeasible operation since the constraint in the reactor pressure $P_{reactor}$ (or M_R) and compressor power (W_S) can be exceeded in some cases. A simple modification would be to control x_B using the separator pressure and keeping the reactor pressure at its set point. This will be discussed later in this chapter.

Table 6.5: *Control structure selection based on the singular perturbation analysis.*

Time scale	Controlled output	Manipulation
Fast	M_R ($P_{reactor)}$	F (z_f)
Fast	M_V ($P_{separator}$)	R (z_p)
Intermediate	M_L	L (z_l)
Intermediate	x_b	$M_{R,setpoint}$ ($P_{reactor,setpoint}$)
Slow	$y_{I,R}$	P

6.4.4 Control configuration arrangements

The objective of this study is to explore how the configurations suggested by the two different approaches can be merged to produce an effective control structure for the system. Thus, as a starting point, the following two "original" configurations are presented:

1. Figure 6.2: This is the original configuration from the singular perturbation approach (Baldea and Daoutidis, 2006).
2. Figure 6.3: This is the simplest self-optimizing control configuration with control of the active constraints ($P_{reactor}$ and x_B) and self-optimizing variable W_S.

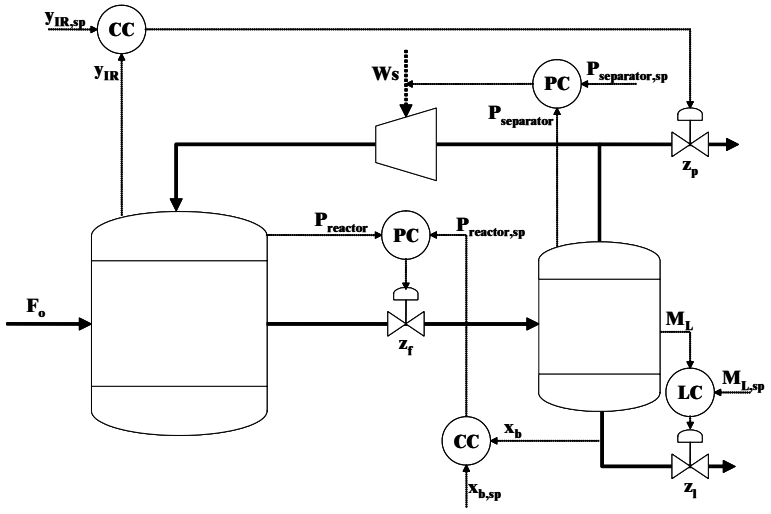

Figure 6.2: *Original configuration based on singular perturbation with control of x_B, $P_{separator}$, and $y_{I,R}$.*

None of these are acceptable. The configuration in Figure 6.2 is far from economically optimal and gives infeasible operation with the economic constraints $P_{reactor}$ exceeded. On the other hand, Figure 6.3 gives unacceptable dynamic performance.

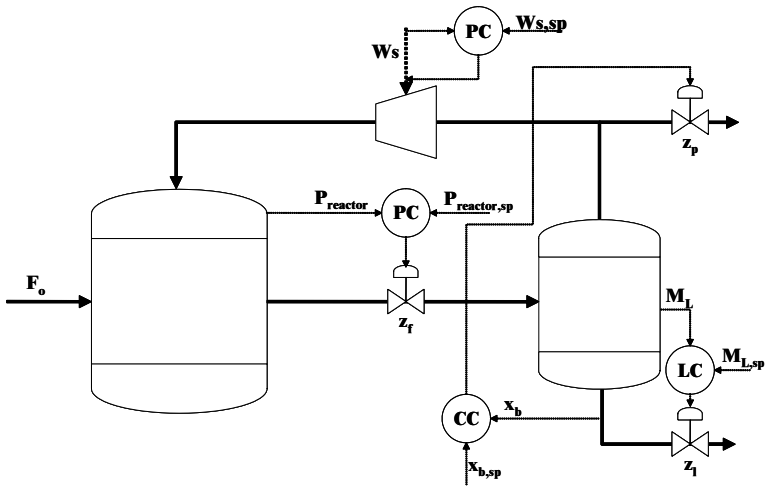

Figure 6.3: *Simplest self-optimizing configuration with control of x_B, $P_{reactor}$, and W_S.*

The idea is to combine the two approaches. Since one normally starts by designing the regulatory control system, the most natural is to start from Figure 6.2. The first evolution of this configuration is to change the pressure control from the separator to the reactor (Figure 6.4). In this case, both active constraints ($P_{reactor}$ and x_b) are controlled in addition to impurity level in the reactor ($y_{I,R}$). The final evolution is to change the primary controlled variable from $y_{I,R}$ to the compressor power W_s (Figure 6.5). The dynamic response for this configuration is very good and the economics are close to optimal.

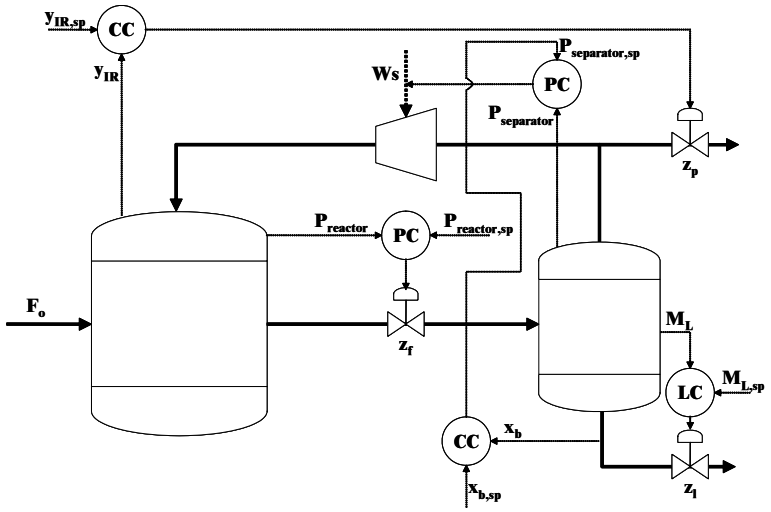

Figure 6.4: *Modification of Figure 6.2: Constant pressure in the reactor instead of in the separator.*

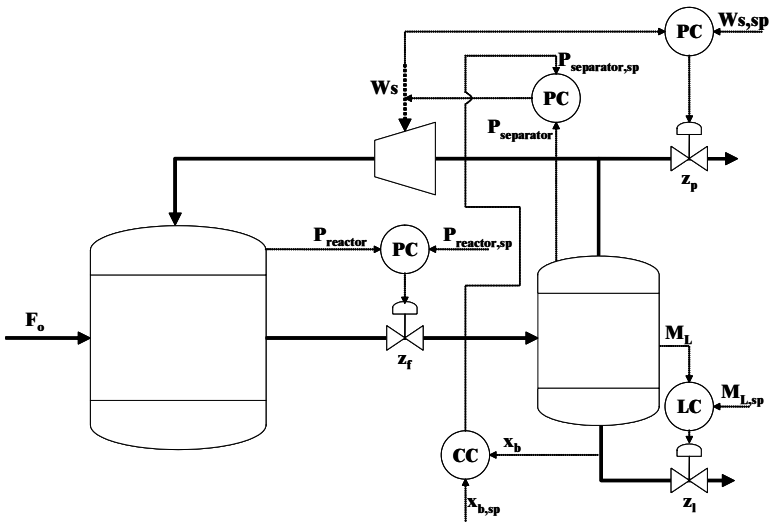

Figure 6.5: *Final structure from modification of Figure 6.4: Set recycle (W_S) constant instead of the inert composition ($y_{I,R}$).*

Simulations

Simulations are carried out so the above configurations are assessed for controllability. Two major disturbances are considered: a sustained reduction of 10% in the feed flow rate F_o at $t = 0$ followed by a 5% increase in the set point for the product purity x_B at $t = 50$h. The results are found in Figures 6.6 through 6.9.

The original system in Figure 6.2 shows an infeasible response when it comes to increasing the set point of x_B since the reactor pressure increases out of bound (see Figure 6.6).

With $P_{reactor}$ controlled (here integral action is brought about) by z_F (fast inner loop), the modified configuration shown in Figure 6.4 gives infeasible operation for set point change as depicted in Figure 6.8.

The proposed configuration in Figure 6.3, where the controlled variables are selected based on economics presents a very poor dynamic performance for set point changes in x_B as seen in Figure 6.7 due to the fact that the fast mode x_B is controlled by the small flow rate z_P and fast responses are obviously not expected, indeed the purge valve (z_P) stays closed during almost all the transient time.

Finally, the configuration in Figure 6.5 gives feasible operation with a very good transient behavior (see Figure 6.9).

In addition, the inert level, although not controlled in some of the proposed configurations, does not build up in the system even for long simulation times. Moreover, the liquid level in the separator is perfectly controlled for all configurations.

The steady-state profit for the two disturbances is shown in the caption of Figures 6.6 through 6.9.

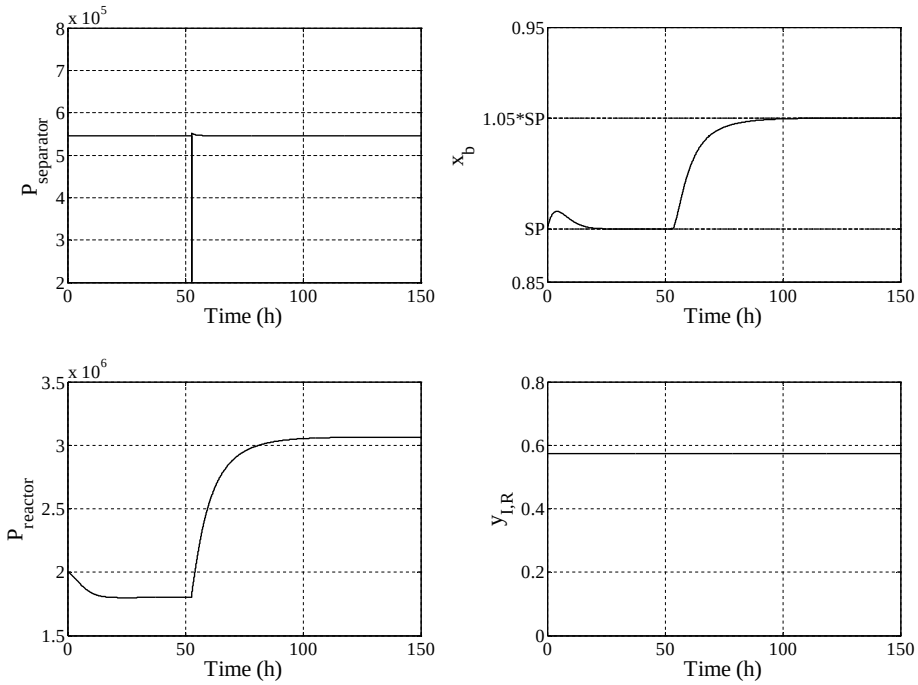

Figure 6.6: *Closed-loop responses for configuration in Figure 6.2: Profit =* $43.13k\$/h$ *and* $43.32k\$/h$ *(good but infeasible).*

6.5 Discussion

In the singular perturbation approach the model analysis may be used to tell which flows (inputs) are suitable for the different time scales. However, it can not be used to tell which outputs are needed to be controlled for economic reasons. Essentially, this approach sets the regulatory control layer in a hierarchical fashion, which represents a great advantage. In contrast, a plantwide control structure design cares for both supervisory and regulatory layers, where the self-optimizing control approach is used to set the former.

So, what is the link between these two approaches? The main link is that the singular perturbation approach can be used to "pair" the inputs (flows) with the outputs in the regulatory control layer resulting in a cascaded control configuration.

An economic analysis of the reactor-separator case study reveals the right variables to control in the slower control layer in order to keep the operation profitable (or at least near optimality). The reactor pressure, $P_{reactor}$ and product purity x_B are both active constraints that, during operation, must be kept constant at its set point together with the self-optimizing variable W_S.

In terms of speed of responses, the expectations are that:

1. Reactor pressure ($P_{reactor}$) is fast (in general, pressure requires fast control): prefer

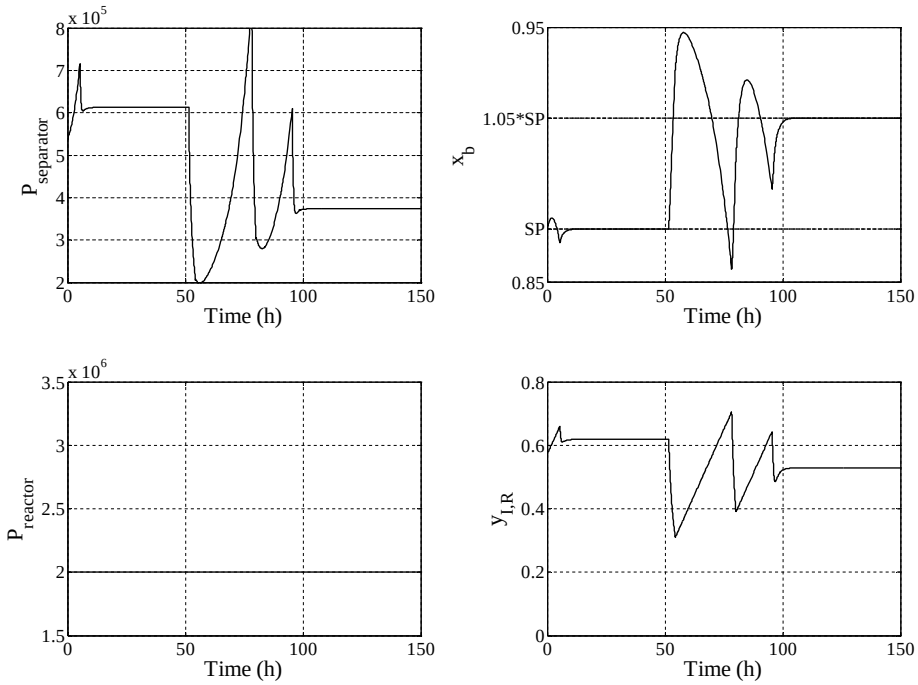

Figure 6.7: *Closed-loop responses for configuration in Figure 6.3: Profit* $= 43.21k\$/h$ *and* $= 43.02k\$/h$.

a large (gas) flow, i.e. F (z_F) or R (W_S). Particularly, one should use F (z_F) since R (W_S) is desired to be constant.

2. Separator liquid level (M_L) has intermediate speed: prefer using L (z_L) (intermediate flow).

3. Product purity (x_B) has also intermediate speed: it needs an intermediate flow, but since there are no such left since it is necessary to keep R (W_S) constant, one solution is to use R (W_S) dynamically for this (This is an interesting result that follows from the singular perturbation analysis!).

4. It is preferable to keep the compressor power (W_S) constant, but allowing it to vary dynamically as long as it is reset back to its desired value at steady state: the rule is to use the small purge flow P (z_P) for this.

6.6 Conclusion

This chapter contrasted two different approaches for the selection of control configurations. The self-optimizing control approach is used to select the controlled outputs that gives the economically (near) optimal for the plant. These variables must be controlled

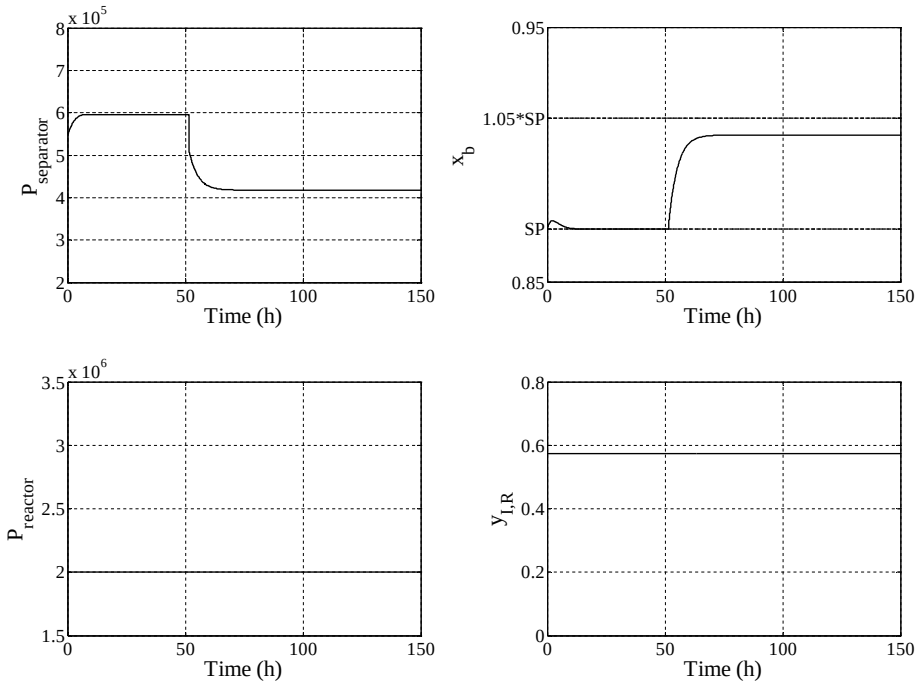

Figure 6.8: *Closed-loop responses for configuration in Figure 6.4: Profit* $= 43.20k\$/h$ *and* $= 43.07k\$/h$.

in the upper or intermediate layers in the hierarchy. The fast layer (regulatory control layer) used to ensure stability and local disturbance rejection is then successfully designed (pair inputs with outputs) based on the singular perturbation framework proposed in Baldea and Daoutidis (2006). The case study on the reactor-separator network illustrates that the two approaches may be combined successfully.

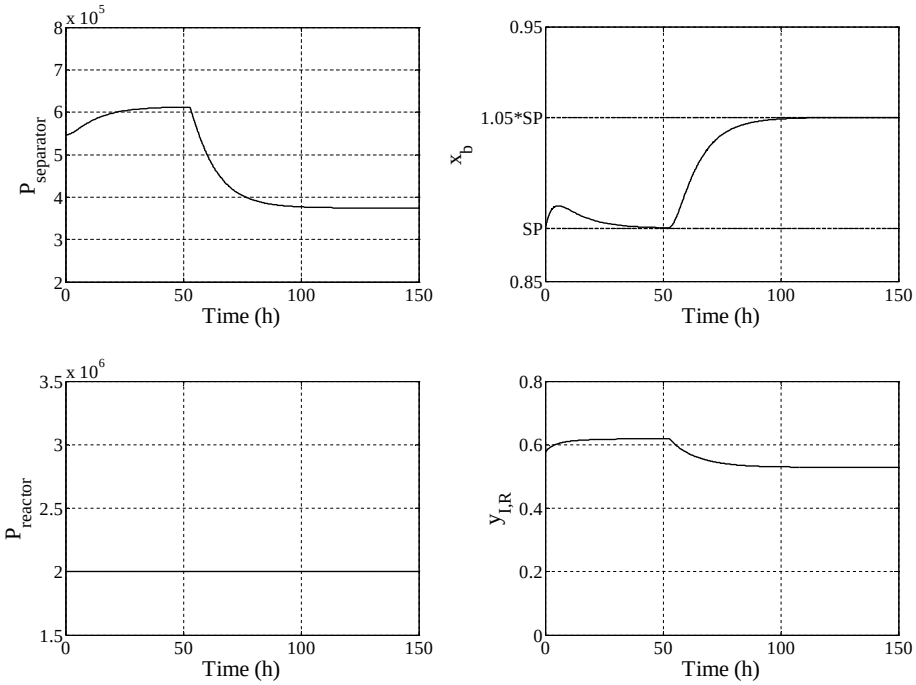

Figure 6.9: *Closed-loop responses for configuration in Figure 6.5: Profit* $= 43.21k\$/h$ *and* $= 43.02k\$/h$.

Chapter 7

Limit cycles with imperfect valves: Implications for controllability of processes with large gains

Based on the paper accepted for publication in
Industrial Engineering Chemistry Research

There is some disagreement in the literature on whether or not large plant gains are a problem when it comes to input-output controllability. In this chapter, controllability requirements are derived for two kinds of input errors, namely restricted (low) input resolution (e.g. caused by a sticky valve) and input disturbances. In both cases, the controllability is limited if the plant gain is large at high frequencies. Limited input resolution causes limit cycle behavior (oscillations) similar to that found with relay feedback. The magnitude of the output variations depends on the plant gain at high frequency, but is independent of the controller tuning. Provided frequent input (valve) movements are acceptable, one may reduce the output magnitude by forcing the system to oscillate at a higher frequency, for example by introducing a faster local feedback (e.g. a valve positioner) or by pulse modulating the input signal.

7.1 Synopsis

The main goal of feedback control is to the keep the plant outputs y within specifications in spite of disturbances, errors and uncertainty. A fundamental question arises: Is the process input-output controllable? There are many factors that need to be considered and one of them is the magnitude of the process gain. The gain depends on the frequency and, for multivariable plants, also on the input direction. To quantify this, the singular values $\sigma_i(G(j\omega))$ of the process transfer function $G(s)$ are considered. Of particular interest are the maximum and minimum singular values, denoted $\bar{\sigma}(G)$ and $\underline{\sigma}(G)$, respectively. In this chapter, for simplicity, mainly SISO systems are considered, where $\bar{\sigma}(G(j\omega)) = \underline{\sigma}(G(j\omega)) = |G(j\omega)|$.

It is well accepted that small process gains may cause problems. For example, the requirement for avoiding input saturation is $\underline{\sigma}(G) \geq 1$, that is, a minimum gain of one is required (Morari, 1983). This assumes that the desired output changes (set points) are of magnitude 1 and the allowed inputs are also of magnitude 1, both expressed in terms of the 2-norm.

It is less clear whether large process gains pose a problem. Skogestad and Postlethwaite (2005) consider the condition number, defined as $\gamma(G) = \bar{\sigma}(G)/\underline{\sigma}(G)$ and make the following statement: *A large condition number may be caused by a small value of* $\underline{\sigma}(G)$*, which is generally undesirable. On the other hand, a large value of* $\bar{\sigma}(G)$ *is not necessarily a problem.*

On the other hand, Moore (1992) claims that high sensitivity (high gains) can be a problem because of low input resolution in valves and actuators. He states: *Valves and other actuators all have a minimum resolution with respect to positioning. These limitations restrict the fine adjustments often necessary for high gain processes to reach a steady operation. If the fine adjustment necessary for steady state is less than the resolution of the valve, sustained oscillations are likely to occur. Consider, for example, a steam valve with resolution of* $\pm 1.0\%$*. If a valve position of* 53.45% *is necessary to meet the target temperature, then the valve will, at best, settle to a limit cycle that hunts over a range from about* 55% *to* 53%*. If the process gain is* 10*, the hunting of the valve will cause a limit cycle in the control temperature of* 20%. In this chapter, we confirm that limit cycles are unavoidable under such conditions, but we find that it is the process gain at the frequency of the limit cycles, and not at steady-state, that matters for controllability.

McAvoy and Braatz (2003) argue along the same lines as Moore (1992) and state that for control purposes the magnitude of steady-state process gain ($\bar{\sigma}(G)$) should not exceed about 50.

In this chapter two main types of input errors are discussed. We first consider the input oscillations caused by restrictions of the input (valve) resolution. Later, in section 7.7, we consider input (load) disturbance which is not related to the valve resolution problems. Most of the results are derived for first-order plus delay processes. When possible, more general derivations are presented.

7.2 Restricted input resolution and limit cycles

As mentioned by Moore (1992) and proved below, feedback control with restricted (low) input resolution results in limit cycles (hunting). A simple representation of restricted (low) input resolution is to use a quantized input as depicted in Figure 7.1.

The output u_q from the quantizer is

$$u_q = q \cdot \mathbf{round}\left(\frac{u}{q}\right), \tag{7.1}$$

where q is the quantization step and the **round** function takes its argument to the nearest integer. This may, for example, represent restricted valve resolution and to

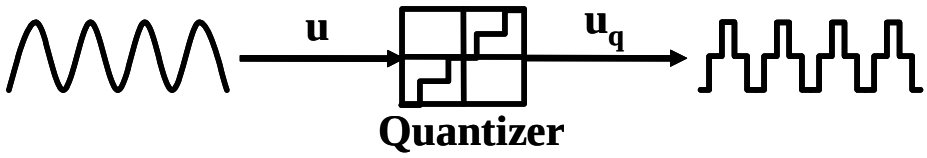

Figure 7.1: *Quantization of a smooth signal.*

some extent valve stiction and valve dead band (Shoukat Choudhory *et al.*, 2005). An extreme case with only one quantization step is an on-off valve.

Figure 7.2 shows a feedback system with a quantizer. Here $G(s)$ is the plant transfer function model, $K(s)$ the controller, y the plant output with reference r, and u the manipulated variable (for simplicity, the Laplace variable s is often omitted). The low input resolution results in a stepwise input "disturbance" of magnitude q. and this again results in oscillations in the plant output $y(t)$ of magnitude a. Note that a here is defined as the "total" amplitude from the bottom to the top of the oscillations.

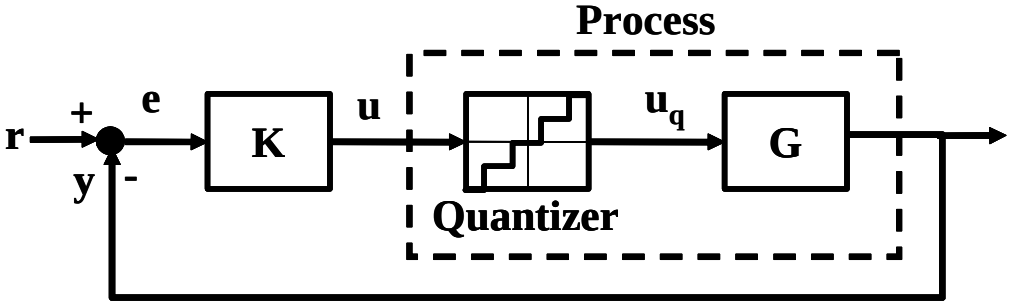

Figure 7.2: *Feedback control of process with restricted input resolution (quantizer)*

Theorem 7.1 *For the feedback system with a quantizer in Figure 7.2 limit cycles are inevitable if there is integral action in the controller such that the output in average has no steady-state offset.*

Proof: At steady-state the average value of the output y is equal to the reference r, that is $y_{ss} = r$ where y_{ss} denotes the average ("steady-state") value of $y(t)$ as $t \to \infty$. To achieve this the input u must on average equal the following value

$$u_{ss} = \frac{y_{ss}}{G(0)} = \frac{r}{G(0)}, \tag{7.2}$$

where $G(0)$ denotes the steady-state plant gain. Except for the special case that u_{ss} happens to exactly correspond to one of the quantizer levels q_i (which in practice with measurement noise will not occur), the quantized input u_q must then cycle between at least two of the quantizer levels. □

Let us consider the most common case where the output cycles between the two neighboring quantizer levels to u_{ss}, here denoted q_1 and q_2. Let f and $(1-f)$ denote the fraction of time spent at each of the two levels. Then, at steady-state (as $t \to \infty$) $u_{ss} = fq_1 + (1-f)q_2$ and we have the following expression for the fraction of time u spends at level q_1:

$$f = \frac{q_2 - u_{ss}}{q_2 - q_1} \tag{7.3}$$

Note that the closer u_{ss} is to one of the quantizer levels, the longer the time u_q will remain on it.

Example 7.1 *As an example consider the system simulated in Figure 7.3 where* $q_1 = 0$ *and* $q_2 = 0.03$ *(this may represent an on/off valve). The third order plant model is*

$$G(s) = \frac{100}{(10s+1)(s+1)^2} \tag{7.4}$$

and we use a PI-controller

$$K(s) = K_c\Big(\frac{\tau_I s + 1}{\tau_I s}\Big); \quad K_c = 0.04, \tau_I = 10 \tag{7.5}$$

Note that the integral time is chosen so that we cancel the dominant pole in $G(s)$ *(IMC tuning rule). The steady-state plant gain is* $G(0) = 100$*. Initially, the system is at steady-state with* $u_q = q_1 = 0$ *and* $y = r = 0$*. We then make a step change* $r = 1$*. The steady-state plant gain is* $G(0) = 100$*, so to achieve* $y_{ss} = 1$ *the required average input is* $u_{ss} = 1/100 = 0.01$ *which is closer to* $q_1 = 0$ *than* $q_2 = 0.03$*. The fraction of time* u_q *remains at* $q_1 = 0$ *is* $f = (0.03 - 0.01)/0.03 = 0.67$*. As expected, this agrees with the simulations.*

Example 7.2 *A similar simulation example with* $q_1 = 0$ *and* $q_2 = 0.03$ *is shown in Figure 7.3, but for a first-order with delay plant*

$$G(s) = \frac{ke^{-\theta s}}{(\tau s + 1)}, \tag{7.6}$$

with $k = 100$*,* $\theta = 1$ *and* $\tau = 10$*. We use the same PI-controller as in (7.5) with* $\tau_I = \tau = 10$ *and* $K_c = 0.04$*. The main difference compared to Example 7.2 is that the step reference change is much smaller,* $r = 0.2$*, such that the input stays a much shorter time at the upper quantizer level of* $q_2 = 0.03$*. The steady-state plant gain is* $k = G(0) = 100$*, so to achieve* $y_{ss} = 0.2$ *the required average input is* $u_{ss} = 0.2/100 = 0.002$*. From (7.3), the fraction of time* u_q *remains at* $q_1 = 0$ *is* $f = (0.03 - 0.002)/0.03 = 0.93$*. Again, this agrees with the simulations.*

For the simulated system in Figure 7.3 (Example 7.2), the magnitude of limit cycles (oscillations) in y is $a = 0.189$ and the period is $T = 6.72$s. The oscillations in $y(t)$ are seen to be quite close to sinusoidal. For the simulated system in Figure 7.4 (Example

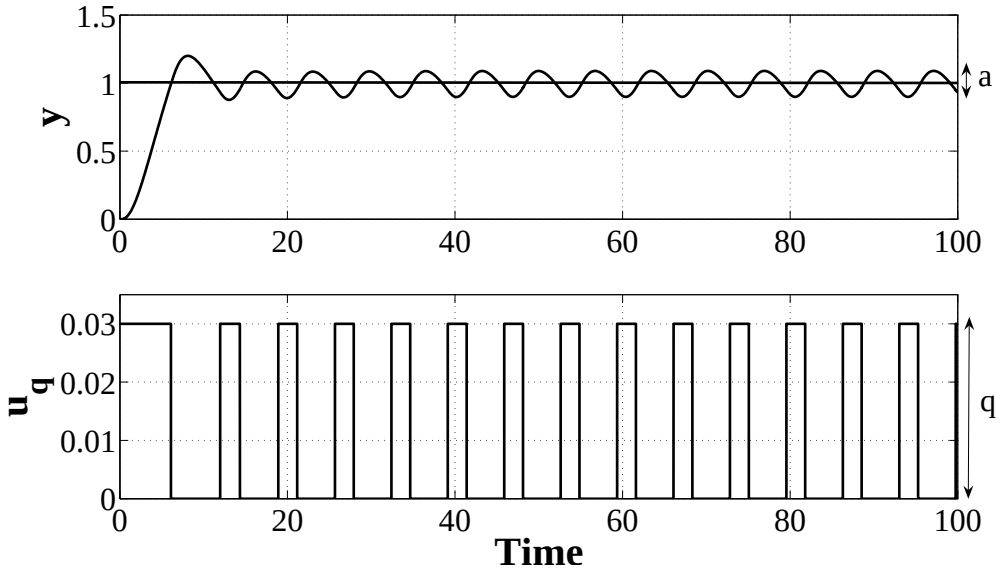

Figure 7.3: *Simulation results for system in Example 7.2.*

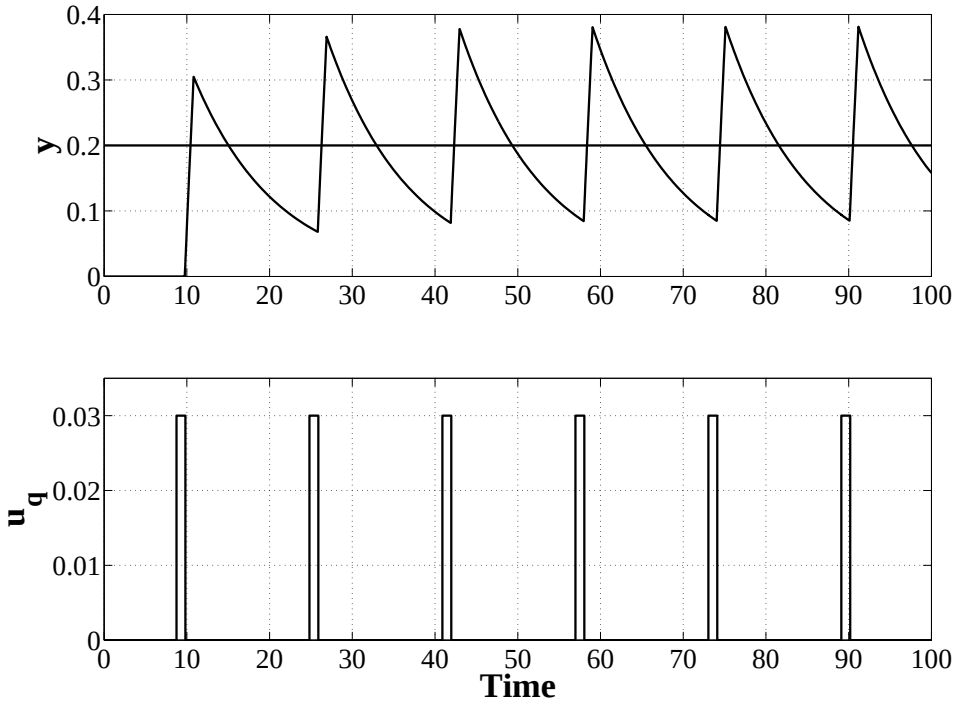

Figure 7.4: *Simulation results for system in Example 7.2.*

7.2), we have $a = 0.3$ and $T = 16.07$s. However, in this case the oscillations in $y(t)$ are far from sinusoidal.

We next want to derive analytic expressions for a and T. We first make the simplifying assumption that the resulting limit cycles are sinusoidal and then study the more general case.

7.3 Describing function analysis of oscillations (assuming sinusoids)

The quantizer (nonlinearity) that causes the limit cycles can be regarded as a relay without hysteresis and is in the following treated as such. As an approximation, the amplitude of the oscillations can then be found analytically from an harmonic linearization or describing function analysis of the nonlinearity. This is analysis is exact if the resulting limit cycle is sinusoidal. For the feedback system in Figure 7.2, the condition for oscillation is given by (Aström and Hägglund, 1988)

$$N(a_u)L(j\omega) = -1, \tag{7.7}$$

where $N(a_u)$ is the describing function of the nonlinearity (quantizer) which is as a function of the amplitude a_u of the oscillations in $u(t)$— at the quantizer input, and $L = GK$ is the loop transfer function (excluding the quantizer). For a relay without hysteresis, the describing function is (Slotine and Li, 1991)

$$N(a_u) = \frac{4q}{\pi a_u}, \tag{7.8}$$

and q is the relay amplitude (quantization step). Since according to (7.8), $N(a_u)$ is a real number, it follows from (7.7) that ω is actually the ultimate frequency $\omega_{L,180}$ and

$$N(a_u) = \frac{1}{|L(j\omega_{L,180})|} = \frac{4q}{\pi a_u} \tag{7.9}$$

The amplitude of the corresponding oscillations at the plant output are

$$a = a_u/|K(j\omega_{L,180})| \tag{7.10}$$

which leads to

$$a = \frac{4q|G(j\omega_{L,180})|}{\pi} \tag{7.11}$$

$$T = \frac{2\pi}{\omega_{L,180}} \tag{7.12}$$

where T is the period of oscillation. This is exact if the limit cycles are sinusoidal.

Example 7.2 (continued). For the system given by (7.4) and (7.5), $\angle L(j\omega_{L,180}) = -\frac{\pi}{2} - 2\arctan(1 \cdot \omega_{L,180}) = -\pi$ which yields $\omega_{L,180} = 1$ [rad/s] and $|G(j\omega_{L,180})| = 4.999$.

From a describing function analysis the period of oscillation is then $T = \frac{2\pi}{\omega_{L,180}} = 6.28$s. and from (7.11) $a = \frac{4}{\pi} q|G(j\omega_{L,180})| = 0.191$. This is in good agreement with the simulation results ($T = 6.72$s, $a = 0.189$).

First-order with delay process. Consider a first-order with delay plant $G()$ controlled by a PI-controller with $tau_I = \tau$,

$$G(s) = \frac{ke^{-\theta s}}{\tau s + 1} \tag{7.13}$$

$$K(s) = K_c \frac{\tau_I s + 1}{\tau_I s},\ \tau_I = \tau \tag{7.14}$$

For this system we have $\angle L(j\omega_{L,180}) = -\frac{\pi}{2} - \omega_{L,180}\theta = -\pi$ which gives $\omega_{L,180} = \frac{\pi}{2}\frac{1}{\theta}$ and $|G(\omega_{L,180})| = k/\sqrt{(\frac{\pi}{2}\frac{\theta}{\tau})^2 + 1}$. From the describing analysis in (7.11) and (7.12) we then have

$$a = \frac{4}{\pi} \frac{qk}{\sqrt{(\frac{\pi}{2}\frac{\tau}{\theta})^2 + 1}} : \quad T = 4\theta \tag{7.15}$$

For small delays ($\theta/\tau \ll 1$) this gives $a \approx \frac{8}{\pi^2} q \frac{k}{\tau}\theta$, and we see that amplitude of the oscillations increases proportionally with $k' = k/\tau$ (intial slope of step response) and θ. For large delays ($\theta/\tau \gg 1$), $a \approx \frac{4}{\pi} qk$, and we see that amplitude of the oscillations increases proportionally with k (steady-state gain) and is independent of θ. In all cases a increases proportionally with q.

Example 7.2 (continued). With $k = 100, \theta = 1, \tau = 10$ and $q = 0.03$ (7.15) gives $T = 4$s and $a = 0.243$. This should be compared with the actual value from the simulations whicha are $T = 16.1$s and $a = 0.296$. Taking into account that the oscillations in $y(t)$ are far from sinusoidal, the value of a in (7.15) obtained from the describing function analysis is quite good (about 20% too low). However, the period T is a factor of four too small.

From the two examples its seems that the amplitude of a in (7.18) from the describing function analysis is quite accurate, but that the actual period may be much larger. This conclusion is confirmed by an exact analysis for a first-order with delay plant presented next.

7.4 Exact analysis of oscillations for first-order plus delay process

In this section, exact results for non-sinusoidal quantized responses are derived for a first-order with delay plant controlled by a PI controller with $\tau_I = \tau$. The following theorem is based on the work by Wang *et al.* (1997).

Theorem 7.2 *For a system given by (7.13) and (7.14) set up according to the configuration of Figure 7.2 with quantizer level q, the amplitude and period of the limit cycle*

oscillations are

$$a = kq\frac{1-e^{\frac{-t_1}{\tau}}+e^{\frac{-T}{\tau}}-e^{\frac{-(T-t_1)}{\tau}}}{1-e^{\frac{-T}{\tau}}} \tag{7.16}$$

$$T = \theta(\frac{1}{1-f}+\frac{1}{f}), \tag{7.17}$$

where $t_1 = \frac{\theta}{1-f}$ *and* f *is calculated from* $u_{ss} = fq_1 + (1-f)q_2$.

Proof: See the appendix. □

Example 7.2 (continued). With $f = 0.933$, the amplitude and period of oscillation calculated using (7.16) and (7.17) are $a = 0.2962$ and $T = 16.07s$, respectively, which matches exactly the observed results in Figure 7.4.

Note that the assumption $\tau_I = \tau$ is the reason why a and T are independent of the controller settings K_c and τ_I.

In Figure 7.5 the amplitude $\frac{a}{kq}$ from (7.16) is plotted as a function of $\frac{\theta}{\tau}$ for various values of f. For small delays ($\theta << \tau$), a increases almost proportionally θ/τ, but for large values of θ it levels off at a constant value of $a = kq$ Note that a depends only weakly on f.

To compare, the dashed line in Figure 7.5 represents (7.15) from the describing function analysis. The agreement is generally very good with a maximum difference of 27% for large values of θ/τ.

On the other hand, note that the period of oscillation can be very different from that found with the describing function analysis. From (7.17) the period T increases proportionally with the delay θ, which agress with the value $T = 4\theta$ in (7.17) from the describing function analysis. However, in the exact analysis, T also depends on f and goes to infinity as f approaches 0 or 1. From (7.17), the minimum value $T = 4\theta$ is obtained when $f = 0.5$, and only this limiting value agrees with the describing function analysis. This is not too surprising as the input is most close to "sinusoidal" when $f = 0.5$.

7.5 Controllability requirements for systems with restricted input resolution

Consider a feedback system with restricted input resolution (quantized input) as shown in Figure 7.2. Assume there is integral action in the controller such that there are limit cycles (Theorem 1). Let $a_{\max}$ denote the maximum allowed amplitude of the limit cycles (oscillations) in y. Then, from (7.11) the following approximate controllability requirement applies:

$$|G(j\omega_{L,180})| < \frac{\pi}{4}\frac{a_{\max}}{q}, \tag{7.18}$$

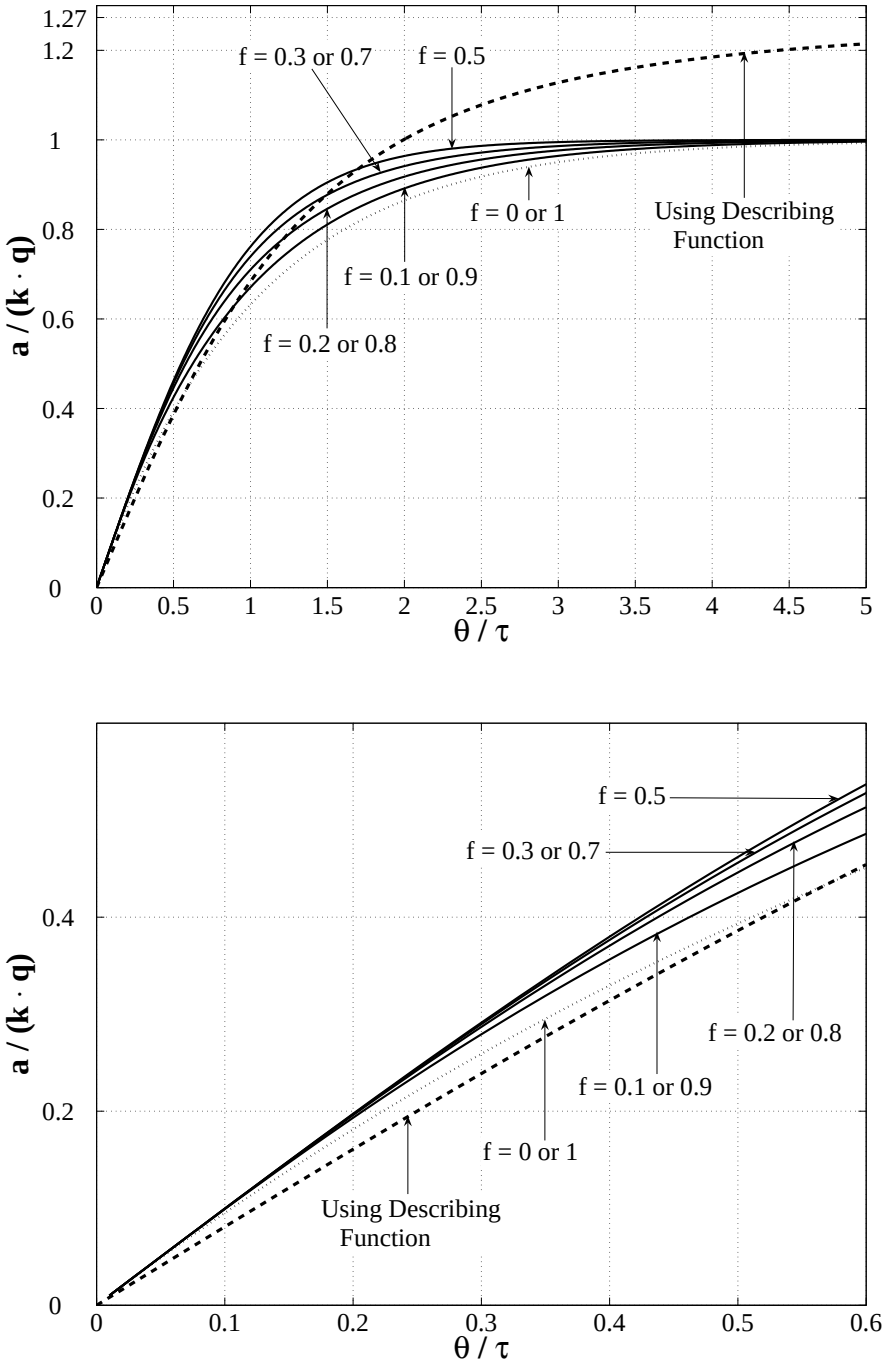

Figure 7.5: *Amplitude a in (7.16) plotted against $\frac{\theta}{\tau}$ for first order plus delay processes. The lower figure is a close-up of the upper figure for small values of $\frac{\theta}{\tau}$.*

Note that this condition depends on the plant only, and more specifically on the plant gain at frequency $\omega_{L,180}$.

Remark 1. The controllability condition (7.18) is approximate because it is based on a describing function analysis which is exact only for sinusoidal oscillations. Nevertheless, the results in the previous section indicates that the gain from the describing function analysis is surpisingly accurate. For a first-order plus delay process, the maximum deviation was only 27% (for large values of θ/τ). Thus, (7.18) is expected to provide a tight controllability condition.

Remark 2. The controller has some effect on the condition, because $\omega_{L,180}$ is the frequency where the sum of the phase lag in the controller K and plant G is 180^o. However, for a well-tuned controller we typically have $\omega_{L,180} \approx 1.57/\theta$, that is, ω_L depends only on on the effective delay θ in the plant. Specifically, this value applies for a first (or second) order plant tuned with a SIMC PI(D)-controller (Skogestad, 2003) (the value is exact when τ_1 is smaller than about 8θ where the SIMC-rule is $\tau_I = \tau_1$, and also applies well for the case when τ_1 is large and the SIMC-rule is $\tau_I = 8\theta$).

Remark 3. Persistent oscillations are generally undesirable. Therefore, the allowed $a_{\max}$ for oscillations is typically considerably much smaller (about 10%) than the maximum allowed output deviation, $y_{\max}$, i.e., $a_{\max} = 0.1 y_{\max}$.

7.6 How to mitigate oscillations caused by restricted input resolution

From the describing function analysis, the magnitude a of the output oscillations for the system in Figure 7.2 is given by (7.15). The magntitude can be reduced, for example by the following means:

(a) Change the valve so that the resolution is better (smaller quantization level q).

(b) Redesign the process or the measurement devices to get a smaller effective delay θ.

(c) Introduce fast, forced cycles at the input with a higher frequency than those generated "naturally". For example, one may use high-frequency pulse modulation or add a high-frequency "dither" signal (forced sinusoidal disturbance at the plant input).

(d) "Valve positioner": Use a measurement of u_q and add a local feedback at the input to generate faster cycling, see Figure 7.6. This may be viewed as a combination of cases (b) and (c).

The problem with approaches (b), (c) and (d) is that fast input cycling may be undesirable, for example, because the valve cannot be moved so fast or because of excessive wear.

Frequency (pulse) width modulation. Let us consider in more detail approaches (c) and (d). A system with restricted (low) input resolution and no (average)

steady-state offset is bound to cycle (Theorem 1) and the amplitude a of the oscillations is given by the process gain at the frequency of oscillations, e.g. see (7.11). So far, we have let the system cycle at its "natural" frequency $\omega_{L,180}$, as given by (7.12) and (7.17). However, since the gain $|G(j\omega)|$ for most processes is lower at high frequencies, an attractive alternative is make the system cycle at a higher frequency.

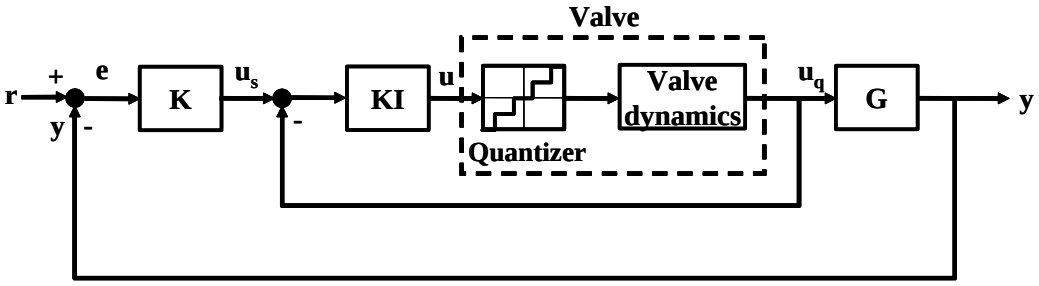

Figure 7.6: *Frequency modulation generated using valve position controller KI.*

One approach (d) is to use a valve position controller based on measuring u_q, as shown in Figure 7.6. Here, the controller K sets the set point u_s for the valve position (input), and the "internal" valve position controller (KI) adjusts the input u signal such that the actual input u_q matches the desired input u_s (at least on average). The valve position controller (KI) should have integral action, or a sufficiently high proportional gain, such that the internal loop cycles. The frequency of the cycling is determined by the effective delay in the "internal" valve position loop, which generally is much smaller than the delay in the overall outer loop. The results is the that the frequency of the oscillations is much higher and the resulting amplitude a of the output is much smaller. This agrees with the recommendations in the Instrument Engineers' Handbook (Liptak, 2006), where it is noted that a positioner can reduce the dead band of a valve/actuator combination from as much as 5% to less than 0.5%.

However, one may not have a measurement of the actual input u_q, and a valve position controller is in fact not necessary to reduce the effect of low input resolution. A more general approach (c) is to introduce forced pulsing by adding a frequency modulator F at the output of the controller. One realization for F is an internal feedback loop as depicted in Figure 7.7. This is similar to the valve positioner controller, except that we need an internal quantizer because there is no measurement of u_q. The modulator forces the system to cycle at a higher frequency than the one that follows "naturally". For example, forced pulsing is commonly used for on/off valves in small-scale plants where the valve may open or close every second and the controller sets the average position.

Example 7.3 *By use of a valve position controller as shown in Figure 7.6, the response of the system in (7.13) and (7.14) is depicted in Figure 7.8. The valve dynamics is assumed to be a delay of* 0.1*, and the remaining process (G) has a delay of* 0.9*. As it*

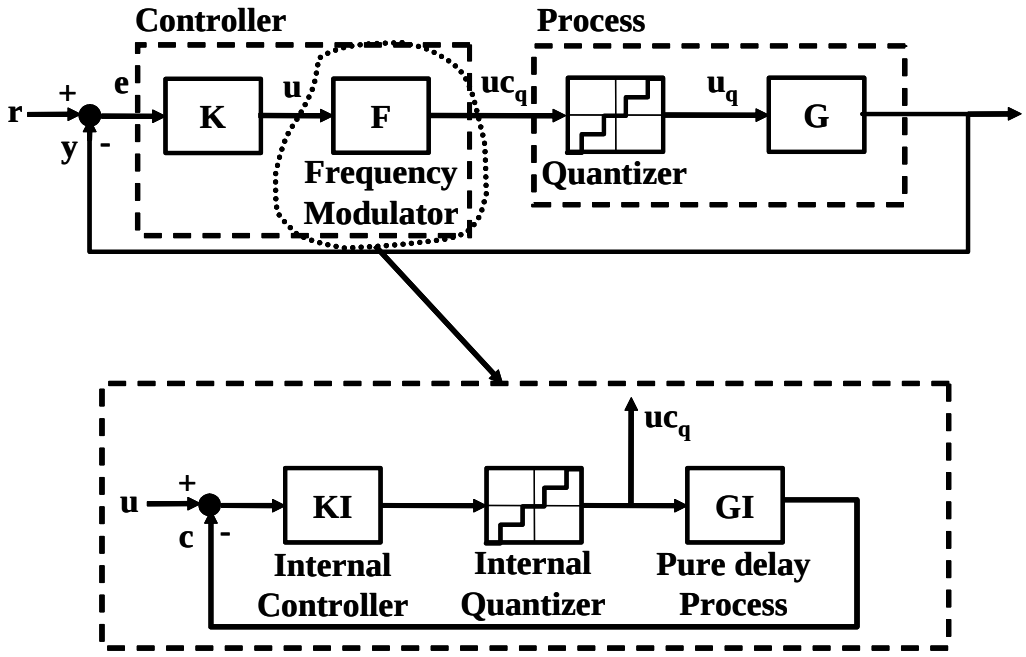

Figure 7.7: *System with frequency modulation. The box shows one way of generating high-frequency oscillations. Alternatively, a clock may be used to set the frequency while the controller sets the pulse width.*

can be seen, the output amplitude is drastically reduced at the expense of high-frequency input oscillations.

P-control. Another potential approach to eliminate oscillations is to use a P-controller (with a sufficiently low controller gain). However, in practice this approach is not acceptable because it results in an unacceptable steady-state offset. Consider a set point change r, for which the desired input to achieve no offset is $u_{ss} = \frac{r}{G(0)}$, see (7.2). Assume that r is such that u_{ss} is in the middle between two quantization levels for the input. Then, for any non-oscillating control system, including feedforward, we have $\Delta u = |u_q - u_{ss}| \geq \frac{q}{2}$ and the resulting offset in the output is

$$|y - r| = |G(0)| \cdot |u_q - u_{ss}| \geq |G(0)|\frac{q}{2} \tag{7.19}$$

From this we conclude that the offset $|y - r|$ will be large for a plant with a large steady-state gain, $|G(0)|$, so P-control is in practice not recommended as a method to mitigate oscillations

7.7 Input (load) disturbance

Consider a plant model in deviation variables

$$y(s) = G(s)u(s) + G_d(s)d(s) \tag{7.20}$$

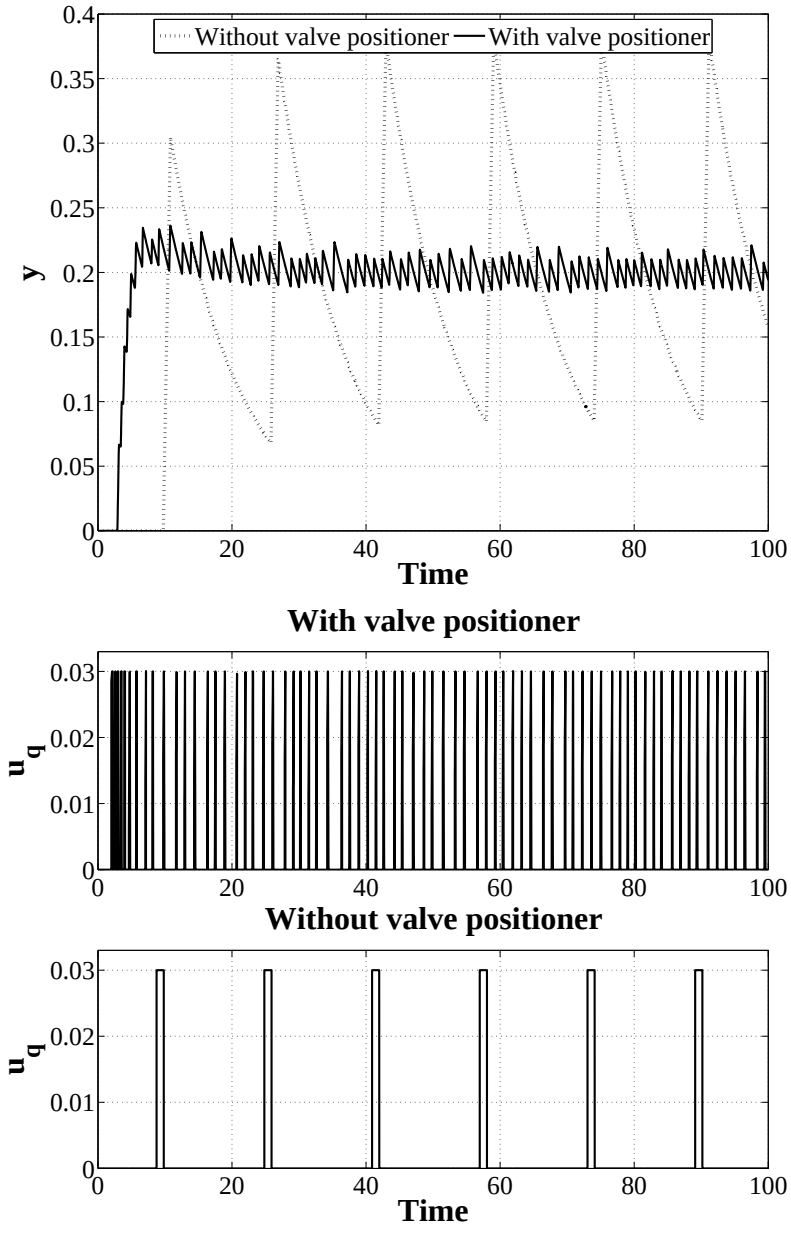

Figure 7.8: *Effect of using valve position control for the system in Example 7.2.*

where G is the plant model, G_d the disturbance model, y the plant output, u the manipulated variable, and d the disturbance (for simplicity, the Laplace variable s is often omitted). Without control the effect of disturbances on the output is $y = G_d(s)d$, and by "large" disturbances is meant that the product $|G_d d|$ is large, such that the output deviation $|y|$ will be large unless we apply control. In this section, input disturbances are mainly considered, i.e., $G_d = G$. This case is illustrated in Figure 7.9 where $d = d_u$ is the disturbance at the plant input.

Feedforward control. As mentioned in the introduction, a large plant gain, especially at steady state, is a problem with feedforward control. As an example, consider a plant $y = G(u + d)$, where $d = d_u$ is the input (load) disturbance. Clearly, if $|G|$ is large, then $|u + d|$ needs to be small to avoid a large $|y|$. With feedforward control u is adjusted based on measuring d. First, an accurate measurement of d is required and it must be possible to adjust u such that $|u - d|$ is small. The latter is not possible with restricted input resolution. For instance, returning to the example of Moore (1992) from the introduction; $|u - d| = 2\%$ and $|G| = 10$ gives $|y| = 20\%$, all at steady state.

Feedback control. On the other hand, with feedback control, "large" disturbances are not necessarily a problem, at least not at steady state. Consider a single disturbance d. Without control the steady-state sinusoidal response from d to the output is $y(\omega) = G_d(j\omega)d(\omega)$, where phasor notation is used and $|d(\omega)|$ denotes the magnitude of the disturbance at frequency ω. We assume that the magnitude is independent of the frequency, i.e. $|d(\omega)| = d_0$ and assume that the control objective is that the output is less than $y_{\max}$ at any given frequency, i.e., $|y(\omega)| < y_{\max}$. From this, one can immediately draw the conclusion that *no control is needed if* $|G_d(j\omega)d_0| < y_{\max}$ *at all frequencies (in which case the plant is said to be "self-regulating").* If $|G_d(j\omega)d_0| > y_{\max}$ at some frequency, then control is needed. With feedback control ($u = -Ky$) we get $y(s) = S(s)G_d(s)d(s)$, where $S = (I + GK)^{-1}$ is the sensitivity function. The requirement $|y(\omega)| < y_{\max}$ then becomes

$$|S(j\omega)| \cdot |G_d(j\omega)||d(\omega)| < y_{\max}, \quad \forall\omega \tag{7.21}$$

With integral action in the controller, $|S|$ is zero at steady state, so in general it does not matter if $|G_d|$ is large at steady state (provided there is no problem with input saturation, but this is mainly a design rather than a control issue). However, $|S|$ increases with frequency and crosses 1 at the bandwidth frequency ω_S, $|S(j\omega_S)| = 1$. At this frequency the requirement (7.21) gives the controllability requirement

$$|G_d(j\omega_S)| < \frac{y_{\max}}{|d(\omega_S)|} \tag{7.22}$$

Input disturbance. However, the purpose of this chapter is not to consider plants for which $|G_d|$ is large, but rather plants for which $|G|$ is large (in practice, these are often related because all plants have disturbances at the input to the plant). To this effect, we consider input (load) disturbances d_u for which $G_d(s) = G(s)$ (see Figure 7.9). Hence, (7.22) gives the following controllability bound on the allowed plant gain at frequency ω_S

$$|G(j\omega_S)| < \frac{y_{\max}}{|d_u(\omega_S)|} \tag{7.23}$$

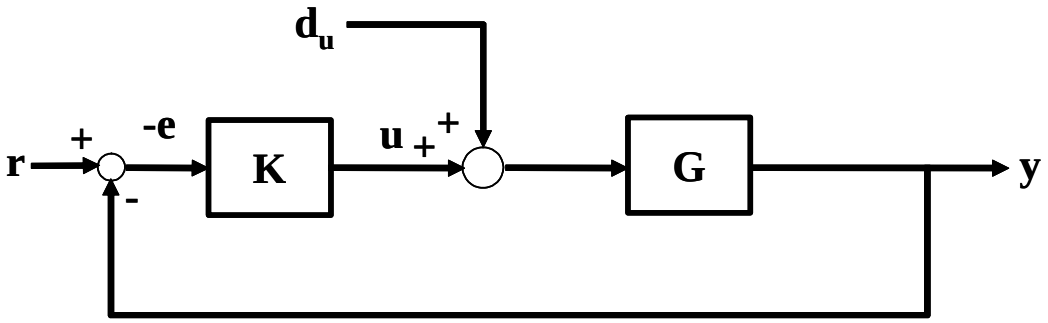

Figure 7.9: *Block diagram of a feedback control system with disturbance at the input of the plant.*

This bound is independent of the controller, and thus provides a fundamental controllability requirement. In most cases $|G|$ is smaller at high frequency, so the bound is easier to satisfy if ω_S is increased. However, for stability reasons the value of ω_S is limited, and a typical upper bound is $\omega_S \approx \frac{0.5}{\theta}$, where θ denotes the "effective delay" around the feedback loop (Skogestad and Postlethwaite, 2005).

Input disturbances are very common, but what is the expected value of $|d_u|$? This is difficult to answer, because input disturbances have many sources. For example, in many cases the input is a valve which receives its power from a hydraulic system (e.g. the brakes of a car) or from pressured air (many process control applications). A change (disturbance) in the power system will then cause an input disturbance. The value of $|d_u|$ will vary depending on the application. If it is assumed that the system has been scaled such that the largest expected input u is of magnitude 1, then it seems reasonable that $|d_u|$ is at least 0.01, and that a typical value is 0.1 or larger.

Steady-state implications. Condition (7.23) provides a bound on the plant gain at frequency ω_S. The implications in terms of the steady-state are discussed next by considering a first-order with delay plant,

$$G(s) = G_d(s) = \frac{ke^{-\theta s}}{(\tau s + 1)}, \tag{7.24}$$

where $k = |G(0)|$ is the steady-state gain of the plant. The high-frequency asymptote is $|G(j\omega)| \approx \frac{k}{\tau\omega} = \frac{k'}{\omega}$, where $k' = \frac{k}{\tau}$ is the initial slope of the step response. With $\omega_S \approx \frac{0.5}{\theta}$, (7.23) gives the controllability requirement

$$\frac{k}{\tau} = k' < 0.5\frac{y_{\max}}{\theta|d_u|} \tag{7.25}$$

(7.25) may seem to indicate that a plant with a large steady-state gain k is fundamentally difficult to control (see case 1 below). However, as discussed in case 2 this

is not always true because from (7.23) it is the gain at frequency ω_S that should be small and a process can have a large steady-state gain while having a small gain at high frequency.

Case 1. In some cases a large steady-state gain k implies a large gain at high frequencies, resulting in not being able to satisfy the controllability requirement in (7.22). A physical example is a pH-neutralization process as studied in chapter 5 in Skogestad and Postlethwaite (2005). The component balance for the excess of acid y gives the model $\tau_h s y(s) = \frac{1}{\epsilon}u(s) - y(s)$. where τ_h is the residence time and u the neutralization flow. This is on the form of (7.24) with $k = 1/\epsilon$ and $\tau = \tau_h$. The reason for the small value of ϵ is that the desired concentration in the tank (y) can be in the order of 10^6 smaller than in the neutralization inflow. Because of the large high-frequency gain, this plant is not controllable according to (7.23), and a design change is required, for example, where the neutralization is done in several steps (tanks) rather than in a single step.

Case 2. As an example of a case where a large steady-state gain does not imply control problems, consider a near-integrating process:

$$G(s) = \frac{k'}{s+\epsilon}e^{-\theta s} \tag{7.26}$$

This is on the form of (7.24) with $k = \frac{k'}{\epsilon}$ and $\tau = \frac{1}{\epsilon}$. Thus, as $\epsilon \to 0$, the steady-state gain $G(0) = \frac{k'}{\epsilon}$ approaches infinity, but the high-frequency slope of the gain k' remains finite as it is independent of ϵ, so (7.25) may not impose any controllability limitation. A physical example is a liquid level where ϵ represents the self-regulating effect. The mass balance may be written as $s\Delta V(s) = \Delta q_{in} - \Delta q_{out}$, where the linearized outflow is $\Delta q_{out} = k'\Delta Z(s) + \epsilon \Delta V(s)$ and Z is the valve position. $\epsilon \to 0$ for the case when the outflow only depends weakly on V. With $y = \Delta V$, $u = \Delta Z$, and $d = \Delta q_{in}$, this results in a model of the form in (7.26) and (7.24).

7.8 Discussion

We have derived expressions for the amplitude and period of oscillations that result with feedback control of a system with restricted input resolution (quantizer). Importantly, the amplitude and period were found (under certain assumptions about the integral time) to be independent of the controller gain. However, note that the time before cycling actually starts may be considerably longer than the period T of the oscillations, and that this start-up time does depend on the controller gain. By detuning the controller (reducing the controller gain) it generally takes longer time for the oscillatings to start. This is confirmed by the simulations in Figure 3 in McAvoy and Braatz (2003) where a detuned controller gives no oscillations with a simulation time of 80 s. However, it is easily confirmed that oscillations do indeed develop if the simulation time is extended to 95 s or more.

In this chapter, we have considered the effect of input (valve) inaccuracy and input

load disturbances, with the corresponding controllability requirements

$$|G(j\omega_{L,180})| < \frac{\pi}{4}\frac{a_{max}}{q} \tag{7.18}$$

$$|G(j\omega_S)| < \frac{y_{\max}}{|d_u(\omega_S)|} \tag{7.23}$$

Which condition is the more restrictive? There is no general answer, but let us first consider two reasons for why the latter (input disturbance) may be more restrictive. First, the input disturbance $|d_u|$ is normally larger than the quantization step q. Second, the bound for input load disturbance occurs at a lower frequency ω_S where the gain $|G(j\omega)|$ is generally larger than at frequency $\omega_{L,180}$. Specially, assume that the magnitude of the first order plus delay plant in the high-frequency range can be approximated by $|G(j\omega)| = \frac{k}{\tau\omega}$. Then, taking the typical values $\omega_S = \frac{0.5}{\theta}$ and $\omega_{L,180} = \frac{1.5}{\theta}$, we get

$$\frac{|G(j\omega_S)|}{|G(j\omega_{L,180}|} \approx \frac{\omega_{L,180}}{\omega_S} \approx 3 \tag{7.27}$$

This leads to the conclusion that the output deviation caused by an input disturbance is likely to be larger than the sustained output varuations caused by restricted input resolution. On the other hand, we are less likely to accept sustained oscillations (a_{max}) than short-time deviations (y_{max}), so one could argue that a_{max} is usually smaller than y_{max} (a typical value may be $a_{max} = 0.2y_{max}$). In summary, it is not clear which is the more restrictive.

McAvoy and Braatz (2003) state that, for control purposes, the magnitude of the steady-state process gain ($k = \overline{\sigma}(G(0))$) should not exceed 50. In this chapter, we have derived controllability conditions, (7.18) and (7.23), that limit the plant gain at frequencies $\omega_{L,180}$ and ω_S, respectively. These conditions have some implications for the steady-state gain which in special cases may provide some justification for the rule-of-thumb of McAvoy and Braatz (2003). Specifically, the expression (7.19) for steady-state offset with P-control gives $k \leq \frac{2|y-r|}{q}$. For example, with $q = 0.02$ and $|y - r|_{max} = a_{max} = 0.2$ this requires $k < 20$. Thus, P-control should only be used for plants with a small steady-state gain. Furthermore, (7.23) may be rewritten as in (7.25) to get $k < 0.5\frac{y_{\max}\tau}{\theta|d_u|}$. If we select $|y_{max}| = 1$, $|d_u| = 0.1$, and $\frac{\tau}{\theta} = 10$ (similar to that used in the simulation in McAvoy and Braatz (2003)) then we derive a bound $k < 50$. However, note that the bounds (7.19) and (7.25) do not imply that large steady-state gains are always a problem for control. First, (7.25) is derived for a first-order with delay model where k and τ are assumed independent, whereas they often are coupled, e.g. see (7.26). Second, (7.19) applies to P-control and the implication is that integral action needs to be added for control of such processes.

In the introduction, we referred to a case by Moore (1992) which seems to prove that a large steady-state gain (i.e. large gain at zero frequency) gives large output variations (poor control) when we have restricted valve resolution. However, in practice the system will not cycle at a low frequency, but at a higher frequency ($\omega_{L,180}$) where

the process gain is smaller and the resulting output variables are therefore smaller. We may also introduce forced cycling or use valve position control to further reduce the output variation.

7.9 Conclusion

In this chapter, controllability requirements are derived for two kinds of input errors, namely

(1) restricted input resolution (e.g. cased by valve inaccuracy) and

(2) input disturbances.

(1) Limited input resolution with integral feedback control (no steady-state offset) causes limit cycle behavior (oscillations) (Theorem 1). The magnitude of the oscillations can be reduced by pulse modulating the input signal or using valve position control, but this assumes that frequent input movements are acceptable. The controllability requirement derived from an approximate describing function analysis, assuming no forced oscillations, is

$$|G(j\omega_{L,180})| < \frac{\pi}{4}\frac{a_{max}}{q}, \tag{7.18}$$

where $L = GK$ and, typically, $\omega_{L,180} \approx \frac{1.5}{\theta}$ (θ is the effective delay in the loop). a_{max} is the allowed magnitude for the resulting sustained output oscillations (limit cycles). This expression agrees well (within 27%) with an exact nonlinear analysis for a first-order plus delay process. With forced oscillations (pulse modulating the input signal), we can select the frequency ω to be much higher than the "natural" cycling frequency $\omega_{L,180}$ and the controllability limitations are generally less restrictive.

(2) For input (load) disturbances of magnitude $|d_u|$, the controllability requirement is

$$|G(j\omega_S)| < \frac{y_{\max}}{|d_u(\omega_S)|}, \tag{7.23}$$

where y_{max} is the allowed magnitude of the resulting short-term output deviation, and and typically $\omega_S \approx \frac{0.5}{\theta}$.

In summary, large gains at frequencies around the closed-loop bandwidth $(\omega_S, \omega_{L,180})$ may cause problems with feedback control. There is no controllability condition that involves the steady-state gain $k = |G(0)|$ only, so a large steady-state gain is not by itself a problem for feedback control.

7.10 Appendix - Proof of Theorem 1

Consider the first-order plus delay process in (7.13). Now, assume this process is excited by a periodic and persistent input (it is applied since $t > 0$) of the form given by Figure 7.10. It represents the signal generated from a relay without hysteresis in which q_1 and q_2 are the limit values, t_1 is the time interval where u_q remains in q_1,

and $T = t_1 + t_2$ is the period of oscillation. This signal can be represented in Laplace domain as a series of steps delayed in time. Assume now, without loss of generality that $q_2 = 0$ and $q_1 = q$. The resulting transformed signal is given by

$$u_q(s) = \frac{q}{s}(1 - e^{-t_1 s} + e^{-Ts} - e^{-(t_1+T)s} + e^{-2Ts} - e^{-(t_1+2T)s} + \cdots) \quad (7.28)$$

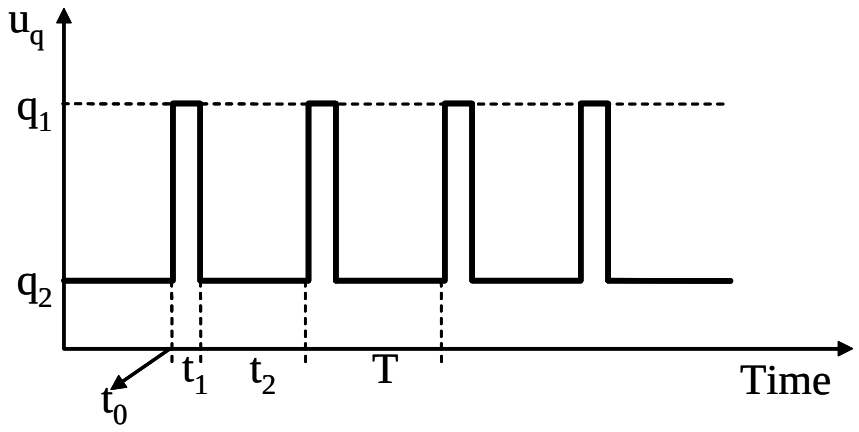

Figure 7.10: *Input to be applied to the system in (7.16).*

When this signal is applied to the process in (7.13), oscillations result in the output.

The set of maximum (or minimum) values of these oscillations are such that $t = \{t|t = t_1 + mT + \theta, \forall m \in \mathbb{N}\}$ and the minimum (or maximum) values are found in the set $t = \{t|t = mT + \theta, \forall m \in \mathbb{N}\}$.

The maximum (or minimum) at $\theta + T < t \leq \theta + t_1 + T$ is

$$y(s) = \frac{k}{\tau s + 1} e^{-\theta s} \frac{q}{s}(1 - e^{-t_1 s} + e^{-Ts}), \quad (7.29)$$

which inverted to the time domain gives

$$y(t) = kq(1 - e^{-(t-\theta-T)/\tau} + e^{-(t-\theta-t_1)/\tau} + e^{-(t-\theta)/\tau}) \quad (7.30)$$

The maximum (or minimum) is thus:

$$y(t_1 + T + \theta) = kq(1 - e^{-t_1/\tau} + e^{-T/\tau} - e^{-(t_1+T)/\tau}) \quad (7.31)$$

Hence, the maximum (or minimum) amplitude y_{ext1} can be extended to

$$y_{ext1} = kq(1 - e^{-t_1/\tau} + e^{-T/\tau} - e^{-(t_1+T)/\tau} + e^{-2T/\tau} - \cdots), \quad (7.32)$$

which can be written as

$$y_{ext1} = kq[(1-e^{-t_1/\tau})(1+e^{-T/\tau}+e^{-2T/\tau}+e^{-3T/\tau}+\cdots)] \tag{7.33}$$

The infinite sum in (7.33) is given by

$$\lim_{n\to\infty}\sum_{j=0}^{n}(e^{-T/\tau})^j = \frac{1}{1-e^{-T/\tau}}, \tag{7.34}$$

where the fact that $(e^{-T/\tau})^n$ converges to zero as n goes to infinity is used.

Accordingly,

$$y_{ext1} = kq\left(\frac{1-e^{-t_1/\tau}}{1-e^{-T/\tau}}\right) \tag{7.35}$$

The minimum (or maximum) at $\theta+t_1+T < t \leq \theta+2T$, y_{ext2}, is found by following the same development used to derive y_{ext1}, i.e.

$$y_{ext2} = kq\left[\frac{e^{-T/\tau}(1-e^{-t_1/\tau})}{1-e^{-T/\tau}}\right], \tag{7.36}$$

The amplitude is calculated by $a = y_{ext1} - y_{ext2}$ or

$$a = kq\left(\frac{1-e^{-t_1/\tau}+e^{-T/\tau}-e^{-(T-t_1)/\tau}}{1-e^{-T/\tau}}\right) \tag{7.37}$$

The formula in (7.37) depends on t_1 and T which must be determined.

From Figure 7.2:

$$u(s) = K(s)[r(s)-y(s)], \tag{7.38}$$

where $K(s)$ is given by (7.14), $r(s)$ is a step change in reference ($r(s) = \frac{r_0}{s}$), and $y(s) = K(s)G(s)u_q(s)$, where $G(s)$ is given by (7.13).

In the limit when $t \to \infty$, the quantizer behaves exactly as the relay depicted in Figure 7.10 and assuming that q_1 and q_2 are arbitrary values, the first three terms of u_q are:

$$u_q(s) = \frac{q_2}{s} + \frac{q_1-q_2}{s}(e^{-t_1 s} - e^{-(t_1+t_2)s}), \tag{7.39}$$

where the fact that $T = t_1 + t_2$ is used.

Consider a PI-controller. Taking (7.39) into (7.38) and inverting it to time domain, the following equation for $u(t)$ in the interval $\theta \leq t < t_0 + \theta$ is found:

$$u(t) = \frac{K_c}{\tau_I}\{r_0(t+\tau_I) - kq_2[(\tau_I-\tau)(1-e^{-(t-\theta)/\tau})+t-\theta]\} \tag{7.40}$$

For the interval $\theta + t_0 \leq t < t_0 + t_1 + \theta$, $u(t)$ is given by

$$\begin{aligned} u(t) &= \frac{K_c}{\tau_I}\{r_0(t+\tau_I) - kq_2[(\tau_I - \tau)(1 - e^{-(t-\theta)/\tau}) + t - \theta] - \\ &\quad k(q_1 - q_2)[(\tau_I - \tau)(1 - e^{-(t-t_1-\theta)/\tau}) + t - t_1 - \theta]\} \end{aligned} \tag{7.41}$$

Likewise, for the interval $\theta + t_0 + t_1 \leq t < t_0 + t_1 + t_2 + \theta$,

$$\begin{aligned} u(t) &= \frac{K_c}{\tau_I}\{r_0(t+\tau_I) - kq_2[(\tau_I - \tau)(1 - e^{-(t-\theta)/\tau}) + t - \theta] - \\ &\quad k(q_1 - q_2)[(\tau_I - \tau)(1 - e^{-(t-t_1-\theta)/\tau}) + t - t_1 - \theta] + \\ &\quad k(q_1 - q_2)[(\tau_I - \tau)(1 - e^{-(t-t_1-t_2-\theta)/\tau}) + t - t_1 - t_2 - \theta]\} \end{aligned} \tag{7.42}$$

So far, no assumptions on the controller settings (K_c and τ_I) have been made. The expressions (7.40)-(7.42) drastically simplify if the integral time is selected as $\tau_I = \tau$, which is an appropriate setting for many plants (Smith *et al.*, 1975).

Furthermore, for a relay without hysteresis its output ($u_q(t)$) changes as its input ($u(t)$) equals to zero and since the quantizer behaves as a relay when $t \to \infty$, the following equations give relations for t_1 and t_2.

For $t = t_0$:

$$r_0(t_0 + \tau_I) = kq_2(t_0 - \theta) \tag{7.43}$$

For $t = t_0 + t_1$:

$$r_0(t_0 + t_1 + \tau_I) = kq_2(t_0 + t_1 - \theta) - k(q_1 - q_2)(t_0 - \theta) \tag{7.44}$$

For $t = t_0 + t_1 + t_2$:

$$\begin{aligned} r_0(t_0 + t_1 + t_2 + \tau_I) &= kq_2(t_0 + t_1 + t_2 - \theta) - k(q_1 - q_2)(t_0 + t_2 - \theta) + \\ &\quad k(q_1 - q_2)(t_0 - \theta) \end{aligned} \tag{7.45}$$

Combining (7.43)-(7.45) the following expressions give the period T of the oscillations:

$$t_1 = \frac{k(q_1 - q_2)\theta}{kq_1 - r_0} \tag{7.46}$$

$$t_2 = \frac{k(q_1 - q_2)\theta}{r_0 - kq_2} \tag{7.47}$$

$$T = t_1 + t_2 \tag{7.48}$$

On average, the input must equal the steady-state value $u_{ss} = \frac{y_{ss}}{G(0)} = \frac{r_0}{k}$ (where $k = G(0)$), and if this does not happen to exactly correspond to one of the quantizer level, the quantized input u_q will cycle between the two neighboring quantizer levels, q_1 and q_2. Let f and $(1-f)$ denote the fraction of time spent at each level. Then, at steady state $u_{ss} = \frac{r_0}{k} = fq_1 + (1-f)q_2$ and from this expression f is found to be

$$f = \frac{r_0 - kq_2}{k(q_1 - q_2)} \tag{7.49}$$

From (7.49),

$$\begin{aligned} t_1 &= \frac{\theta}{1-f} \\ T &= \theta\Big(\frac{1}{1-f} + \frac{1}{f}\Big), \end{aligned} \tag{7.50}$$

which completes the proof.

Chapter 8

Concluding remarks and further work

8.1 Concluding remarks

This thesis has dealt with the application of the plantwide control structure design procedure of Skogestad (2004*a*). One of the main results was that the technique is very effective to handle large-scale complex process flowsheets, leading to efficient control structures that are economically (near) optimal with good dynamic performance characteristics.

In chapter 3, the well-known test-bed HDA process was extensively used to demonstrate the effectiveness of the plantwide control design procedure by Skogestad (2004*a*). Since the task of selecting primary controlled variables for this (or any other process one considers) process is of paramount importance, we used the self-optimizing control technique by Skogestad (2000) which gives a natural and systematic way of deciding for the variables that should be controlled in order to achieve (near) optimal operation without the need to re-optimize when disturbances occur. We performed this computation for the case where the feed flow rate is given, what we called Mode I of operation. The large number of variable combinations makes the HDA process a challenging problem, and a local (linear) analysis based on the SVD of the linearized model of the plant was used to select good candidate sets for the unconstrained controlled variables. Namely, 16 candidate sets were found to be suitable to select from. Moreover, Aspen Plus^{TM} proved to be a valuable tool for the evaluation of self-optimizing control structures for large-scale processes.

After having selected the primary variables to be controlled in the HDA process in order to get optimal operation, a major task is then to design the regulatory control layer and decide for the way the supervisory control should be conducted. This was accomplished in chapter 4 and one very important issue considered there was the way the control structure was set in order to deal with maximum production rate, here called Mode II of operation. For this process, the bottleneck for maximum production rate (Mode II) was found to be the furnace heat duty Q_{fur}. However, this heat duty is needed to stabilizer the reactor, so the throughput manipulator was selected as the

toluene feed rate F_{tol}. The final regulatory control layer shows good dynamic responses, as seen from the simulation results. The reason for this is that the systematic procedure ensures that the process does not drift away from its nominally optimal operating point (both Mode I and II). Note that no "intermediate" control layer was introduced in the hierarchy which contributed to the low complexity of the overall control structure.

In chapter 5, we demonstrated another yet very important mode of operation when it is not economically optimal to maximize throughput, even if feed is available. This happens if the profit reaches a maximum, for example, because purge streams increase sharply at high feed rates. This was discussed in details when we applied the plantwide design procedure to the ammonia synthesis process. It has been found that is not economically attractive to operate the process beyond the production rate determined by the "economic" bottleneck corresponding to the maximum gas feed rate. By applying the self-optimizing technique of Skogestad (2000), we also found that it is (near) optimal to operate the supervisory control layer by keeping constant set point policy for the feed compressor power, recycle compressor power, and purge flow rate when the gas feed rate is given (Mode I), which corresponds to the practice currently adopted in industrial ammonia synthesis plants. In case of optimized throughput (Mode IIb), the pressure of the system and the mole fraction of CH_4 should be controlled to achieve (near) optimal operation. The regulatory layer is enhanced by controlling the reactor temperature so to avoid the deteriorating effects of oscillations caused by variations in the reactor inlet conditions (temperature and/or pressure) (Morud and Skogestad, 1998).

Chapter 6 discussed that an interesting perspective on the plantwide control design procedures dealt with in this thesis can be drawn if we consider the application of two seemingly related fields: Self-optimizing control (Skogestad, 2000) and singular perturbation analysis (Baldea and Daoutidis, 2006). The self-optimizing control approach is used to select the controlled outputs that gives the economically (near) optimal for the plant. These variables must be controlled in the upper or intermediate layers in the hierarchy. The fast layer (regulatory control layer) used to ensure stability and local disturbance rejection is then successfully designed (pair inputs with outputs) based on the singular perturbation framework proposed in Baldea and Daoutidis (2006). The case study on the reactor-separator network illustrates that the two approaches may be combined successfully.

Last but not least, in chapter 7 we saw that the issue of imperfect valves has important implications on the plantwide control strategy since it impacts on the decisions involving lower hierarchy layers, specially on the regulatory control layer. We then derived some controllability requirements when we have restricted input resolution (e.g. cased by valve inaccuracy) and input disturbances. We found out that limited input resolution with integral feedback control causes limit cycle behavior and also that the magnitude of the oscillations can be reduced by pulse modulating the input signal or using valve position control, but this assumes that frequent input movements are acceptable.

8.2 Directions for further work

8.2.1 Effect of valve imperfection on multivariable large-scale systems

The results of limit cycles with imperfect valves should be applied to the design of regulatory control layers for multivariable systems since they correspond to the majority and most important applications in the process industry. Specially, problems related to stiction are the rule rather than the exception in process plants.

8.2.2 Effective off-line handling of active constraints operating regions

In the available literature for self-optimizing control (e.g. Halvorsen *et al.* (2003)), it is assumed that the set of active constraints does not change with disturbances. Then, with the elimination of the state variables x, the resulting problem can be treated as an unconstrained optimization problem in the reduced space. Though this assumption greatly simplifies the analysis, it can be very restrictive in some cases. The active constraints form a subset of controlled variables and thus a change in the set of active constraints require changing the set of controlled variables. One possible way to overcome this limitation is to find the optimal controlled variables for every possible set of active constraints (off-line) and then use of a logic-based switching algorithm (on-line). Similar ideas have been used recently in the context of moel predictive controllers (MPC) (Bemporad *et al.*, 2002). Recent research has demonstrated that for different sets of active constraints, the entire feasible region can be efficiently divided into polyhedra for the quadratic problem involved in MPC (Bemporad *et al.*, 2002). For the nonlinear program used at the optimization layer, such a decomposition is difficult, as the boundaries of the regions corresponding to different sets of active constraints can take arbitrary shapes. One strategy to get across this problem is to sacrifice optimality in favor of practicality by dividing the feasible region into polyhedra or ellipses based on loss due to suboptimal strategy. The proposed work will then focus on efficient computational methods for finding the minimal number of divisions of the feasible region and devising a simple switching algorithm.

8.2.3 Model reduction of solution

For many chemical processes, it may not be possible to find a set of controlled variables that give near-optimal operation with a constant set point policy, for instance, when the anticipated set of disturbances is very large. In such cases, self-optimizing control is still useful as it can reduce the frequency of on-line optimization. The on-line optimization can be simplified by eliminate some of the variables using the model equations and also the set of active constraints, when the elimination is carried out over a subset feasible regions with the same active constraints. This results in a simplified optimization problem in the reduced space. By “reduced space” we here mean in the

number of degrees of freedom left for optimization. The idea is to investigate the use of symbolic computation for elimination of implicit variables, for example, using the available techniques of (Wang, 2001).

8.2.4 Varying set points

An alternative to solve the optimization problem on line (preferably using a reduced model), is to generate optimal variations in the set points of the controlled variables as a function of disturbances or the system state. For the nonlinear case, one may attempt to find symbolically the optimal function, or generate it numerically by fitting a polynomial function to the solution, for instance.

8.2.5 Selection of primary controlled variables

Previous work on selection of primary controlled variables for self-optimizing control used brute-force method and local analysis. The local analysis has resulted in the approximate but highly useful and insightful "maximum gain rule" (Skogestad and Postlethwaite, 2005). Though useful, the maximum gain rule needs to be applied to all possible alternatives for controlled variables, which increase exponentially with the problem size. Recent developments indicate that a deterministic branch and bound algorithm can be used to reduce the involved computational complexity. The plan is to fully develop this idea and seek its generalizations to the exact local method (Halvorsen *et al.*, 2003) and also to the original nonlinear program (possibly with the assumption of local convexity).

8.2.6 Selection of secondary controlled variables

There has been made significant progress in terms of the selection of primary (economic) controlled variables. However, the selection of secondary (dynamic) controlled variables is also very important. These variables are primarily controlled in order to "stabilize" the process. The word stabilize has here been put in quotes because we are not only concern with "stabilization" in the broader sense as used by the lay person, which may be loosely defined as "keeping the system reasonably close to its desired operation point". A key point here is to reduce the disturbance sensitivity. In practice, this is done by controlling selected secondary controlled variables. The set points for these variables are then degrees of freedom for the higher layers in the hierarchy, resulting in a cascade control system. It would be then interesting to investigate more systematic methods for selecting secondary controlled variables. Pairing and decentralized control is also an issue here.

8.2.7 Dynamic self-optimizing control

So far we have focused on self-optimizing control on steady-state models. This is justified as for most chemical processes, economics are primarily governed by the steady-

state of the process. In some cases, however, e.g., batch processes, grade transitions, and start up, the consideration of dynamics becomes important. Some useful work in this are has bee reported by Visser *et al.* (2000) and Srinivasan *et al.* (2002). Based on these works, the idea would be to develop this further, including the issue of directly controlling the first-order optimality conditions at zero. The local analysis has proved to be extremely useful for steady-state optimizing control and this future work would aim at generalizing these results to dynamic models.

Bibliography

Araujo, A. C. B., M. Govatsmark and S. Skogestad (2006). Application of plantwide control to the HDA process. I - steady-state optimization and self-optimizing control. *Control Engineering Practice*.

Arbel, A., I. H. Rinard and R. Shinnar (1996). Dynamics and control of fluidized catalytic crackers, 3 designing the control system: Choice of manipulated and measured variables for partial control. *Industrial Engineering Chemistry Research* **35**(7), 2215–2233.

Arkun, Y. and G. Stephanopoulos (1980). Studies in the synthesis of control structures for chemical processes: part iv. design of steady-state optimizing control structures for chemical process units. *AICHE journal* **26**(6), 975–991.

Aström, K. J. and T. Hägglund (1988). *Automatic Tuning of PID Controllers*. Instrument Society of America. USA.

Baldea, M. and P. Daoutidis (2006). Dynamics and control of integrated networks with purge streams. *AICHE Journal* **52**(4), 1460–1472.

Bemporad, A., M. Morari, V. Dua and E. N. Pistikopoulos (2002). The explicit linear quadratic regulator for constrained systems. *Automatica* **38**(1), 3–20.

Brognaux, C. (1992). A case study in operability analysis: The `HDA` plant. Master thesis. University of London, London, England.

Buckley, P. S. (1964). *Techniques of process control*. John Wiley and Sons. New York, USA.

Cao, Y. and D. Biss (1996). New screening techniques for choosing manipulated variables. In: *Preprints IFAC '96, 13th World Congress of IFAC, Volume M*. San Francisco, CA.

Cao, Y. and D. Rossiter (1997). An input pre-screening technique for control structure selection. *Computers and Chemical Engineering* **21**(6), 563–569.

Cao, Y. and D. Rossiter (1998). Input selection and localized disturbance rejection. *Journal of Process Control* **8**(3), 175–183.

Cao, Y., D. Rossiter and D. Owens (1997*a*). Input selection for disturbance rejection under manipulated variable constraints. *Computers and Chemical Engineering* **21**(Suppl.), S403–S408.

Cao, Y., D. Rossiter and D. Owens (1997*b*). Screening criteria for input and output selection. In: *Proceedings of European Control Conference, ECC 97*. Brussels, Belgium.

Cao, Y., D. Rossiter and D. Owens (1998*a*). Globally optimal control structure selection using branch and bound method. In: *Proceedings of DYCOPS-5, 5th IFAC Symposium on Dynamics and Control of Process Systems*. Corfu, Greece.

Cao, Y., D. Rossiter, D.W. Edwards, J. Knechtel and D. Owens (1998*b*). Modelling issues for control structure selection in a chemical process. *Computers and Chemical Engineering* **22**(Suppl.), S411–S418.

Cui, H. and W. Jacobsen (2002). Performance limitations in decentralized control. *Journal of Process Control* **12**, 485–494.

Douglas, J. M. (1988). *Conceptual Design of Chemical Processes*. McGraw-Hill. USA.

Froment, G. F. and K. B. Bischoff (1990). *Chemical Reactor Analysis and Design, 2nd ed.*. Wiley. New York.

Halvorsen, I J., S. Skogestad, J. C. Morud and V. Alstad (2003). Optimal selection of controlled variables. *Ind. Eng. Chem. Res.* **42**, 3273–3284.

Heath, J. A., I. K. Kookos and J. D. Perkins (2000). Process control structure selection based on economics. *AIChE Journal* **46**, 1998–2016.

Herrmann, G., S. K. Spurgeon and C. Edwards (2003). A model-based sliding mode control methodology applied to the hda-plant. *Journal of Process Control* **13**, 129–138.

Hicks, R. C., G. R. Worrell and R. J. Durney (1966). Atlantic seeks improved control; studies analog-digital models. *Oil and Gas Journal* **24**, 97.

Hori, E. S. and S. Skogestad (2006). Self-optimizing control configuration for two-product distillation columns. In: *Proceedings Distillation and Absorption*. London, UK.

Hovd, M. and S. Skogestad (1993). Procedure for regulatory control structure selection with application to the fcc process. *AIChE Journal* **39**(12), 1938–1953.

Konda, N. V. S. N. M., G. P. Rangaiah and P. R. Krishnaswamy (2005*a*). Plantwide control of industrial processes: an integrated framework of simulation and heuristics. *Industrial Engineering Chemistry Research* **44**, 8300–8313.

Konda, N. V. S. N. M., G. P. Rangaiah and P. R. Krishnaswamy (2005*b*). Simulation based heuristics methodology for plant-wide control of industrial processes. In: *Proceedings of 16th IFAC World Congress*. Praha, Czech Republic.

Kumar, A. and P. Daoutidis (2002). Nonlinear dynamics and control of process systems with recycle. *Journal of Process Control* **12**(4), 475–484.

Lee, W. and V. W. Weekman (1976). Advanced control practice in the chemical process industry: A view from industry. *AIChE Journal* **22**(1), 27–38.

Liptak, B.G (2006). *Instrument Engineers' Handbook. Volume II: Process control and optimization, 4th edition*. CRC Press. New York.

Luyben, W. L. (2002). *Plantwide dynamic simulators in chemical processing and control*. Marcel Dekker, Inc.. New York, USA.

Luyben, W. L., B. D. Tyréus and M. L. Luyben (1998). *Plantwide process control*. McGraw-Hill. USA.

Maarleveld, A. and J. E. Rijnsdorp (1970). Constraint control on distillation columns. *Automatica* **6**, 51–58.

McAvoy, T. J. and R. D. Braatz (2003). Controllability of process with large singular values. *Ind. Eng. Chem. Res.* **42**, 6155–6165.

McKetta, J. J. (1977). *Benzene design problem*. Encyclopedia of Chemical Processing and Design. Dekker, New York, USA.

Moore, C. F. (1992). Selection of controlled and manipulated variables. *In "Practical Distillation Control", W. L. Luyben, Van Nostrand Reinhold, New York*.

Morari, M. (1983). Design of resilient processing plants III - a general framework for the assessment of dynamic resilience. *Chemical Engineering Science* **38**, 1881–1891.

Morari, M. and J. D. Perkins (1995). Design for operations.. In: *L. Biegler and M. Doherty, Fourth International Conference on Foundations of Computer-Aided Process Design.*

Morari, M., G. Stephanopoulos and Y. Arkun (1980). Studies in the synthesis of control structures for chemical processes, part I: formulation of the problem, process decomposition and the classification of the control task, analysis of the optimizing control structures. *AIChE Journal* **26**(2), 220–232.

Morud, J. C. and S. Skogestad (1998). Analysis of instability in an industrial ammonia reactor. *AIChE Journal* **44**(4), 888–895.

Narraway, L. T. and J. D. Perkins (1993). Selection of process control structure based on linear dynamic economics. *Industrial Engineering Chemistry Research* **32**(11), 2681–2692.

Narraway, L. T. and J. D. Perkins (1994). Selection of process control structure based on economics. *Compuers and Chemical Engineering* **18**, S511–S517.

Narraway, L. T., J. D. Perkins and G. W. Barton (1991). Interaction between process design and process control: economic analysis of process dynamics. *Journal of Process Control* **1**, 243–250.

Ng, C. and G. Stephanopoulos (1996). Synthesis of control systems for chemical plants. *Computers and Chemical Engineering* **20**, S999–S1004.

Ponton, J.W. and D.M. Laing (1993). A hierarchical approach to the design of process control systems. *Trans IChemE* **71**(Part A), 181–188.

Price, R. M. and C. Georgakis (1993). Plantwide regulatory control design procedure using a tiered framework. *Industrial and Engineering Chemistry Research* **32**, 2693–2705.

Price, R. M., P. R. Lyman and C. Georgakis (1994). Throughput manipulation in plantwide control structures. *Industrial and Engineering Chemistry Research* **33**, 1197–1207.

Qiu, Q. F. and P. R. Krishnaswamy (2003). Application of a plant-wide control design to the hda process. *Computers and Chemical Engineering* **27**, 73–94.

Shinnar, R. (1981). Chemical reactor modeling for purposes of controller design. *Chemical engineering Communications* **9**, 73–99.

Shoukat Choudhory, M. A. A., N.F. Thornhill and ShaH N. L. (2005). Modelling valve stiction. *Control Engineering Practice* **13**(5), 641–658.

Skogestad, S. (2000). Plantwide control: The search for the self-optimizing control structure. *Journal of Process Control* **10**, 487–507.

Skogestad, S. (2002). Plantwide control: Towards a systematic procedure. In: *Proceedings of the European Symposium on Computer Aided Process Engineering 12.* pp. 57–69.

Skogestad, S. (2003). Simple analytic rules for model reduction and PID controller tuning. *Journal of Process Control* **13**, 291–309.

Skogestad, S. (2004*a*). Control structure design for complete chemical plants. *Computers and Chemical Engineering* **28**, 219–234.

Skogestad, S. (2004*b*). Simple analytic rules for model reduction and PID controller tuning. *Modeling, Identification and Control* **25**(2), 85–120.

Skogestad, S. and I. Postlethwaite (2005). *Multivariable Feedback Control: Analysis and Design.* John Wiley & Sons. Chichester, UK.

Skogestad, S., P. Lundstrom and E. W. Jacobsen (1990). Selecting the best distillation control configuration. *AIChE Journal* **36**(5), 753–764.

Slotine, J. E. and W. Li (1991). *Applied Nonlinear Control*. Prentice-Hall International Editions. New Jersey, USA.

Smith, C. L., A. B. Corripio and J. Jr. Martin (1975). Controller tuning from simple process models. *Instrumentation Technology*.

Srinivasan, B., E. Visser, S. Palanki and D. Bonvin (2002). Dynamic optimization of batch processes: I. role of measurements in handling uncertainty. *Computers and Chemical Engineering* **27**, 27–44.

Stephanopoulos, G. (1984). *Chemical process control*. Prentice-Hall International Editions. New Jersey, USA.

Stephanopoulos, G. and C. Ng (2000). Perspectives on the synthesis of plant-wide control structures. *Journal of Process Control* **10**, 97–111.

Visser, E., B. Srinivasan, S. Palanki and D. Bonvin (2000). A feedbac implementation scheme for batch process optimization. *Journal of Process Control* **10**, 399–410.

Wang, D. (2001). *Elimination Methods - Texts and Monographs in Symbolic Computation*. Springer. New York.

Wang, P. and T. McAvoy (2001). Synthesis of plantwide control systems using a dynamic model and optimization. *Industrial and Engineering Chemistry Research* **40**, 5732–5742.

Wang, Q., C. Hang and B. Zou (1997). Low-order modelling from relay feedback. *Process Design and Control* **36**, 375–381.

Wolff, E. A. (1994). Studies on control of integrated plants. PhD thesis. Norwegian University of Science and Technology, Trondheim, Norway.